

1-1-2000

Synthesis and characterization of fluorinated high performance polymeric materials

Pamela Ann Havelka
Iowa State University

Follow this and additional works at: <https://lib.dr.iastate.edu/rtd>

Recommended Citation

Havelka, Pamela Ann, "Synthesis and characterization of fluorinated high performance polymeric materials" (2000). *Retrospective Theses and Dissertations*. 21256.
<https://lib.dr.iastate.edu/rtd/21256>

This Thesis is brought to you for free and open access by the Iowa State University Capstones, Theses and Dissertations at Iowa State University Digital Repository. It has been accepted for inclusion in Retrospective Theses and Dissertations by an authorized administrator of Iowa State University Digital Repository. For more information, please contact digirep@iastate.edu.

Synthesis and characterization of fluorinated high performance polymeric materials

by

Pamela Ann Havelka

A thesis submitted to the graduate faculty
in partial fulfillment of the requirements for the degree of
MASTER OF SCIENCE

Major: Organic Chemistry

Major Professor: Valerie V. Sheares

Iowa State University

Ames, Iowa

2000

Graduate College
Iowa State University

This is to certify that the Master's Thesis of
Pamela Ann Havelka
has met the thesis requirements of Iowa State University

Signatures have been redacted for privacy

TABLE OF CONTENTS

LIST OF FIGURES	v
LIST OF SCHEMES	vii
LIST OF TABLES	viii
LIST OF ABBREVIATIONS	ix
GENERAL INTRODUCTION	1
Introduction	1
Thesis Organization	14
EXPERIMENTAL	15
Materials	15
Characterization	15
Synthetic Procedures	17
RESULTS AND DISCUSSION	24
Monomer Synthesis	28
Polymer Synthesis	29
Polymer Characterization	
GENERAL CONCLUSIONS	57
APPENDIX. SUPPORTING DATA	60
REFERENCES	136
ACKNOWLEDGEMENTS	140

LIST OF FIGURES

Figure 1. Poly(tetrafluoroethylene)	1
Figure 2. 2,2-Bis(trifluoromethyl)-4,5-difluoro-1,3-dioxole	2
Figure 3. Poly(2-fluoro1,3-butadiene)	3
Figure 4. Poly[methyl(3,3,3-trifluoropropyl)siloxane]	3
Figure 5. Poly[tetrafluoroethylene-co-(1,1,1-trifluoromethoxy)ethylene]	3
Figure 6. Structure of hexafluorisopropylidene	8
Figure 7. Poly[2-(4-phenoxyphenyl)hexafluoro-2-propanal]	8
Figure 8. Poly(bisphenol AF ether ketone)	9
Figure 9. Poly(bisphenol AF ether sulfone)	9
Figure 10. HFIP containing poly(urethane)	10
Figure 11. HFIP containing poly(ester)	11
Figure 12. HFIP containing poly(acrylate)	11
Figure 13. Poly(hexafluoropropane diphthalimido-1,4-phenylene)	12
Figure 14. UV-vis trace of the 6F polymer	34
Figure 15. GPC and MALLS chromatograms of the 6F polymer	35
Figure 16. DSC thermogram of the 6F polymer	36
Figure 17. WAXD of the 6F polymer	37
Figure 18. TGA thermogram of the 6F polymer	38
Figure 19. Gas permeability of the 6F polymer based on penetrant kinetic diameter	45

Figure 20. UV-vis trace of crosslinkable 6F polymer	49
Figure 21. GPC and MALLS chromatograms of the crosslinkable 6F polymer	48
Figure 22. TGA thermogram of the uncrosslinked 6F polymer	51
Figure 23. TGA thermogram of the crosslinked 6F polymer	51
Figure 24. UV-Vis trace of the 3F polymer	54
Figure 25. GPC and MALLS chromatograms of the 3F polymer	55
Figure 26. DSC thermogram of the 3F polymer	56
Figure 27. TGA thermogram of the 3F polymer	57

LIST OF SCHEMES

Scheme 1. Synthesis of 2,2-bis(4-chlorophenyl)hexafluoropropane	25
Scheme 2. Synthesis of 1,1-bis(4-chlorophenyl)-2,2,2-trifluoro-1-phenylethane	26
Scheme 3. Synthesis of 2,2-bis[[trifluoromethylsulfonyloxybenzene]hexafluoropropane and 1,1-bis[[trifluoromethylsulfonyl]oxybenzene]-2,2,2-trifluoro-1-phenylethane	28
Scheme 4. Synthesis of 2,2-bis[[4-acetylene]phenyl]hexafluoropropane	29
Scheme 5. Synthesis of the 6F polymer	30
Scheme 6. Synthesis of the crosslinkable 6F polymer	48
Scheme 7. Synthesis of 3F polymer	53

LIST OF TABLES

Table 1. Commercially available 6F monomers	14
Table 2. Effect of reaction temperature on the 6F monomer polymerization	31
Table 3. Effect of amount of catalyst on the 6F monomer polymerization	31
Table 4. Effect of reaction solvent on the 6F monomer polymerization	32
Table 5. Effect of solvent concentration on the 6F monomer polymerization	32
Table 6. Effect of reaction time on the 6F monomer polymerization	33
Table 7. Isothermal gravimetric analysis of the 6F polymer	39
Table 8. Polymer flammability	40
Table 9. Fractional free volume (FFV) of selected glassy polymers	42
Table 10. Gas permeability of the 6F polymer	43
Table 11. Permeability coefficients for oxygen in various polymers	44
Table 12. Separation factors of the 6F polymer	47
Table 13. Effect of solvent concentration on the 3F monomer polymerization	53

LIST OF ABBREVIATIONS

AlCl ₃	aluminum chloride
bipy	2,2'-bipyridine
°C	degrees Celsius
calcd	calculated
CHCl ₃	chloroform
cm	centimeter(s)
conc.	concentration
d	doublet
DMAc	<i>N,N</i> -dimethylacetamide
DMSO	dimethylsulfoxide
dn/dc	change in refractive index/change in concentration
DSC	differential scanning calorimetry
g	gram(s)
GC	gas chromatography
GC/MS	gas chromatography-mass spectrometry
GPC	gel permeation chromatography
HCl	hydrochloric acid
HFIP	hexafluoroisopropylidene
IR	infrared

kHz	kilohertz
m	multiplet
MALLS	multiple angle laser light scattering
MHz	megahertz
mol	mole(s)
mp	melting point
Ni	nickel
NiCl ₂	nickel(II) chloride
NMP	1-methyl-2-pyrrolidinone
NMR	nuclear magnetic resonance
PDT	polymer decomposition temperature
PPh ₃	triphenylphosphine
PPP	poly(<i>p</i> -phenylene)(s)
PTFE	poly(tetrafluoroethylene)
s	singlet
t	triplet
TFE	tetrafluoroethylene
T _g	glass transition temperature (softening temperature)
TGA	thermogravimetric analysis
THF	tetrahydrofuran
UV-vis	ultraviolet-visible
Zn	zinc

GENERAL INTRODUCTION

Introduction

Evolution of fluoropolymers

Historically, fluorinated polymers have been linked to applications in the military and for national defense. Almost immediately after the discovery of poly(tetrafluoroethylene) (Figure 1) in 1938, by Dr. Roy Plunkett, it was used in equipment developed for separating uranium isotopes in the Manhattan project.¹ It was also used as a coating for artillery shells during World War II.² Both applications required light-weight materials with enhanced thermal, chemical and oxidative stability. During that time, poly(tetrafluoro-ethylene) (PTFE) was the only synthetic material available, which could provide those unique properties.

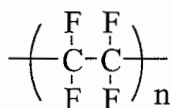


Figure 1. Poly(tetrafluoroethylene)

Although PTFE possessed unique properties that had not been observed in other synthetic materials, it did have limitations. Examining those limitations helps to explain the evolution of fluorinated materials. As a highly crystalline polymer, PTFE was noted for its high purity, chemical resistance, excellent dielectric properties and low surface energy.²

However, it was not the solution to every high performance material needed. Unless PTFE was reinforced, creep (cold flow) caused early deformation which led to the failure of the material.² Also, processing PTFE was difficult due to its high molecular weight and high crystallinity.² In order to further enhance PTFE's properties, other functional groups were incorporated into the polymer chain. For example, combining 2,2-bis(trifluoromethyl)-4,5-difluoro-1,3-dioxole (Figure 2) with tetrafluorethylene (TFE) lowered the crystallinity and molecular weight of the resulting polymer, allowing for easier processability while retaining the outstanding chemical, thermal and electrical properties of PTFE.²

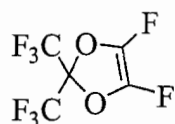


Figure 2. 2,2-bis(trifluoromethyl)-4,5-difluoro-1,3-dioxole

Due to the success of copolymers made with TFE, new classes of fluorinated polymers began to emerge. During the late 1940's, a fluorinated elastomer appeared on the market. It was made from 2-fluoro-1,3-butadiene (Figure 3).² This new material began with a promising future. The newly developed aerospace industry was placing higher demands on existing rubber materials in seals and hoses. This prompted the exploration for new materials with better heat and fuel resistance. Fluoroelastomers provided the aerospace industry with robust materials that could perform under harsh conditions. As technology continued to advance over the next twenty years, new materials were again needed. Fluorosilicones (Figure 4) and perfluoroelastomers (Figure 5) became the new choice for seals, gaskets and

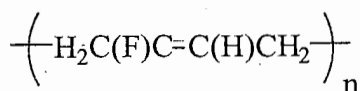


Figure 3. Poly(2-fluoro-1,3-butadiene)

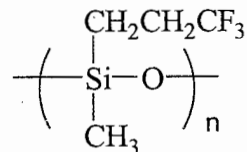


Figure 4. Poly[methyl(3,3,3-trifluoropropyl)siloxane]

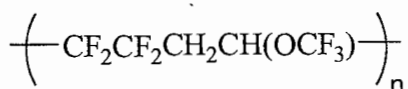


Figure 5. Poly[tetrafluoroethylene-co-(1,1,1-trifluoromethoxy)ethylene]

lubricants used in military equipment.² Today, these kinds of fluoropolymers also appear in the automotive industry as gaskets, washers, diaphragms and seals.

Military technological advancement continues to initiate research and development of fluoropolymers. In addition to military applications, fluorinated products are also being developed and marketed for the general population. Gortex® materials and Scotchgard® coatings are commonly found in many households in items such as clothing, shoes, and spray on coatings for fabrics.² Fluoropolymers are present in our cars, computers and watches and can even be found as protective barriers on skyscrapers.²

Currently, the microelectronic industry is a rapidly expanding market for fluoropolymers. The two main areas of interest deal with high speed data transmission over cables for the internet and optical communication cables.² In this industry, materials with

low refractive indices, low signal losses and low water absorption are desired.² In addition, it is necessary for these materials to maintain structural integrity after a thermal or electrical overload as well as be highly flame retardant and form non-conductive char.² Due to their unique properties, fluoropolymers are excellent candidates for these types of applications.²

Fluorine's effect on polymer properties

As technology advances, new materials are continuously being synthesized to replace existing materials that can no longer perform to the increased specifications or withstand the rigors placed upon them. Often, the versatility of fluoropolymers makes them ideal materials for these new technological advancements. Fluorinated polymers can have a wide spectrum of uses, such as insulating, highly capacitive or even piezoelectric materials.³ These unique characteristics of fluoropolymers are due to the presence of fluorine. It is fluorine's inherent properties such as its electronegativity, size, effective nuclear charge and bond strength with carbon that help create these remarkable macromolecules.³

By looking at the molecular level, we can begin to explain these extraordinary properties of fluoropolymers. Fluorine's small size and effective nuclear charge gives it the highest electronegativity of any element.⁴ Bonds between fluorine and other atoms are more ionic than covalent because of fluorine's high electronegativity. Most of the unique behavior of fluorinated materials can be directly associated with the ionic distribution of electrons in C-F bonds.³ The ionic nature of these bonds account for the favorable thermal and chemical inertness observed in fluorinated materials.³ The chemical inertness of fluoropolymers stems from the high charge density centered on fluorine, which acts like a sheath. The sheath

creates a barrier to chemical attack, protecting the weaker bonds in a molecule.² In addition to this increase in thermal and chemical inertness, fluorinated materials are difficult to polarize. Since the electrons are held so tightly by the fluorine atom, polarization of fluorinated polymers is minimized, resulting in materials with low dielectric constants.³

The low polarizability of the C-F bond also influences molecular interactions. Molecular attraction energy decreases significantly with decreasing polarizability, leaving weak intermolecular forces between fluorinated materials.³ Without dipole forces, induction forces or hydrogen bonding, the intermolecular forces associated with most fluorinated materials are classified as dispersion forces.³ These weak intermolecular interactions lead to low surface tension.³ Surface tension is a measure of the difference in interaction energy between molecules in the bulk phase compared with those at the surface.³ It is defined as the change in free energy with a change in surface area.³ Fluorinated materials, with their weak intermolecular interactions, lose minimal free energy when their surface area is increased; therefore, most fluoropolymers have low surface energies.³

Weak intermolecular interactions also minimize the frictional forces of fluorinated materials. Frictional forces are defined as the energy required to move an object across the surface of a material.³ The energy required is directly proportional to the molecular interactions that are disturbed when the object is moved across the surface of the material.³ The weak intermolecular forces of fluoropolymers minimize the interactions that are disturbed. It is the low surface energies of fluorinated materials that give them their non-stick surfaces.³

Also related to surface properties is repellency. Repellency is the ability to make liquids bead on a surface.³ It is measured by observing the contact angles formed between

the liquid and the surface of the material.³ Since fluoropolymers have low surface energies, liquids with strong intermolecular forces will bead up when placed on their surface.³ For example, water with its high surface tension will generally have contact angles greater than 100° on fluorinated materials.³ With its strong hydrogen bonding and the resulting large surface tension, water has very few intermolecular interactions with fluorinated materials. This explains the beads that are formed when water is placed on the surface of highly fluorinated materials. Generally, materials with similar surface tensions will adhere to one another and materials with dissimilar surface tensions will repel one another.³

Different types of fluorinated polymers have different surface tensions. There are two main types of fluorinated polymers; PTFE based materials and perfluoroalkyl materials. Normally, perfluoroalkyl materials have lower surface tensions than PTFE based materials.³ The difference between the two types of fluorinated materials can be explained by looking at surface packing characteristics. Generally, the less material per given unit area of a surface, the lower the surface tension.³ Therefore the surface densities of fluorinated materials will determine their surface tension.³ PTFE chains lie parallel to the air/material interface and perfluoroalkyl chains lie almost perpendicular.³ Perfluoroalkyl materials which can aggregate CF₃ groups at the surface will have less dense surfaces than PTFE based materials due to the bulky nature of the CF₃ groups.³ PTFE based materials have more dense surfaces because of the parallel orientation of the chain to the surface.³ This allows for tighter packing of the CF₂ repeat units at the surface.³

There is one more factor that helps in determining the surface tension of fluorinated materials: surface activity. Surface activity is the excess of fluorinated materials at the air/material interface.³ Perfluoroalkyl materials normally have high surface activities.³ If

perfluoroalkyl groups can converge at a surface and lower surface tension, they will.³ This means that a minimal amount of fluorine can be incorporated into a polymer to achieve low surface tension; however, the bulk properties of the polymer will be different.³

Hexafluoroisopropylidene polymers

The interesting properties that can be achieved by the incorporation of fluorine into polymers can easily be accomplished through the use of a hexafluoroisopropylidene group (HFIP) (Figure 6). The monomers of hexafluoroisopropylidene substituents can be readily obtained through condensation, Friedel Crafts or Grignard reactions involving hexafluoroacetone. Due to synthetic ease many high performance polymers have been prepared with the HFIP group to improve upon existing polymer properties. The HFIP group is highly stable, bulky-yet flexible and non-conjugating.³ Incorporation of the group into a polymer increases the free volume and decreases the crystallinity.³ Dramatic improvements in thermal and mechanical properties can be observed when comparing a fluorinated polymer to its non-fluorinated analog.³ In general, solubility, thermal stability, thermooxidative stability, optical transparency, flame resistance and UV radiation resistance are increased when HFIP is included.³ At the same time, the dielectric constant, crystallinity, water absorption and surface energy decrease.³

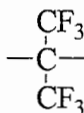


Figure 6. Structure of hexafluoroisopropylidene

Step growth polymers containing a hexafluoroisopropylidene linkage have been around since the mid-1960's. The first high performance polymer synthesized containing HFIP was a poly(ether) (Figure 7). It was patented as a thermally stable polymer which exhibited excellent mechanical properties.² All HFIP poly(ether)s prepared tended to have low dielectric constants, low water absorption and high tensile strength, making them useful to the microelectronics industry as insulating materials.⁵

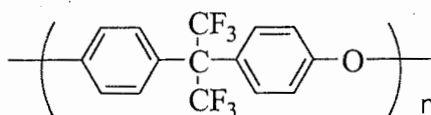


Figure 7. Poly[2-(4-phenoxyphenyl)hexafluoro-2-propanal]

From this initial fluorinated high performance polymer, a series emerged. Incorporation of HFIP into poly(arylene ether ketone and sulfone)s (Figures 8 and 9) soon followed. HFIP replaced the standard non-fluorinated isopropylidene linking group. Replacing this linkage with HFIP caused dramatic changes in the oxidative stability, tensile strength, dielectric constant and permeability of the materials.^{6,7} For example, membranes made from HFIP containing poly(arylene ether sulfone)s were more permeable and more selective towards He, CO₂, and CH₄ than the non-fluorinated analogues.⁸ The HFIP substituents changed the pore size and enhanced polymer-solute interactions.⁹ In addition, substantial increases in the glass transition temperatures and polymer decomposition temperatures were evident. With the inclusion of HFIP groups, the continuous use temperatures were shifted from 485 °C for the non-fluorinated polymers to 553 °C for the

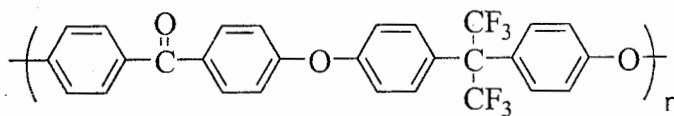


Figure 8. Poly(bisphenol AF ether ketone)

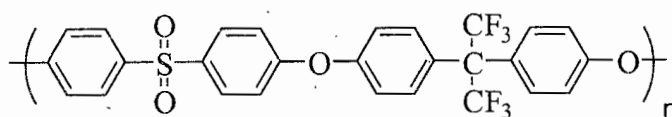


Figure 9. Poly(bisphenol AF ether sulfone)

fluorinated polymers.¹⁰ When compared to non-fluorinated poly(arylene ether ketone)s the HFIP analogues showed dramatic improvements in both oxidative stability and tensile strength.¹¹

Besides poly(ether)s, researcher have examined at fluorinating poly(urethane)s. Fluorinated poly(urethane)s (Figure 10) containing the HFIP group are largely used for surface coatings, medical products and as surface-enhancing treatments for textiles, leather and carpeting.¹² By creating a surface composed of closely packed trifluoromethyl groups, extremely low surface energies are produced, which are comparable to those of PTFE. Several resins synthesized from hexafluoroacetone and diisocyanates take advantage of this fact.¹³ Endcapping these polymers with perfluoroalkyl groups allows for the self assembly of these groups at the surface which in turn allows for minimal surface tension.¹⁴ The resins

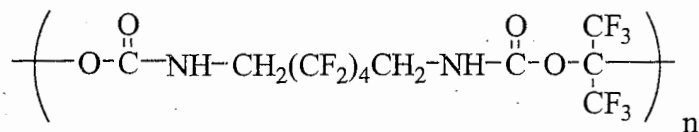


Figure 10. HFIP containing poly(urethane)

have excellent resistance to water, chemicals and corrosive agents and form durable fluorinated coatings, which act as protective barriers in bulk fuel tanks and on sea vessels.^{15,16}

Poly(ester)s and poly(acrylate)s such as the ones shown in Figure 11 and 12 also have benefited from the incorporation of HFIP. The poly(ester)s prepared with HFIP form clear, colorless films and have improved thermal stabilities with 10% weight losses ranging from 440-490 °C.¹⁷ These polymers are water repellent and have increased water contact angles of 95° compared to the non-fluorinated analogues which have a water contact angles of 85°.¹⁸ HFIP containing poly(acrylate)s show the same types of improvement. Low moisture absorption and improved film properties can be achieved when HFIP is incorporated into the non-fluorinated analogues.¹⁹ The water contact angles were recorded as high as 160°, which is remarkable when considering the contact angle of PTFE is only 108°.^{20,21} This phenomenon can be explained by examining the way the polymer backbone aligns at the surface. The fluorocarbon tails are projected into the air, minimizing the surface tension.²² These types of materials have been used in biomedical devices such as artificial prosthesis and dental materials.²³

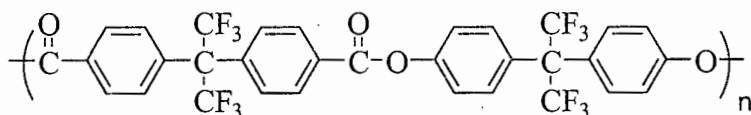


Figure 11. HFIP containing poly(ester)

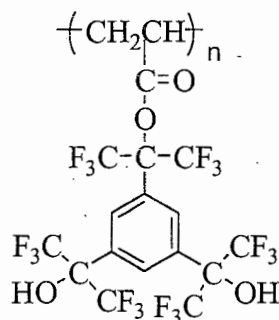


Figure 12. HFIP containing poly(acrylate)

Poly(imide)s (Figure 13) are another type of high performance polymer that has benefitted from the incorporation of HFIP. These robust high performance polymers are difficult to process; however, they are used in aerospace applications and in the microelectronics industry as optical fiber sheaths, fiber composites and gas separation membranes.²⁴ Due to their insolubility and intractability, formation of the finalized product is extremely difficult. The normal two-step polymerization is not trivial; the poly(amic acid) is produced and then subsequently dehydrated. Incorporation of HFIP has increased the

processability and solubility of the poly(imide)s while improving the polymer properties. Tough, flexible, transparent films with improved thermal properties are reported when hexafluoroisopropylidene diphthalic anhydride is condensed with a diamine.²⁵ HFIP decreased the coloration, the dielectric constants and the moisture absorption of the films.^{26,27} Thermal decomposition temperatures of these polymers reached well above 600 °C.^{28,29} In addition, the miscibility of poly(imide)s can be improved by including HFIP. This inclusion has resulted in fully miscible alloys.³⁰

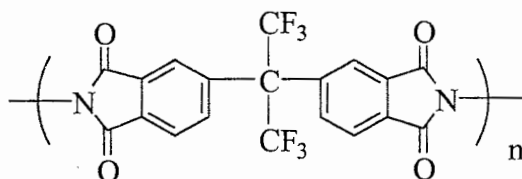
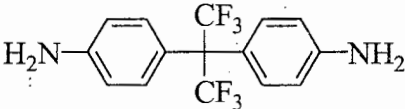
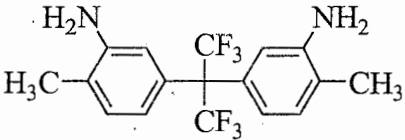
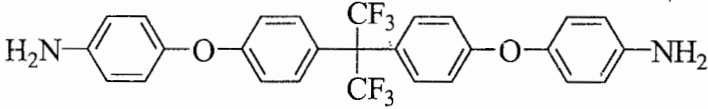
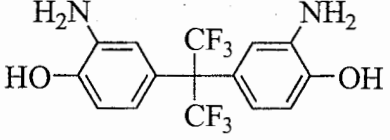
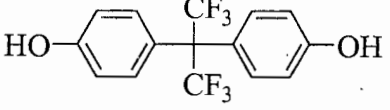
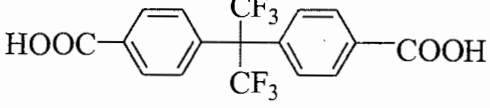
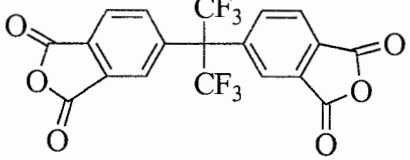


Figure 13. Poly(hexafluoropropanedipthalimido-1,4-phenylene)

The inclusion of hexafluoroisopropylidene linkages within a polymer backbone or from pendant groups continues to be an important method for improving polymer properties. Since HFIP's initial use in 1965, many polymers have been synthesized from monomers containing trifluoromethyl groups. Table 1 shows several different types of HFIP monomers that have been used in the synthesis of fluorinated materials. These monomers have two common functional groups: HFIP and benzene. Many of the monomers listed are commercially available and are prepared by Friedel-Crafts or Grignard condensation reactions.³¹ HFIP's ability to enhance polymer properties is quite interesting; however, its effects have not been recorded without the presence of other functional groups. The work in

Table 1. Commercially available 6F monomers

Structure	Name
	2,2-bis(4-aminophenyl)-hexafluoropropane
	2,2-bis(3-amino-4-methylphenyl)hexafluoropropane
	2,2-bis[4-(4-aminophenoxy)-phenyl]hexafluoropropane
	2,2-bis(3-amino-4-hydroxyphenyl)hexafluoropropane
	2,2-bis(4-hydroxyphenyl)-hexafluoropropane
	2,2-bis(4-carboxyphenyl)-hexafluoropropane
	4,4'-(hexafluoropropane)diphthalic anhydride

this thesis describes the efforts to produce polymers containing only hexafluoro-isopropylidene and phenyl groups. The results and properties are presented, along with the initial work done to prepare a crosslinkable polymer by incorporating acetylene groups into the backbone of the polymer

Thesis Organization

This thesis is divided into two main chapters. The first chapter contains experimental methods for the synthesis of the desired monomers and polymers, along with a description of the characterization methods. The second chapter discusses the results obtained from the work presented in this manuscript. This second chapter is divided into two sections of work. The first section details the results from the monomer synthesis. The second section details the results and characterization of the polymers synthesized.

The general conclusion chapter summarizes the results of this thesis and the potential applications of these materials, as well as the relevance of these novel polymers to the field of polymer science.

The appendices contain the data for the monomers and polymers discussed within this thesis.

The references are listed as a comprehensive listing of the works cited within this thesis.

EXPERIMENTAL

Materials

All reagents were purchased from Aldrich and used as received unless otherwise indicated. Dipyrityl and triphenylphosphine were purified by recrystallization from ethanol. Trimethylsilylacetylene, bis(trimethylsilyl)acetylene, DMF, THF, DMAc, and NMP were purified by distillation. All monomers synthesized were purified until their ^1H -NMR spectra corresponded to the expected structure and purity was greater than 99% by DSC melting point and HRMS.

Characterization

General. ^1H NMR and ^{13}C NMR were measured in CDCl_3 with a Bruker 400 MHz spectrometer. A Varian gas chromatograph fitted with a Finnigan Mat Magnum mass spectrometer was used for product identification and purity confirmation. High resolution mass spectrometry was performed with a Kratos MS50TC at a resolution (R) of 14,300 in electron impact (EI) mode with an electron beam energy of 70 eV. Monomer melting point temperatures were determined using a Perkin-Elmer Pyris 1 differential scanning calorimeter (DSC) at a heating rate of $10\text{ }^\circ\text{C}/\text{min}$. The UV-Vis absorption spectrum was obtained with a Shimadzu UV-2101PC UV-Vis scanning spectrophotometer. Elemental analysis of the monomers and polymers was performed using a Perkin-Elmer model 2400 Series II CHN/S instrument.

Thermal Analysis. Polymer glass transition temperatures were determined using a Perkin-Elmer Pyris 1 differential scanning calorimeter (DSC) at a heating rate of $20\text{ }^\circ\text{C}/\text{min}$

and a heating range of 25 °C to 350 °C, with nitrogen purge. Glass transition temperatures are reported as the inflection point of the change in heat capacity during the second heat. Thermogravimetric analyses (TGA) were performed on a Perkin-Elmer TGA with heating rates of 10 °C/min.

Molecular Weight Analysis. Molecular weights were determined by gel permeation chromatography (GPC) and multiple angle laser light scattering (MALLS) using a Waters gel permeation system coupled with a Wyatt miniDAWN. The chromatography system was equipped with three Waters styragel columns and measurements were made at 40 °C with THF as the solvent at a flow rate of 1.0 mL/min. Molecular weights (GPC) were calculated with a calibration plot constructed with polystyrene standards.

Morphology Analysis. Wide-angle X-ray diffraction (WAXD) experiments were conducted using a Phillips diffractometer. Diffraction data was collected in the range $10^\circ < 2\theta < 75^\circ$ with a step size of 0.05° (2θ) and a counting time of 10 seconds per step using Cu K α radiation. The contact angle was measured using a Ramé-Hart goniometer equipped with an image analysis attachment.

Gas Permeability Analysis. Pure gas permeabilities of the 6F polymer films were determined at 35 °C using the constant pressure/variable volume method. The gases used were hydrogen, helium, nitrogen, oxygen, methane, and carbon dioxide. The feed pressure was 50 psig except for methane (methane: 100 psig), and the permeate pressure was maintained at 0 psig [i.e., $p_2 - p_1 = 50$ psig = 3.4 atm, $p_2 - p_1 = 100$ psig = 6.8 atm (methane)]. The permeability coefficients are reported in Barrers, where 1 Barrer = 10^{-10} cm³(STP)cm/(cm²·s·cm Hg).

Polymer Fire Resistance. Heat release capacities of the polymer were determined using a Perkin-Elmer Pyris 7 TGA. The polymer samples were pyrolyzed under anaerobic conditions. Anaerobic pyrolysis and oxidative combustion of the pyrolysis gases occurred sequentially. The heat released by combustion was deduced from the oxygen depletion measurements of the flow stream.

Synthetic Procedures

2,2-Bis(4-chlorophenyl)hexafluoropropane. To a 250 mL round bottom flask equipped with a nitrogen inlet was added dichlorotriphenylphosphorane (35.7 g, 0.107 mol) and 4,4'-(hexafluoroisopropylidene)diphenol (18.1 g, 0.0536 mol). The flask was placed in a heating mantle, insulated with sand and heated to 350 °C for 4h. The reaction temperature was monitored with a thermocouple. The brown reaction mixture was cooled to room temperature and dissolved in 50 mL of methylene chloride. The resulting solution was eluted through a short basic aluminum oxide column using 300 mL of hexane as the eluting solvent. The product was distilled and 12.4 g (0.0332 mol, 67 %) of white solid formed: mp = 60 °C (DSC); ¹H-NMR: δ 7.35 (doublet, *J* = 8.7 Hz, 4H), 7.29 (doublet, *J* = 8.7 Hz, 4H); ¹³C-NMR; δ 135.89, 132.72, 131.73, 128.87, 124.12 (quartet, *J* = 1140 Hz), 64.55 (septet, *J* = 102 Hz). The theoretical weight percents are 48.29 % C and 2.14 % H. Elemental analysis showed 48.25 % C and 2.16 % H. Theoretical mass was calculated to be 371.99073 g/mol; high resolution mass spectrometry showed a measured mass of 371.99044 g/mol with a deviation of -0.78 ppm.

1,1-Bis(4-hydroxyphenyl)-2,2,2-trifluoro-1-phenylethane. To a three neck, 500 mL round bottom flask equipped with a water condenser, addition funnel, and nitrogen purge

was added phenol (37.7 g, 0.40 mol) and 1,1,1-trifluoroacetophenone (17.4 g, 0.10 mol). The round bottom flask was heated to 40 °C and trifluoromethyl-sulfonic acid (15.0 g, 0.10 mol) was added dropwise over a 30-minute period. The peach colored reaction mixture was poured into 500 mL of boiling water and left to stir for 8 hours. The crude product was filtered using a water aspirator and then purified by stirring in 300 mL of methylene chloride to give 30.0 g (0.087 mol, 87 %) of a white powder: mp = 232 °C (DSC); $^1\text{H-NMR}$: δ 6.74 (doublet, $J = 9$ Hz, 4H), 6.82 (doublet, $J = 9$ Hz, 4H), 7.05 (multiplet, 1H), 7.36 (multiplet, 4H), 9.62 (singlet, 1H); $^{13}\text{C-NMR}$: δ 156.75, 140.43, 130.53, 129.97, 129.96, 129.27, 128.21, 128.19 (quartet, $J = 1139$ Hz), 128.00, 114.86, 63.30 (quartet, $J = 93$ Hz). The theoretical weight percents are 69.76 % C and 4.39 % H. Elemental analysis showed 69.70 % C and 4.55 % H. Theoretical mass was calculated to be 344.10241 g/mol; high resolution mass spectrometry showed a measured mass of 344.10208 g/mol with a deviation of -0.97 ppm.

1,1-Bis(4-chlorophenyl)-2,2,2-trifluoro-1-phenylethane. To a 250 mL round bottom flask equipped with a nitrogen inlet was added dichlorotriphenylphosphorane (19.4 g, 0.0583 mol), and 1,1-bis(4-hydroxyphenyl)-2,2,2-trifluoro-1-phenylethane (18.1 g, 0.0536 mol). The flask was placed in a heating mantle, insulated with sand and heated to 350 °C for 4h. The reaction temperature was monitored with a thermocouple. The brown reaction mixture was cooled to room temperature and dissolved in 100 mL of methylene chloride. The resulting solution was eluted through a short basic aluminum oxide column using 400 mL of hexane as the eluting solvent. The product was distilled and 6.92 g (0.0182 mol, 45 %) of white solid formed: mp = 103 °C (DSC); $^1\text{H-NMR}$: δ 7.10 (multiplet, 8H), 7.35

(multiplet, 5H); ^{13}C -NMR; δ 139.45, 138.46, 134.34, 131.349, 130.25 (quartet, $J = 1140$ Hz), 129.94, 128.66, 128.462, 128.35, 64.66 (quartet, $J = 96$ Hz). The theoretical weight percents are 63.01 % C and 3.44 % H. Elemental analysis showed 61.54 % C and 3.81 % H. Theoretical mass was calculated to be 380.03464 g/mol; high resolution mass spectrometry showed a measured mass of 380.03389 g/mol with a deviation of -1.98 ppm.

2,2-Bis[[trifluoromethylsulfonyl]oxybenzene]hexafluoropropane. To a three neck, 500 mL round bottom flask equipped with a water condenser, addition funnel, and nitrogen purge was added 4,4'-(hexafluoroisopropylidene)diphenol (50.0 g, 0.148 mol) to 120 mL of dry pyridine and stirred for 1 hour. Trifluoromethylsulfonic anhydride (96.5 g, 0.342 mol) was slowly added dropwise over a 2 hour period. The crude product was filtered and washed with three 100mL portions of 10 % hydrochloric acid solution, two 100 mL portions of distilled water, and three 100 mL portions of 10 % sodium bicarbonate solution. The crude product was purified by recrystallization from ethanol to give 86.4 g (0.144 mol, 97 %) of white crystals: mp = 97°C (DSC); ^1H -NMR: δ 7.50 (d, $J = 8.7$ Hz, 4H), 7.36 (d, $J = 8.7$ Hz, 4H); ^{13}C -NMR; δ 149.94, 133.14, 132.25, 123.63 (quartet, $J = 1152$ Hz), 121.55, 118.72 (quartet, $J = 1152$ Hz), 64.04 (septet, $J = 103.5$ Hz). The theoretical weight percents are 34.01 % C and 1.34 % H. Elemental analysis showed 33.84 % C and 1.46 % H. Theoretical mass was calculated to be 600.99073 g/mol; high resolution mass spectrometry showed a measured mass of 600.99044 g/mol with a deviation of -0.78 ppm.

1,1-Bis[[trifluoromethylsulfonyl]oxybenzene]-2,2,2-trifluoro-1-phenylethane.

To a three neck, 500 mL round bottom flask equipped with a water condenser, addition funnel and nitrogen purge was added 2,2-bis(4-hydroxyphenyl)1,1,1-trifluoro-2-phenylethane (33.0 g, 0.096 mol) to 80 mL of dry pyridine and stirred for 1 hour.

Trifluoromethylsulfonic anhydride (62.2 g, 0.220 mol) was slowly added dropwise over a 2 hour period. The crude product was filtered and washed with three 100 mL portions of 10 % hydrochloric acid solution, two 100 mL portions of distilled water and three 100 mL portions of 10 % sodium bicarbonate solution. The crude product was purified by recrystallization from ethanol to give 47.2 g (0.079 mol, 83 %) of white crystals: mp = 90 °C (DSC); ¹H-NMR: δ 7.34 (multiplet, 3H), 7.25 (doublet, *J* = 9 Hz, 4H), 7.20 (doublet, *J* = 9 Hz, 4H), 7.04 (multiplet, 2H); ¹³C-NMR: δ 149.27, 140.05, 138.75, 132.06, 129.43, 128.92, 128.86, 127.53 (quartet, *J* = 1140 Hz, C-6), 121.45, 118.93 (quartet, *J* = 1276 Hz), 64.74 (quartet, *J* = 96.9 Hz). The theoretical weight percents are 43.43 % C and 2.15 % H. Elemental analysis showed 43.44 % C and 2.36 % H. Theoretical mass was calculated to be 608.000985 g/mol; high resolution mass spectrometry showed a measured mass of 608.0010618 g/mol with a deviation of 0.12 ppm.

2,2-Bis[[4-trimethylsilylacetylene]phenyl]hexafluoropropane. To a three neck, 500 mL round bottom flask equipped with a water condenser and nitrogen purge was added 2,2-bis[[trifluoromethylsulfonyl]oxybenzene]hexafluoropropane (6.0 g, 0.010 mol), trimethylsilylacetylene (7.4 g, 0.025 mol), tetrakis(triphenylphosphine)palladium (1.7 g, 0.0005 mol), and copper (I) iodide (0.3 g, 0.001 mol) to 60 mL of dry pyridine and stirred for 24 hours at 80 °C. The reaction was quenched in 400 mL of 10% HCl/methanol solution, the solids were collected and dissolved into hexane. The crude product was washed with two 100 mL portions of distilled water, three 100 mL portions of 10 % sodium bicarbonate solution, one 100 mL portion of saturated sodium chloride solution and rinsed with one 100 mL portion of distilled water. The crude product was purified by flash chromatography using hexane as the eluting solvent to give 1.0 g (0.002 mol, 20 %) of a white solid: mp = 50 °C; ¹H-NMR: δ

7.45 (doublet, $J = 9$ Hz, 4H), 7.28 (doublet, $J = 9$ Hz, 4H), 0.25 (singlet, 18H); ^{13}C -NMR; δ 133.34, 132.83, 131.91, 130.22, 124.44, 103.89, 96.65, 0.44. The theoretical weight percents are 60.46 % C and 5.28 % H. Elemental analysis showed 60.463% C and 5.52 % H. Theoretical mass was calculated to be 496.14846 g/mol; high resolution mass spectrometry showed a measured mass of 496.14793 g/mol with a deviation of 1.5 ppm.

2,2-Bis[[4-acetylene]phenyl]hexafluoropropane. To a one neck, 500 mL round bottom flask equipped with nitrogen purge was added 2,2-bis[[4-trimethylsilyl=acetylene]phenyl]hexafluoropropane (1.0 g, 0.020 mol) and potassium carbonate (1.0 g, 0.025 mol) to a mixture of 50 mL of tetrahydrofuran and 100 mL of methanol and stirred for 24 hours at room temperature. The reaction was quenched in 400 mL of distilled water and the crude product was extracted with hexane. The crude product was purified by flash chromatography using hexane as the eluting solvent to give 0.7 g (0.0018 mol, 90%) of a clear liquid: ^1H -NMR: δ 7.49 (doublet, $J = 9$ Hz, 4H), 7.33 (d, $J = 9$ Hz, 4H), 3.15 (singlet, 2H); ^{13}C -NMR; δ 149.94, 138.90, 132.25, 123.63 (quartet, $J = 1152$ Hz), 118.72 (quartet, $J = 1152$ Hz), 64.04 (septet, $J = 103.5$ Hz). The theoretical weight percents are 64.78 % C and 2.86 % H. Elemental analysis showed 64.71 % C and 3.73 % H. Theoretical mass was calculated to be 352.06867 g/mol; high resolution mass spectrometry showed a measured mass of 352.069310 g/mol with a deviation of 1.8 ppm.

Poly[[1,1'-biphenyl]-4,4'-diyl[2,2,2-trifluoro-1-(trifluoromethyl)ethylidene]]. To a three-necked 250 mL pear-shaped flask equipped with an overhead stirrer was added zinc (2.17 g, 0.0332 mol), nickel chloride (0.104g, 0.000803 mol), triphenylphosphine (2.8 g, 0.0107 mol), and dipyridyl (0.1253 g, 0.000803 mol). *N,N*-Dimethylformamide (10 mL) was added via syringe and the mixture was stirred at 90 °C until a deep red-brown color was

observed. At that time, 2,2-bis(*p*-chlorophenyl)hexafluoropropane (4.00 g, 0.0107 mol) was added. The reaction continued at 90 °C for 72 hours. The catalyst was quenched by pouring the reaction mixture into 400 mL of 25 % HCl/methanol solution and stirred overnight. The polymer was filtered and rinsed with a 10 % sodium bicarbonate solution, dissolved in 30 mL of chloroform and reprecipitated in 400 mL of methanol. The polymerization gave 95 % yield of a white powder. ¹H-NMR: δ 7.62 (d, *J* = 8.1 Hz, 4H), 7.50 (d, *J* = 8.1 Hz, 4H); ¹³C-NMR: δ 140.51 (C-4), 133.00 (C-1), 130.84 (C-3), 126.94 (C-2), 124.28 (quartet, *J* = 1134 Hz, C-6), 64.41 (septet, *J* = 100.8 Hz, C-5). The theoretical weight percents are 59.61 % C and 2.67 % H. Elemental analysis showed 59.38 % C and 2.59 % H.

Poly[biphenyl-4,4'-diyl(1-phenyl-2,2,2-trifluoroethane-1,1-diyl)]. To a three-necked 250 mL pear-shaped flask equipped with an overhead stirrer was added zinc (2.12 g, 32.5 mmol), nickel chloride (0.102g, 0.788 mmol), triphenylphosphine (2.75 g, 10.5 mmol), and dipyridyl (0.1230 g, 0.788 mmol). *N,N*-Dimethylformamide (10 mL) was added via syringe and the mixture was stirred at 90 °C until a deep red-brown color was observed. At that time, 2,2-bis(4-chlorophenyl)1,1,1-trifluoro-2-phenylethane (4.00g, 10.5 mmol) was added. The reaction continued at 90 °C for 72 hours. The catalyst was quenched by pouring the reaction mixture into 400 mL of 25 % HCl/methanol solution and stirred overnight. The polymer was filtered and rinsed with a 10 % sodium bicarbonate solution, dissolved in 30 mL of chloroform and reprecipitated in 400 mL of methanol. The polymerization gave 93 % yield of a white powder. ¹H-NMR: δ 7.34 (m, 3H), 7.20 (d, *J* = 9 Hz, 4H), 7.25 (d, *J* = 9 Hz, 4H), 7.04 (m, 2H); ¹³C-NMR; δ 149.27, 140.05, 138.75, 132.06, 129.76, 121.45, 118.93

(quartet, $J = 1276$ Hz), 64.74 (quartet, $J = 96.9$ Hz). The theoretical weight percents are 48.29 % C and 2.14 % H. Elemental analysis showed 48.25 % C and 2.16 % H.

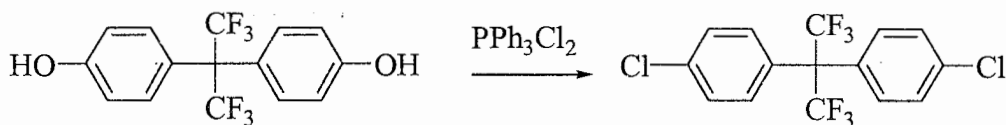
Poly(2,2-Bis[[4-acetylene]phenyl]hexafluoropropane). To a one neck, 250 mL round bottom flask equipped with oxygen purge was added 2,2-bis[[4-acetylene]phenyl]hexafluoropropane (0.44 g, 0.0013 mol) and cupric acetate (1.45 g, 0.008 mol) to 5 mL of tetrahydrofuran and 50 mL of pyridine and stirred for 72 hours at 80 °C. The catalyst was quenched by pouring the reaction mixture into 400 mL of 25 % HCl/methanol solution and stirred overnight. The polymer was filtered and rinsed with a 10 % sodium bicarbonate solution. The polymerization gave 99 % yield of a brown-green powder. $^1\text{H-NMR}$: δ 7.54 (doublet, $J = 8.4\text{Hz}$, 4H), 7.36 (doublet, $J = 8.4$ Hz, 4H); $^{13}\text{C-NMR}$: δ 140.51 (C-4), 133.00 (C-1), 130.84 (C-3), 126.94 (C-2), 124.28 (quartet, $J = 1134$ Hz, C-6), 64.41 (septet, $J = 100.8$ Hz, C-5). The theoretical weight percents are 64.78 % C and 2.86 % H. Elemental analysis showed 58.97 % C and 3.07 % H.

RESULTS AND DISCUSSION

Monomer Synthesis

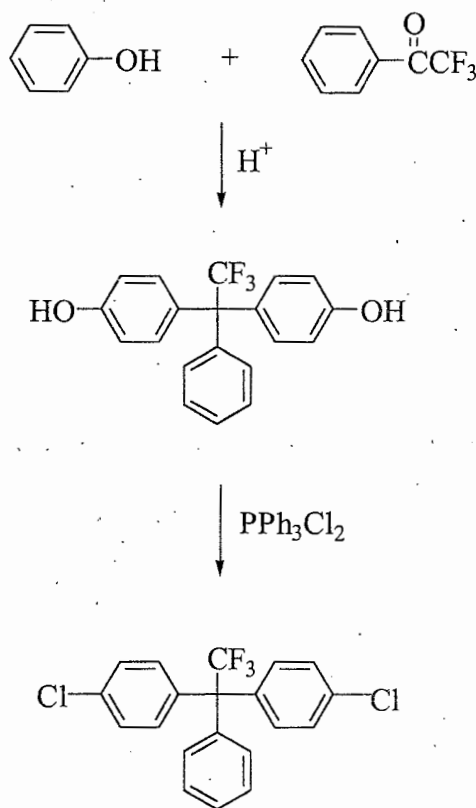
2,2-Bis(4-chlorophenyl)hexafluoropropane (6F monomer). The 6F monomer was selected because of the enhanced properties expected upon incorporation of fluorine into the resulting polymer. In addition, the resulting polymer structure would contain only HFIP and benzene groups. This would allow for the study of a unique polymer structure without the presence of other functionalities. The 6F monomer was prepared according to a previous patent which described the nucleophilic substitution reaction of dibromotriphenylphosphorane and 4,4'-(hexafluoroisopropylidene)diphenol, the synthesis is shown in Scheme 1.³²

The 6F monomer was soluble in hexane, chloroform, acetone, tetrahydrofuran, methylene chloride, *N,N*-dimethylformamide, *N,N*-dimethylacetamide, dimethylsulfoxide, methanol, and partially soluble in ethanol. Due to the monomer's high solubility, recrystallization was difficult. Therefore, it was further purified by distillation to insure polymer grade monomer. It was made with a 67 % yield and exhibited a sharp melting point at 60 °C. High resolution mass spectra and elemental analysis data were used to confirm the purity and chemical composition of 2,2-bis(4-chlorophenyl)hexafluoropropane.



Scheme 1. Synthesis of 2,2-bis(4-chlorophenyl)hexafluoropropane

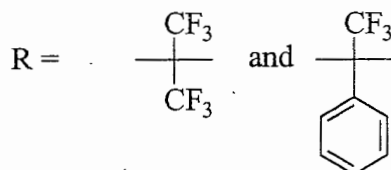
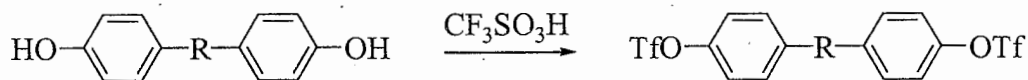
1,1-Bis(4-chlorophenyl)-2,2,2-trifluoro-1-phenylethane (3F monomer). The 3F monomer was designed as a comparison between its trifluorinated system and the hexafluorinated system of the HFIP group. A two step synthetic process was used to prepare the 3F monomer, shown in Scheme 2. 1,1,1-Trifluoroacetophenone was condensed with phenol in the presence of triflic acid; the product was then chlorinated by using the same synthetic procedure as described in the 6F monomer synthesis.



Scheme 2. Synthesis of 1,1-bis(4-chlorophenyl)-2,2,2-trifluoro-1-phenylethane

The 3F monomer was soluble in hexane, chloroform, acetone, tetrahydrofuran, methylene chloride, *N,N*-dimethylformamide, *N,N*-dimethylacetamide, dimethylsulfoxide, methanol, and partially soluble in ethanol. It was also purified by distillation to insure polymer grade monomer. The 3F monomer was made with a 45 % yield and exhibited a sharp melting point at 103 °C. High resolution mass spectra and elemental analysis data were used to confirm the purity and chemical composition of 1,1-bis(4-chlorophenyl)-2,2,2-trifluoro-1-phenylethane.

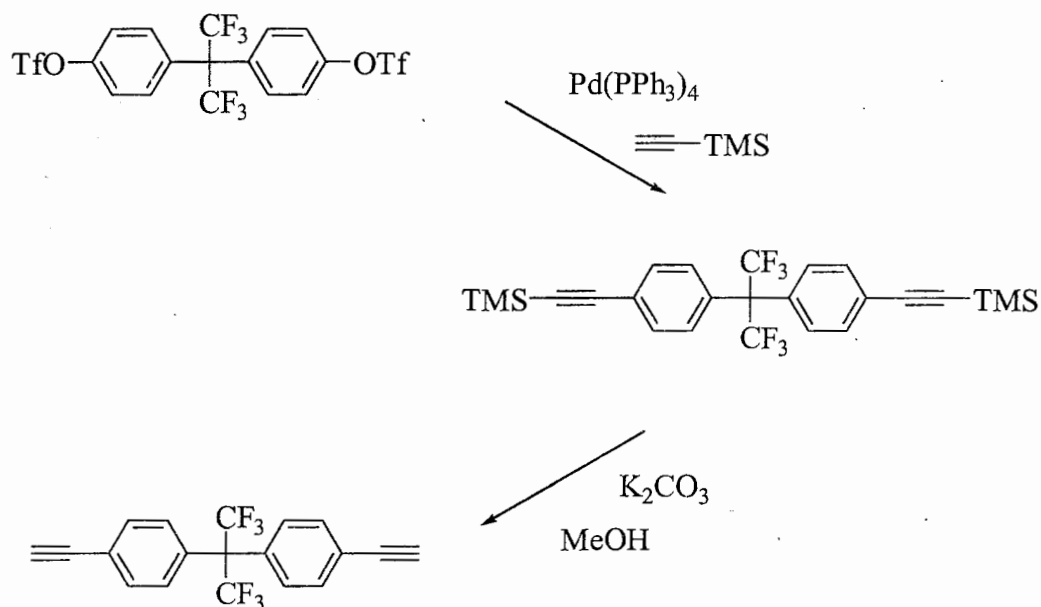
2,2-Bis[[trifluoromethylsulfonyl]oxybenzene]hexafluoropropane (6F triflate) and 1,1-bis[[trifluoromethylsulfonyl]oxybenzene]-2,2,2-trifluoro-1-phenylethane (3F triflate). The two monomers were synthesized for their use in a palladium catalyzed coupling reaction. They were prepared according to the standard reactions conditions used to synthesize triflates. The synthesis is shown in Scheme 3. The 6F and 3F triflates were soluble in hexane, chloroform, acetone, tetrahydrofuran, methylene chloride, *N,N*-dimethylformamide, *N,N*-dimethylacetamide, dimethylsulfoxide, methanol and ethanol. They were purified by recrystallization from ethanol to insure polymer grade monomer. The 6F triflate was synthesized with a 97 % yield and exhibited a sharp melting point at 97 °C. The 3F monomer was made with an 83 % yield and exhibited a sharp melting point at 90 °C. High resolution mass spectra and elemental analysis data were used to confirm the purity and chemical compositions of 2,2-bis[[trifluoromethylsulfonyl]oxybenzene]hexafluoropropane and 1,1-bis[[trifluoromethylsulfonyl]oxybenzene]-2,2,2-trifluoro-1-phenylethane.



Scheme 3. Synthesis of 2,2-bis[[trifluoromethylsulfonyl]oxybenzene]hexafluoropropane and 1,1-bis[[trifluoromethylsulfonyl]oxybenzene]-2,2,2-trifluoro-1-phenylethane

2,2-Bis[[4-trimethylsilylacetylene]phenyl]hexafluoropropane and 2,2-Bis[[4-acetylene]phenyl]hexafluoropropane. A two step synthetic procedure was used to prepare the acetylene containing 6F monomer. The resulting monomer was designed to be used in a copper coupling polymerization, which ultimately could produce a crosslinkable polymer. The monomer was prepared according to the standard reactions conditions used in a Sonogashira-Hagihara coupling; the synthesis is shown in Scheme 4.³³ Both, the protected and deprotected monomer were soluble in hexane, chloroform, acetone, tetrahydrofuran, methylene chloride, *N,N*-dimethylformamide, *N,N*-dimethylacetamide, dimethylsulfoxide, methanol and ethanol. The monomers were purified by flash column chromatography to insure polymer grade monomer. The protected 6F entity was synthesized with a 20 % yield, the deprotected 6F monomer was made with a 99 % yield and exhibited a sharp melting point

at 90 °C. High resolution mass spectra and elemental analysis data were used to confirm the purity and chemical compositions of both 2,2-Bis[[4-trimethylsilylacetylene]phenyl]-hexafluoropropane and 2,2-Bis[[4-acetylene]phenyl]hexafluoropropane.

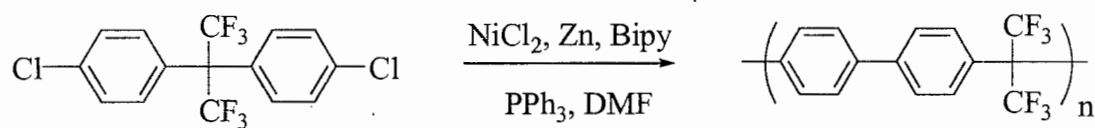


Scheme 4. Synthesis of 2,2-bis[[4-acetylene]phenyl]hexafluoropropane.

Polymer Synthesis

Poly[[1,1'-biphenyl]-4,4'-diyl[2,2,2-trifluoro-1-(trifluoromethyl)ethylidene]] (6F polymer). The polymerization reactions used to prepare the 6F polymer utilized a procedure first reported by Colon *et al.*³⁴ Reaction conditions for the polymerization were

optimized by varying the solvent, solvent volume, reaction time, temperature, and catalyst ratio. Table 2 shows the effect of temperature on the polymerization reaction. A range of temperatures were used and the highest molecular weight was achieved at 90 °C. Catalyst ratios were varied and the results are shown in Table 3. It was found that when a molar equivalent of triphenylphosphine to monomer was added, the best results were obtained. In addition, excess zinc in the molar ratio of 3.1:1 to monomer also improved the molecular weight. Only when *N,N*-dimethylformamide and a one molar monomer concentration were used could high molecular weight be obtained (Tables 4 and 5). The reaction time had the greatest effect on the polymerization. Particularly, a long reaction time of 72 hours produced the highest molecular weight (Table 6). Furthermore, excessively pure and dry reagents were needed to insure high molecular weight polymer could be synthesized using the optimized conditions. The polymerization reaction is shown in Scheme 5.



Scheme 5. Polymerization of the 6F monomer

Polymer characterization

Surprisingly, the 6F polymer was completely soluble at room temperature in a number of common organic solvents such as chloroform, acetone, tetrahydrofuran,

Table 2. Effect of reaction temperature on the 6F monomer polymerization^a

Entry	Time (hr)	Temperature (°C)	$\langle M_n^b \rangle$	$\langle M_w^b \rangle$
1	24	55	4,300	6,860
2	24	80	7,212	11,400
3	24	90	8,876	12,877
4	24	115	3,600	6,160

^a Molar ratios of catalyst system: monomer 1, NiCl₂ 0.075, Zn 3.1, PPh₃ 1, Bipy 0.075. Polymerization run in 10mL of DMAc. ^b Determined by gel permeation chromatograph (polystyrene standards).

Table 3. Effect of amount of catalyst on the 6F monomer polymerization^a

Entry	NiCl ₂	Zn	PPh ₃	Bipy	$\langle M_n^b \rangle$	$\langle M_w^b \rangle$
5 ^c	0.02	3.1	0.4	0.1	1,160	1,980
6	0.20	3.1	1	0.075	1,300	2,150
7	0.075	6	1	0.075	9,420	13,260
8	0.075	3.1	2	0.075	7,500	11,770
9 ^d	0.075	3.1	1	0.075	7,800	15,400

^a Polymerization run in 10mL of DMAc for 24 hours. ^b Determined by gel permeation chromatograph (polystyrene standards). ^c Catalyst ratio's published in *J. Polym. Sci., Part A: Polym. Chem.* **1998**, 36, 2611. ^d Catalyst ratio's published in *Macromolecules* **1998**, 31, 6769.

Table 4. Effect of reaction solvent on the 6F monomer polymerization^a

Reaction	Solvent	Temperature (°C)	$\langle M_n^b \rangle$	$\langle M_w^b \rangle$
10	NMP	55	4,170	6,708
11	THF	60	4,258	6,900
12	DMAc	90	7,908	5,200
13	DMF	90	13,400	21,800

^a Molar ratios of catalyst system: monomer 1, NiCl₂ 0.075, Zn 3.1, PPh₃ 1, Bipy 0.075. 24 hour polymerization time. ^b Determined by gel permeation chromatograph (polystyrene standards).

Table 5. Effect of solvent concentration on the 6F monomer polymerization.^a

Reaction	Solvent	Concentration (M)	$\langle M_n^b \rangle$	$\langle M_w^b \rangle$
14	DMF	0.01	---	---
15	DMF	0.5	2,350	7,400
16	DMF	1.0	9,440	15,000
17	DMF	2.0	6,200	12,670

^a Molar ratios of catalyst system: monomer 1, NiCl₂ 0.075, Zn 3.1, PPh₃ 1, Bipy 0.075. 24 hour polymerization time. ^b Determined by gel permeation chromatograph (polystyrene standards).

Table 6. Effect of reaction time on the 6F monomer polymerization^a

Entry	Time (hr)	Temperature (°C)	$\langle M_n \rangle^b$	$\langle M_w \rangle^b$
18	4	90	2,786	5,840
19	8	90	4,160	6,300
20	12	90	5,940	9,050
21	16	90	7,850	11,760
22	18	90	9,400	6,170
23	24	90	9,800	11,760
24	28	90	10,600	20,200
25	32	90	11,800	20,800
26	36	90	12,600	21,300
27	42	90	13,900	22,700
28	56	90	16,400	24,600
29	72	90	19,200	31,020

^a Molar ratios of catalyst system: monomer 1, NiCl₂ 0.075, Zn 3.1, PPh₃ 1, Bipy 0.075. Polymerization run in 10mL of DMF (1M). ^b Determined by gel permeation chromatograph (polystyrene standards).

methylene chloride, *N,N*-dimethylformamide; it is insoluble in hexane, methanol, and ethanol. It was synthesized in a 95 % yield. The 6F polymer was white with a λ_{max} value of 254.8 nm in a chloroform solution, and no absorption occurs above 340 nm. See Figure 14 for the UV-vis trace.

The 6F polymer had a number average molecular weight of 19.2×10^3 g/mol by GPC and 27.5×10^3 g/mol by MALLS ($dn/dc = 0.075$ ml/g in THF at 40 °C). The degree of

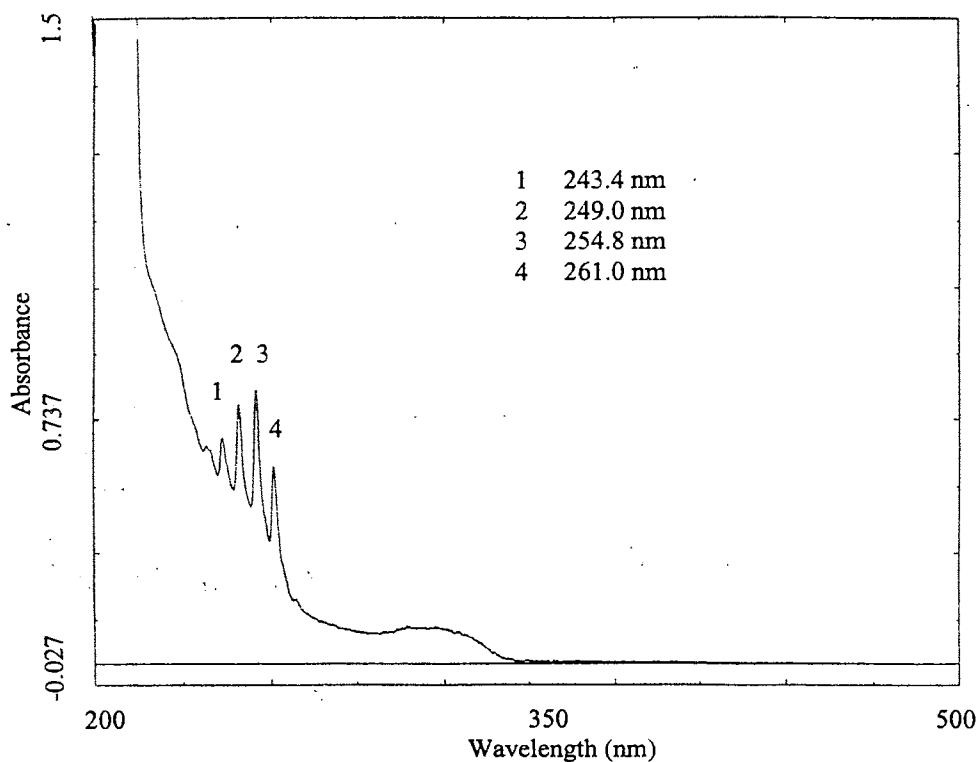


Figure 14. UV-vis trace of the 6F polymer

polymerization (DP) determined by light scattering was 91. This is in good agreement with the DP calculated from end group analysis by proton NMR, which was 95. Since the GPC data reflects the hydrodynamic volume based on polystyrene standards, the MALLS data more accurately reflects the molecular weight of the 6F polymer. This was evident from the DP calculated from the proton NMR. The GPC and MALLS chromatograms are shown in Figure 15. Previously in a series of poly(2,5-benzophenone)s prepared, the Sheares' group observed the opposite trend in molecular weights. The poly(2,5-benzophenone)s had lower molecular weight values calculated by MALLS than by GPC.³⁵ The hydrodynamic volume for such rigid rod polymers probably influences the molecular weight correlations resulting

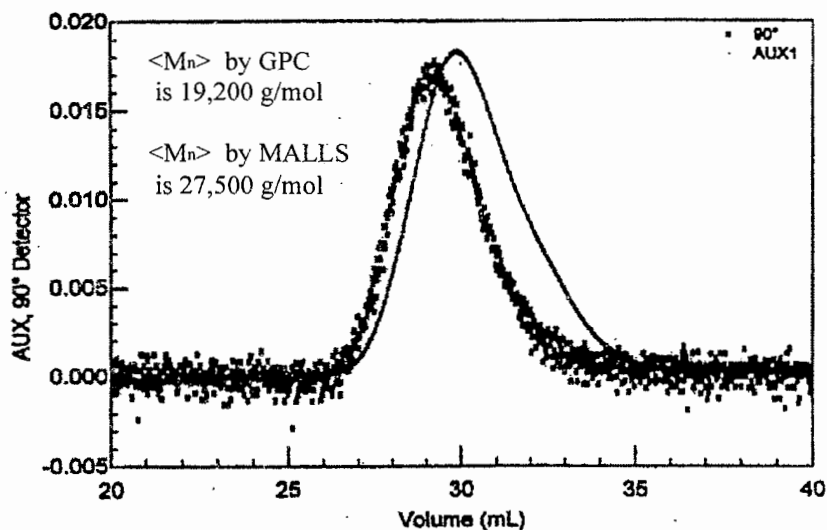


Figure 15. GPC and MALLS Chromatograms of the 6F polymer

in a large deviation between the two methods. With the HFIP group present within the polymer backbone the rigidity is broken up, which allows for a better correlation between the DPs calculated by MALLS and NMR. The 6F polymer had a polydispersity index of 1.61 by GPC and 1.25 by MALLS. The deviation from the theoretical value of 2.0 is consistent with other polymers prepared by Ni(0) catalysis and may be due to the loss of some lower molecular weight polymer during workup.³⁵⁻³⁹

The 6F polymer had a glass transition temperature (T_g) of 255 °C, shown in Figure 16. Poly(arylene ether sulfone)s with the same HFIP component had substantially lower glass transition temperatures ($T_g = 180$ °C), presumably due to the flexible ether linkages. The 6F polymer exhibited no evidence of crystallinity by DSC or by wide-angle

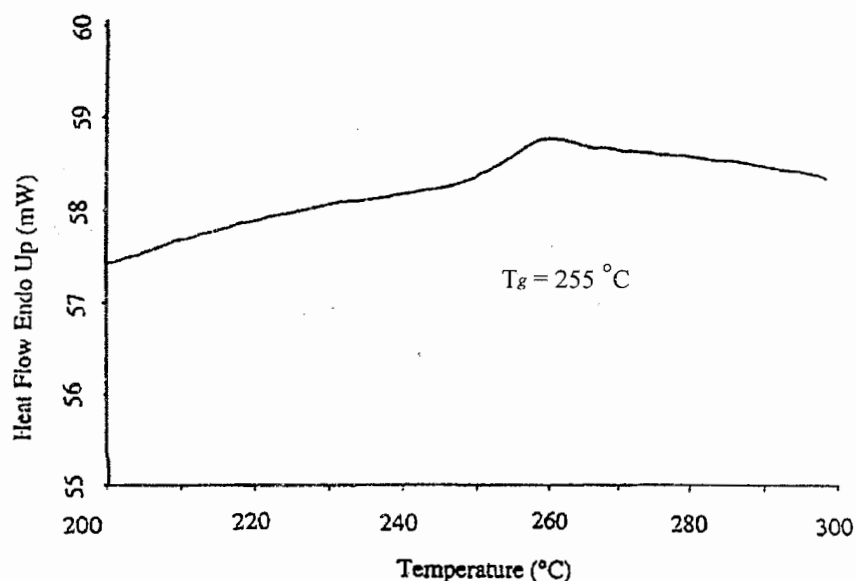


Figure 16. DSC thermogram of 6F polymer

X-ray diffraction (Figure 17). The WAXD pattern showed an amorphous halo. There are two peaks at 2θ between 10 - 20° . In poly(ethylene terephthalate) PET, a double peak in the amorphous halo was also observed. Murthy *et al.* separated the amorphous halo of PET into two peaks.⁴⁰ One peak was ascribed to interchain spacing normal to the plane of aligned aromatic rings. The other peak was attributed to the interchain spacing in the plane of the aligned aromatic rings.⁴⁰ It is possible that the same explanation may be applied to the two peaks observed in the 6F polymer; however, extensive TEM experiments would be needed.

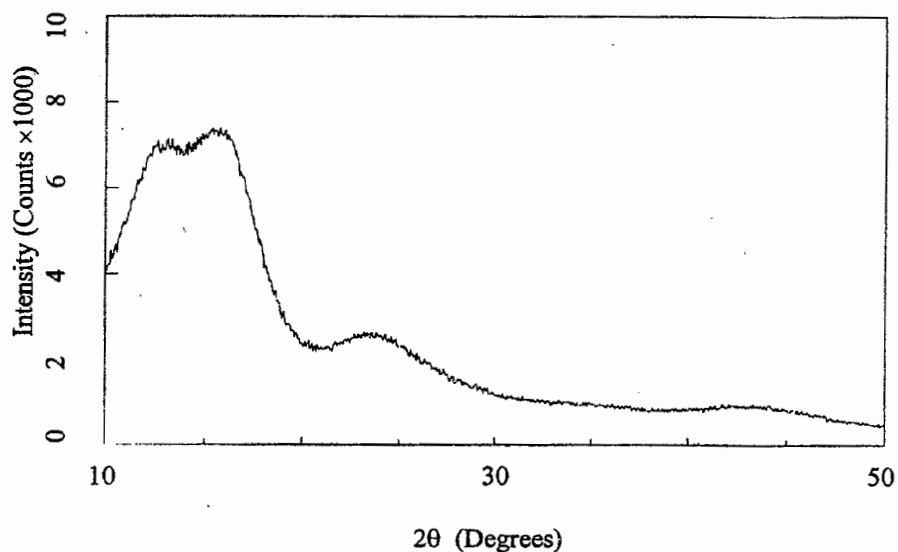


Figure 17. WAXD of 6F polymer

Thermogravimetric analysis, Figure 18, showed 5% weight loss values at 515 °C for both nitrogen and air. It also showed 10% weight loss values at 533 °C in nitrogen and 535 °C in air. The thermal stability of the 6F polymer was comparable to a polyimide based on 2,2'-bis(trifluoromethyl)-4,4'-dianimobiphenyl and 1,4-bis(trifluoromethyl)-2,3,5,6-benzene tetracarboxylic dianhydrides.⁴¹ This particular polyimide had a T_g of 332 °C and a 5% weight loss value of 569 °C in nitrogen and 549 °C in air. The new 6F polymer had only slightly lower 10% weight loss numbers. However, the new 6F polymer had better solubility than these polyimides, which would aid in the processability of the polymer.

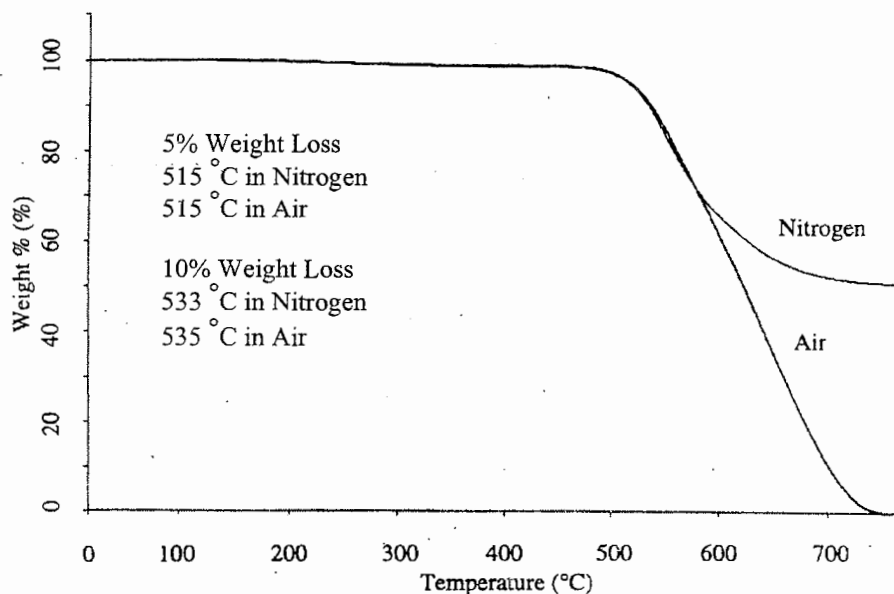


Figure 18. TGA thermogram of the 6F polymer

Isothermal gravimetric analysis was performed on the high molecular weight 6F polymer and the data collected is shown in Table 7. It is important to note that at 300 °C and 350 °C, virtually no weight loss occurs. After 100 hours at 400 °C, only 0.03% of the initial weight is lost. These numbers indicate that the polymer's continuous use temperature would approach 350 °C, making it useful as a high performance polymer.

Table 7. Isothermal gravimetric analysis of the 6F polymer^a

Temperature (°C)	Initial Weight (mg)	Final Weight (mg)	Wt loss/hr (%)
300	12.059	12.059	0
350	4.948	4.948	~0
400	7.722	7.484	0.031
450	6.526	4.229	0.35

^a Data collected for 100 hours in nitrogen at indicated temperature.

The 6F polymer has a heat release capacity of 25 J/g-K, a total heat of combustion of volatiles of 3.3 kJ/g-solid, and a pyrolysis residue of 50.4% at 650 °C. Table 8 lists several polymers' flammability rankings released by the Federal Aviation Administration. The table ranks the fire resistivity of the polymers: flammability decreases down the table. The 6F polymer is comparable to other high performance polymers with respect to microscale heat release capacity.⁴² The fire resistant values for the new 6F material surpass the values for RADEL R[®] (polyphenylsulfone), and are more comparable to TORLON[®] (polyamideimide). Although TORLON[®] exceeds the char yields of PDTFE, PDTFE does surpass the FAA char

yield requirement of 45%. The FAA's future goal is to find a material with a heat release capacity of 8 J/g-K, a total heat of combustion of volatiles of 1 kJ/g-solid, and a pyrolysis residue of 45% at 650 °C. The 6F polymer has slightly higher values for the heat release capacity and total heat of combustion for the FAA's future goals. However, based on existing correlations it would be expected to meet or exceeds the FAA's current requirement for flaming heat release rate when tested according to FAR 25.853(a-1) Heat Release Rate Test for Aircraft Cabin Materials.⁴³

Table 8. 6F Polymer Flammability^a

Polymer	Heat Release Capacity (J/g-K)	Total Heat Released (kJ/g)	Char Yield (%)
Nylon 6-6	348	32	0
PMMA	297	25	0
KEVLAR [®]	170	14	35
RADEL R [®]	92	12	52
TORLON [®]	28	6	64
New 6F Polymer	25	3	50
KAPTON [®]	14	4	66
PBO	3	1	97

^a Data taken from the FAA Data Base on Fire Resistant Materials.

Water absorption data and contact angles were also measured on the 6F polymer. After 100 hours submerged in distilled water, films showed virtually no increase in weight at temperatures of 25, 35, 45, and 55 °C. At 8, 12 and 24 hours in boiling water, the films showed no detectable changes in appearance or weight. The 6F polymer structure contained

no hydrogen bonding sites that made it hydrophilic. With the highly nonpolar aromatic rings and the hydrophobic fluorine atoms, the films did not absorb significant amounts of moisture. The contact angle was measured immediately after a drop of water was placed on a 6F polymer film, it was 73.9 °. Although, the polymer film had perfluoroalkyl groups present, they were not end groups. This diminished the number of CF_3 groups that could aggregate on the surface of the film, keeping the contact angle small.

The dielectric constant for the 6F polymer was 2.56. This number is extremely low and indicates that the 6F polymer has potential use as an inner layer dielectric. The highly hydrophobic nature of the new 6F polymer insures that the dielectric constant would not be significantly influenced by humidity, making it even more desirable as an inner layer dielectric. Comparisons can be made between the 6F polymer's dielectric constant and the dielectric constants of several poly(imide)s. Recently, several fluorinated poly(imide)s showed higher dielectric constants, ranging from 2.6 to 3.2.⁴⁴ However, moisture absorption was cited as a problem. Once the polyimides absorbed moisture the dielectric constants increased to 2.8 to 3.6. Even though the poly(imide)s initially had lower dielectric constants, moisture would have effected those values, ultimately limiting their use as inner layer dielectrics.

Films of this polymer prepared from a chloroform solution were colorless, transparent, and flexible. The fractional free volume (FFV) was estimated to be 0.29 using an average film density of 1.24 g/cm^3 .⁴⁵ This FFV value is much higher than that of low permeability, conventional, glassy polymers such as polysulfone (0.16) and polycarbonate (0.17).⁴⁶ The FFV is the same as that of highly permeable glassy polymers such as poly(1-trimethylsilyl-1-propyne) [PTMSP] (0.29), and is similar to the FFV values of random

copolymers of tetrafluoroethylene [TFE] and 2,2-bistrifluoromethyl-4,5-difluoro-1,3-dioxole [PDD] (0.30 for PPD 87 mol % and 0.28 PPD 65 mol %).⁴⁷ These numbers are shown below in table 9.

Table 10 summarizes permeability coefficients of this polymer film to various gases at 35 °C. The permeability coefficient to oxygen was 120 Barrers, which is very high relative to conventional glassy, aromatic polymers. The O₂ permeability of PDTFE is similar to that of other very high free volume, glassy, fluorinated polymers. For example, poly(TFE-co-PDD) (PDD content = 65 mol %, DuPont AF1600) has an O₂ permeability of 365 Barrers. These values are lower than those of the most permeable fluoropolymer known, poly(TFE-co-PDD) (PDD content = 87 mol %: DuPont AF2400), which has an O₂ permeability

Table 9. Fractional Free Volume (FFV)^a of Selected Glassy Polymers

Polymer	FFV
PTMSP	0.290
6F Polymer	0.290
Poly(sulfone)	0.159
Poly(carbonate)	0.166
PET	0.152

^a *J. polym. Sci. Pt. B. Polym. Phys.* **1996**, *34*, 2209.

Table 10. Gas Permeability of the 6F polymer

Gases	Permeability Coefficients [Barrers] ^a
He	390
H ₂	470
CO ₂	470
O ₂	120
N ₂	41
CH ₄	34

^a 1 [Barrer] = $1 \times 10^{-10} \text{ cm}^3(\text{STP})\text{cm}/(\text{cm}^2\text{-s-cm Hg})$

Film thickness: 30.3 μm

coefficient of 1,380 Barrers. Moreover, the permeability is substantially lower than that of the most permeable polymer known, PTMSP, which has an O₂ permeability of 9,860 Barrers.⁴⁸⁻⁴⁹ These results are shown in Table 11. Figure 19 presents gas permeability coefficients as a function of kinetic diameter, a parameter frequently used to characterize relative penetrant size for light gases.⁵⁰ The permeability coefficients of He, H₂, and CO₂ were rather similar, independent of gas size, and higher than those of the other gases considered. The permeability of this polymer to O₂, N₂, and CH₄ decreased with increasing penetrant size.

The permeability coefficient of gases in polymers is typically expressed as the product of gas solubility and gas diffusivity in the polymer⁵¹:

$$P_A = S_A \times D_A$$

Where P_A is the permeability coefficient of gas A, S_A is the solubility coefficient of gas A in the polymer, and D_A is the effective, concentration averaged diffusion coefficient of the gas in the polymer. As a result, both solubility and diffusivity contribute to overall permeability characteristics. The ability of a polymer to separate two gases depends on the polymer being more permeable to one gas than the other.

Table 11. Permeability coefficients for oxygen in various polymers^a

Polymers	$P(O_2) \times 10^{10}$	$P(O_2)/P(N_2)$
PTMSP	10,000	1.5
Poly(dimethylsiloxane)	600	2.0
6F Polymers	121	3.0
Poly(4-methyl-1-pentene)	32	4.0
Natural Rubber	18	5.0
Ethyl cellulose	15	3.4
Poly(carbonate)	1	4.7
Poly(propylene)	0.8	4.3
Poly(vinylidene chloride)	0.005	5.0

^a *The Physical Chemistry of Membranes* Marcel Dekker, 1992, 13. Units are in $\text{cm}^3(\text{STP})\text{cm}/(\text{cm}^2\text{-s-cm Hg})$

The permeability coefficient of carbon dioxide in this polymer was essentially the same as that of hydrogen, despite the larger size of CO_2 . This result is unusual. Typically, polymers that are as permeable or more permeable to CO_2 than to H_2 are either rubbery polymers or ultrahigh free volume, disubstituted polyacetylenes, such as PTMSP.⁵²⁻⁵⁴ High carbon dioxide solubility (relative to other gases) has been reported for other organic polymers having high concentrations of accessible fluorine groups. Examples include organopolysiloxanes bearing fluorinated side chains and poly(bistrifluoroethoxy-phosphazene).^{55,56} These authors suggest that favorable interactions between fluorinated units in the polymer and carbon dioxide contribute to high CO_2 solubility. In this regard, the HFIP units in this polymer may interact favorably with carbon dioxide, which would enhance the permeability coefficient of this polymer to CO_2 .

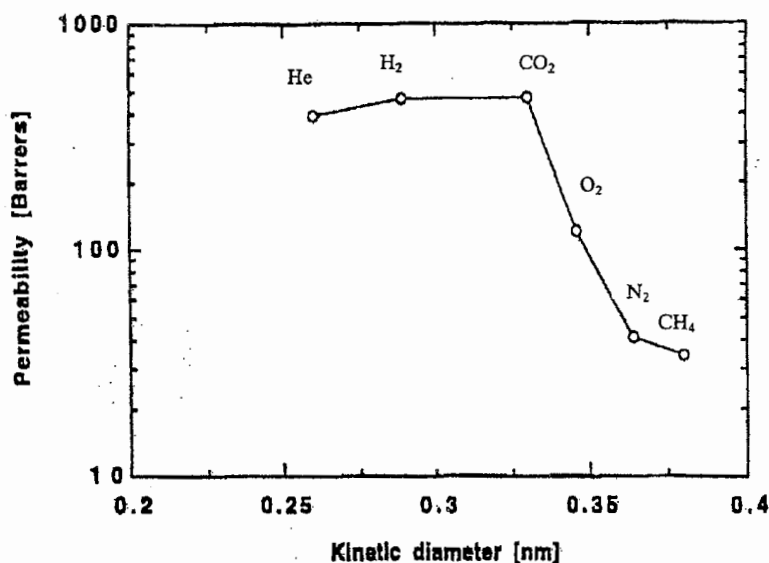


Figure 19. Gas permeability of the 6F polymer based on penetrant kinetic diameter

Separation factors of several industrial gas pairs are summarized in Table 10. Based on an exhaustive search of the polymer permeation literature, Robeson reported that the best combinations of permeability and selectivity obeyed a tradeoff rule: more permeable polymers are less selective and vice versa.⁵⁷ Polymers which have permeability and selectivity combinations beyond the so-called upper bound limits identified by Robeson are extremely rare. Robeson reported quantitative relations between gas permeability and selectivity for many common gas pairs. Based on the measured permeability coefficients in this polymer, estimates of the selectivity of a hypothetical upper bound polymer with the same permeability coefficients were computed using the relations published by Robeson. These estimated selectivity values are also listed in Table 10 along with the selectivity values determined from the ratios of experimentally determined, pure gas permeability coefficients. All of the separation factors calculated based on the experimental permeability coefficients were lower than their calculated upper bound values. For example, the separation factors of oxygen over nitrogen and carbon dioxide and methane were 2.9 and 13.8, respectively. These values were 73% of their calculated upper bound values and are closer to the upper bound selectivity values than those of the other gas pairs. Given the excellent thermal stability of the polymer and its separation properties, which are near the upper bound limits for some gas pairs, this polymer might be of interest as a high temperature membrane material.

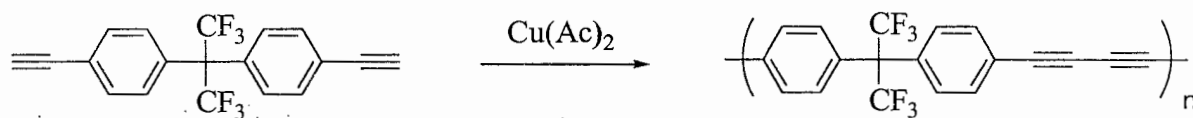
Table 12. Separation factors of the 6F polymer

Gas pairs	Robeson's Parameters ^a		Gas _i	P _i Barrers]	Separation Factors	
	k [Barrers]	n [-]			Exp.	Calc.
H ₂ /N ₂	52,918	-1.5275	H ₂	470	11	22
H ₂ /O ₂	35,760	-2.2770	H ₂	470	3.9	6.7
H ₂ /CH ₄	18,500	-1.2112	H ₂	470	14	21
O ₂ /N ₂	389,224	-5.8000	O ₂	120	2.9	4.0
CO ₂ /CH ₄	1,073,700	-2.6264	CO ₂	470	14	19

^a data from L. M. Robeson, *J. Membrane Sci.* **1991**, 62, 165.

Separation factor = $(P_i/k)^{1/n}$

Poly(2,2-Bis[[4-acetylene]phenyl]hexafluoropropane). Due to the extraordinary properties of the 6F polymer, a crosslinkable structure was devised. By incorporating a crosslinking group into the polymer backbone, polymer films could be cast and then crosslinked by heat or light. This would insure chemical resistance, since the original 6F polymer was highly soluble in common organic solvents. Several palladium cross coupling reactions were tried; however, only a copper coupling reaction resulting in high molecular weight polymer. The polymerization is shown below in scheme 6.



Scheme 6. Synthesis of the crosslinkable 6F polymer

Initially, the polymer was soluble at room temperature in a number of common organic solvents such as acetone, tetrahydrofuran, methylene chloride, *N,N*-dimethylformamide; it was partially soluble in chloroform and it was insoluble in hexane, methanol, and ethanol. The polymer was green with a λ_{max} value of 340.0 nm in a chloroform solution, and no absorption occurred above 350 nm (Figure 20). Polymer films were cast from THF. These films were green, opaque and flexible. After heating a polymer film to 80 °C for 2 hours the polymer was no longer soluble in solvents such as tetrahydrofuran, methylene

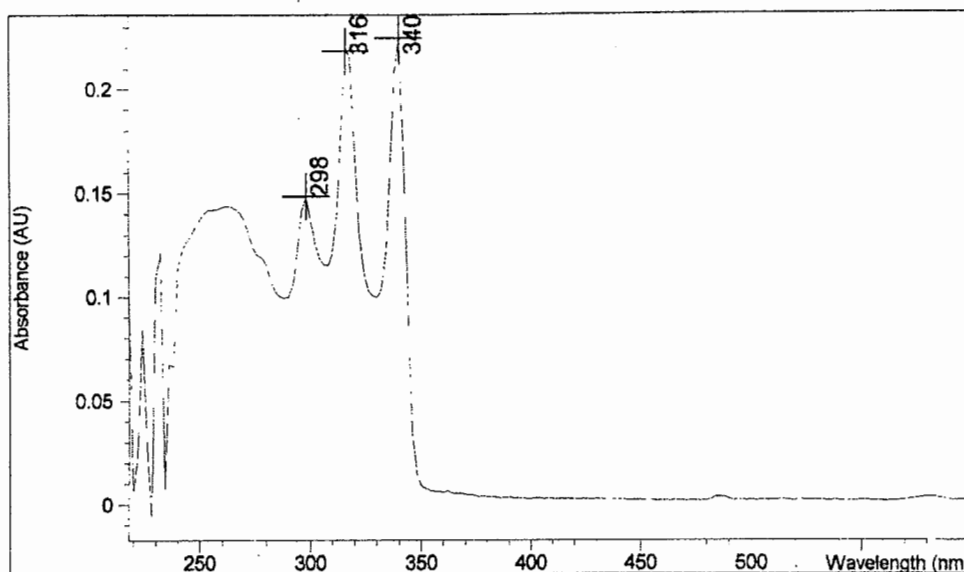


Figure 20. UV-vis of the crosslinkable 6F polymer

chloride, *N,N*-dimethyl-formamide. A color change was evident in the crosslinked polymer; it turned brown and the films became brittle.

The crosslinkable 6F polymer was synthesized in a 99 % yield. It had a number average molecular weight of 22.9×10^3 g/mol by GPC and 35.6×10^3 g/mol by MALLS ($dn/dc = 0.09$ ml/g in THF at 40 °C). The degree of polymerization (DP) determined by light scattering was 89. This is in good agreement with the DP calculated by proton NMR, which was 91. The GPC and MALLS chromatograms are shown in Figure 21. The polymer showed no evidence of a glass transition temperature in the DSC. It is very possible that the polymer crosslinks before the glass transition temperature can be observed. Thermogravimetric analysis, Figure 22, showed 5 % weight loss values at 139 °C and 146 °C in

nitrogen and air, respectively. It also showed 10 % weight loss values at 195 °C in nitrogen and 221 °C in air. Those numbers increased significantly after the polymer film was crosslinked. After crosslinking the temperatures increased by over 200 °C. The polymer's new weight loss numbers were 362 °C in nitrogen and 377 °C in air for the 5 % numbers. It also showed 10 % weight loss values at 410 °C for both nitrogen and air. See Figure 23.

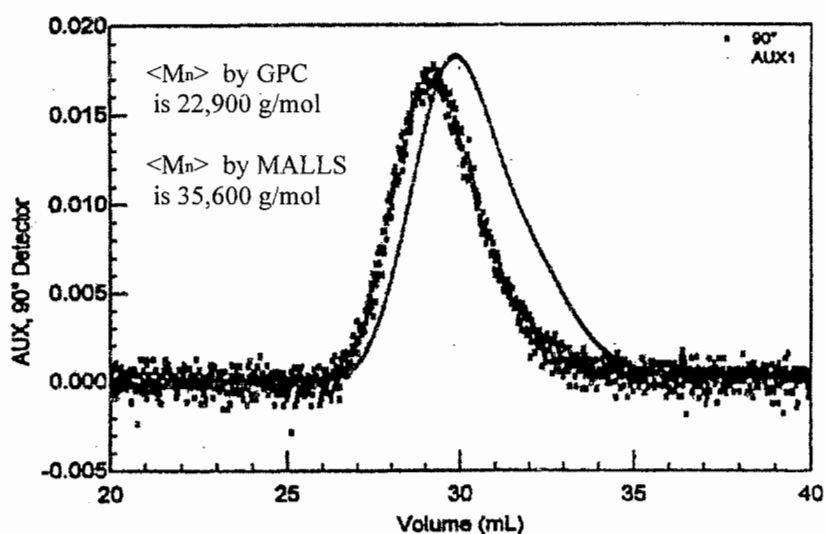


Figure 21. GPC and MALLS chromatograms of the crosslinkable 6F polymer

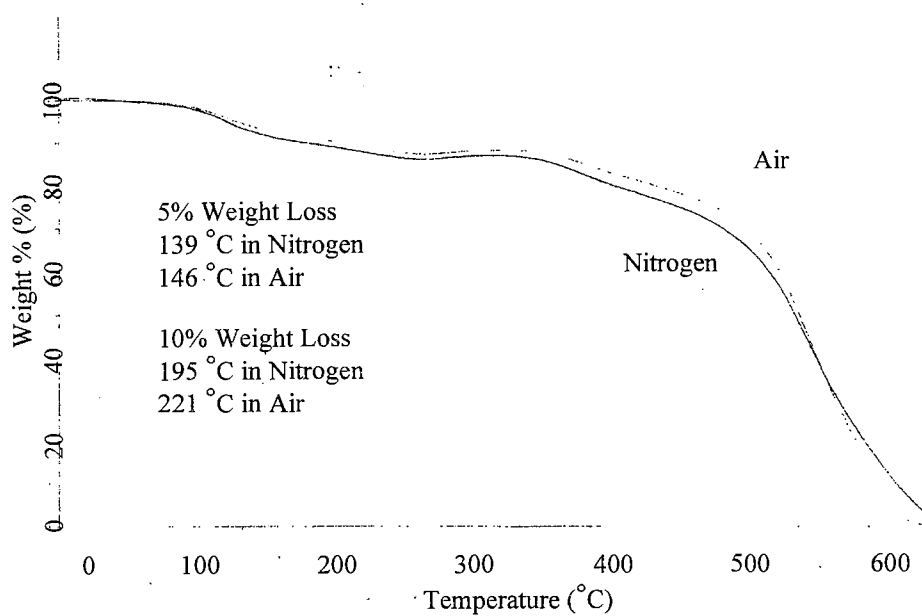


Figure 22. TGA thermogram of the uncrosslinked 6F polymer

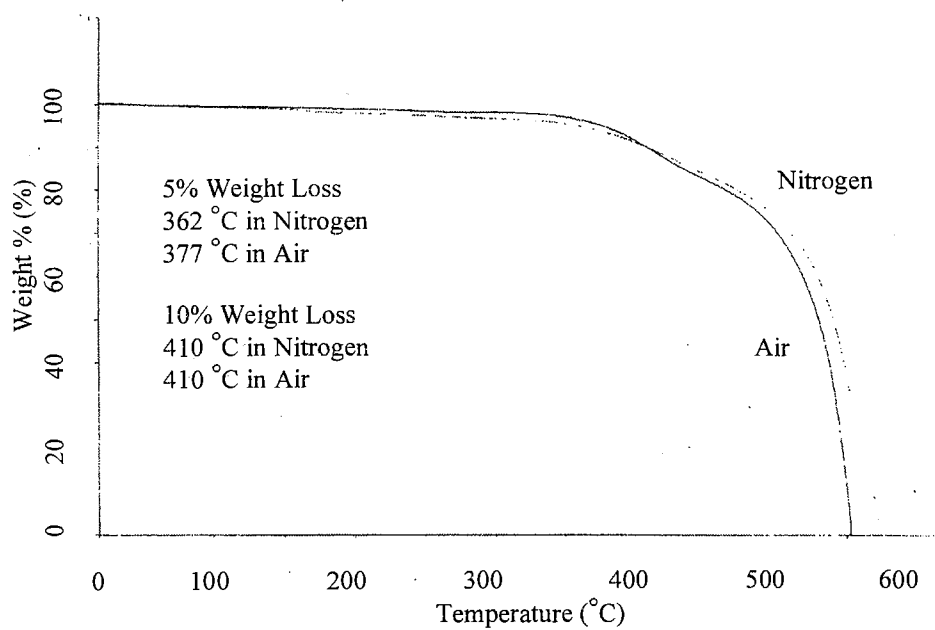
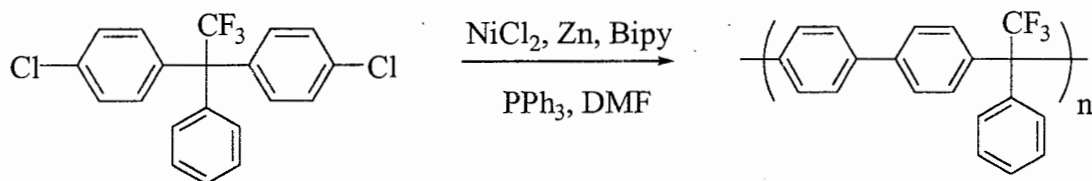


Figure 23. TGA thermogram of the crosslinked 6F polymer

Poly[biphenyl-4,4'-diyl(1-phenyl-2,2,2-trifluoroethane-1,1-diyl)]. The success of the 6F polymer spurred interest in other perfluorinated polymers. Logically, the 3F monomer was prepared and polymerized to use as a comparison to the 6F polymer. The optimized 6F reaction conditions were used for the polymerization of the 3F polymer (Scheme 6). However, these reaction conditions resulted in only low molecular weight 3F polymer. One major difference between the 6F polymerization and the 3F polymerization was reaction viscosity. The 3F polymerization viscosity increased dramatically. A concentration study was performed in hopes of achieving high molecular weight. Table 13 shows the different concentrations that were attempted along with the molecular weights results. Even by diluting the reaction 100× high molecular weight could not be obtained. These results can be explained by the following factors. First, the slightly polar monomer is not as soluble in hexane as was the 6F monomer. This made it difficult to remove all traces of the triphenylphosphine oxide by-product and led to decreased monomer purity compared to the 6F monomer. Without excessively pure monomer, the stoichiometry of the polymerization was not balanced and ultimately it led to low molecular weight. Secondly, with only one trifluoromethyl group the 3F monomer was not as electron withdrawing as the 6F monomer. The nickel-catalyzed coupling reaction shows the best results when strong electron withdrawing groups are present in the monomer ortho or para to the coupling site. Due to the nature of the polymerization mechanism, this difference could be partially responsible for the lower molecular weight of the 3F polymer. Finally, the lower yield of the 3F polymer provided another clue to its low molecular weight. Without extremely high conversion, high molecular weight is not achieved in traditional step growth polymerizations. All of these

factors undoubtedly influenced the 3F polymerization, making it more difficult to achieve high molecular weight.



Scheme 5. Synthesis of the 3F polymer

Table 13. Effect of solvent concentration on the 3F monomer polymerization^a

Reaction	Solvent	Concentration (M)	$\langle M_n^b \rangle$	$\langle M_w^b \rangle$
30	DMF	0.01	1,730	2,590
31	DMF	0.5	3,560	6,240
32	DMF	1.0	7,033	15,020
33	DMF	2.0	5,260	9,700

^a Molar ratios of catalyst system: monomer 1, NiCl₂ 0.075, Zn 3.1, PPh₃ 1, Bipy 0.075. 24 hour polymerization time. ^b Determined by gel permeation chromatograph (polystyrene standards).

The 3F polymer also was completely soluble at room temperature in a number of common organic solvents such as chloroform, acetone, tetrahydrofuran, methylene chloride, *N,N*-dimethylformamide; it is insoluble in hexane, methanol, and ethanol. Due to the low molecular weight films did not form. The polymer was a white powder with a λ_{max} value of 268.0 nm in a chloroform solution. No absorption occurred above 310 nm (Figure 24).

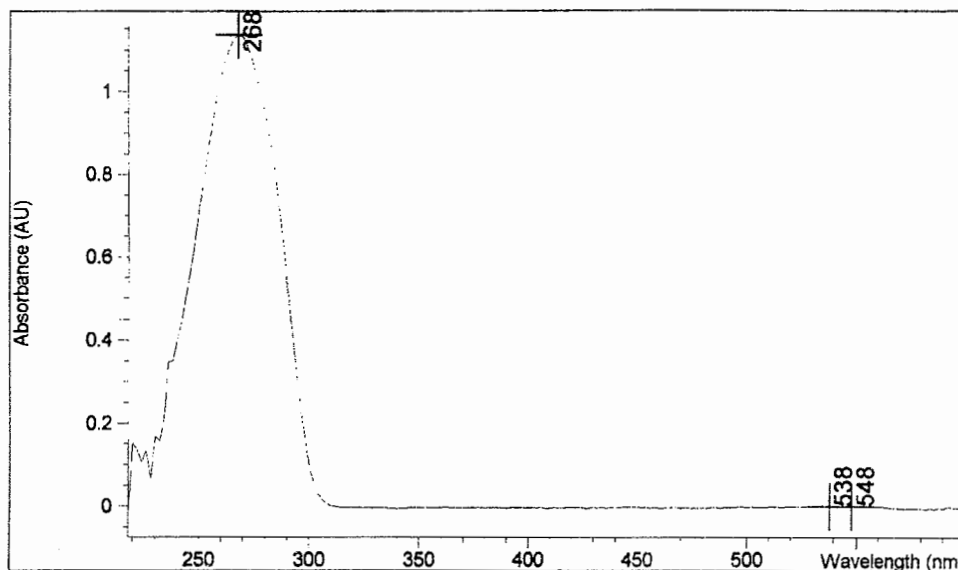


Figure 24. UV-Vis trace of the 3F polymer

The 3F polymer was synthesized in a 93 % yield. The number average molecular weight was 8.5×10^3 g/mol by GPC and 12.6×10^3 g/mol by MALLS ($dn/dc = 0.08$ ml/g in THF at 40 °C). The degree of polymerization (DP) determined by light scattering was 42. Proton NMR could not be used to calculate DP due to the overlap of chemical shifts in the aromatic region. The GPC and MALLS chromatograms are shown in Figure 25.

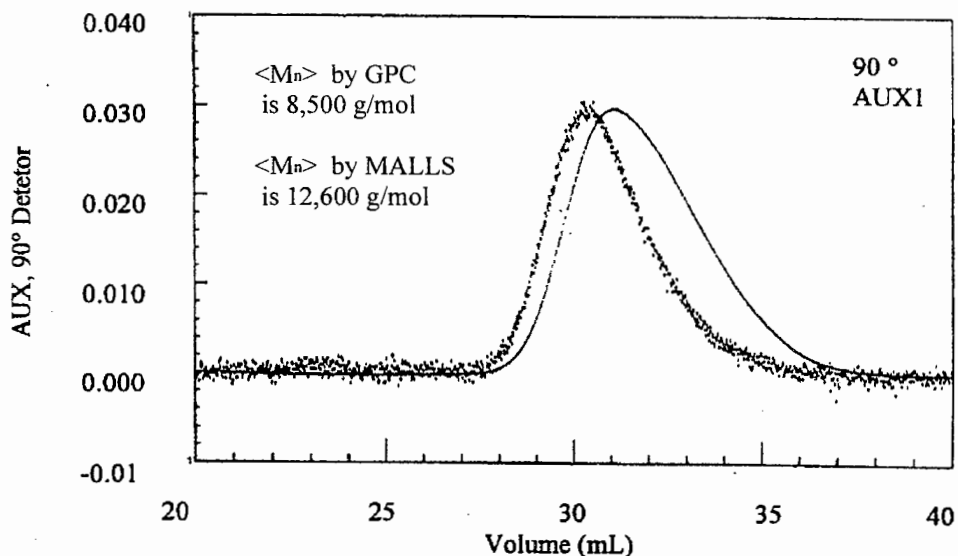


Figure 25. GPC and MALLS chromatograms of the 3F polymer

Although, only low molecular weight was achieved with the 3F polymer the glass transition temperature of the material was quite high. It had a glass transition temperature of 275 °C, see Figure 26. This was substantially higher than the 6F polymer when comparing the molecular weights that were used to determine the T_g . At the same molecular weight, the

6F polymer's T_g was only 180 °C. The 6F polymer reached its critical molecular weight at 13,000 g/mol, at this molecular weight the T_g was 250 °C. The T_g of the 3F polymer should also continue to increase until the critical molecular weight of the polymer is reached. The large difference between the two T_g 's can be explained by the addition of the phenyl group to the repeat unit of the polymer. This increases the rigidity of the polymer repeat unit and in turn increases the glass transition temperature.

Thermogravimetric analysis of the 3F polymer, Figure 27, showed 5% weight loss values at 515 °C and 520 °C for nitrogen and air, respectively. It also showed 10%

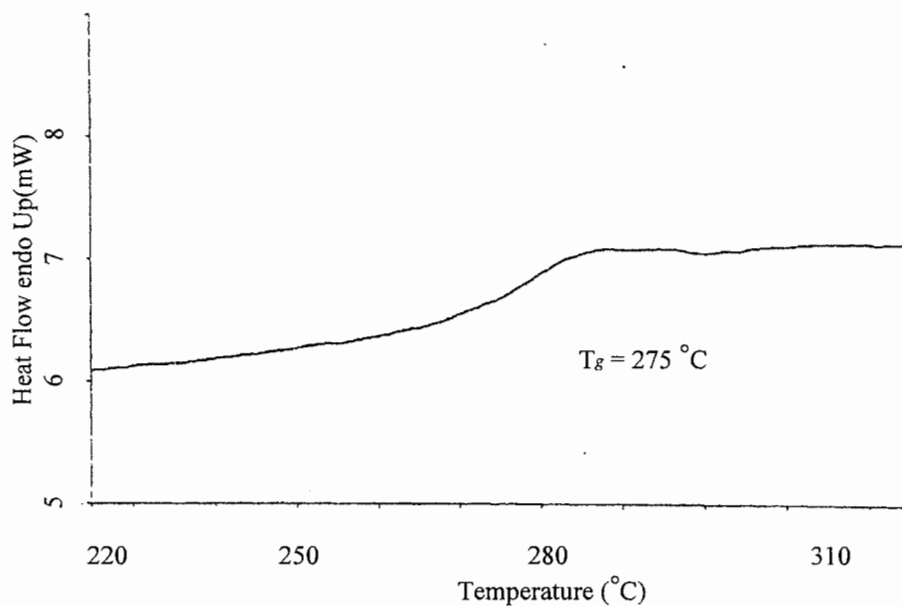


Figure 26. DSC thermogram of the 3F polymer

weight loss values at 540 °C in nitrogen and 550 °C in air. The thermal stability of the 3F polymer was comparable to the 6F polymer. However, these values for the 3F polymer are not optimized considering that the critical molecular weight had not been synthesized. With the optimization of the molecular weight these values are expected to rise significantly.

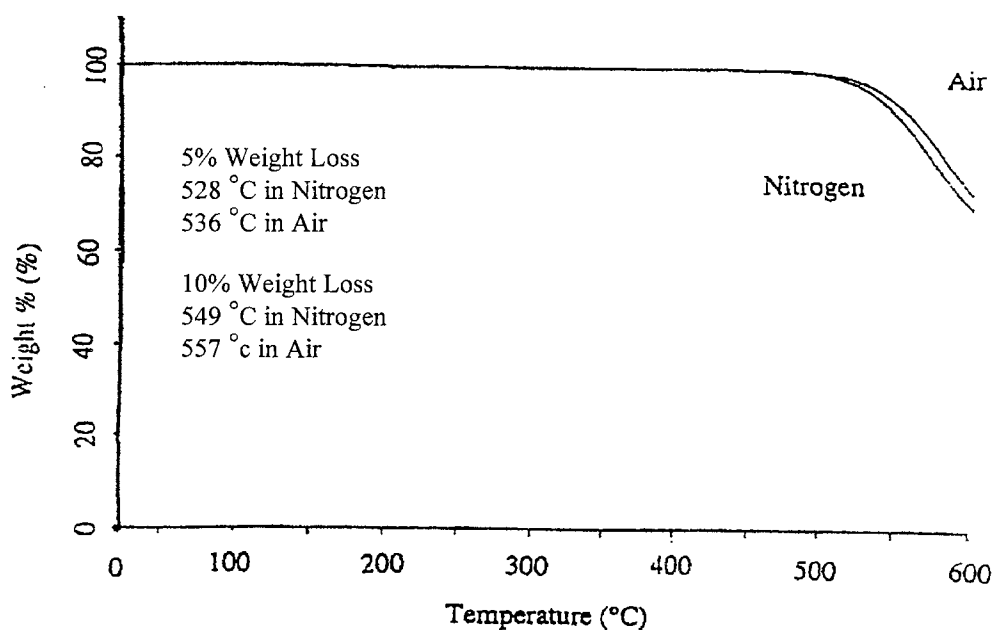


Figure 27. TGA thermogram of the 3F polymer

GENERAL CONCLUSIONS

Poly[[1,1'-biphenyl]-4,4'-diyl[2,2,2-trifluoro-1-(trifluoromethyl)ethylidene]] and poly[biphenyl-4,4'-diyl(1-phenyl-2,2,2-trifluoroethane-1,1-diyl)] were successfully prepared by the Ni(0)-catalyzed coupling polymerization of 2,2-bis(*p*-chlorophenyl)-hexafluoropropane and 1,1-bis(4-chlorophenyl)-2,2,2-trifluoro-1-phenylethane, respectively. This unique polymerization technique has allowed for the synthesis of two new materials. These new materials and the study of their properties have isolated the enhancing effects of trifluoromethyl groups within polymers. Both of these unique polymers and their properties can be used as a comparison to other polymers that have incorporated the hexafluoroisopropylidene linkage. The 6F polymer is especially useful, it specifically separates out the properties attributed to the hexafluoroisopropylidene linkage from other functionalities contained within a polymer. Ultimately, it leads to the ability to assess the extent of the property enhancing effects of HFIP.

The 6F polymer has even greater potential as a useful commercial material. Poly[[1,1'-biphenyl]-4,4'-diyl[2,2,2-trifluoro-1-(trifluoromethyl)ethylidene]] exhibits excellent thermal and thermooxidative stability. The combination of its thermal stability, minimal moisture absorption, and low dielectric constant indicates that this material and its analogues are promising for electronic applications. The fire resistance testing shows that this new polymer is comparable with other polymers in its class and exceeds present FAA standards. The 6F polymer has a high free volume and is very gas-permeable for an aromatic, glassy polymer. Selectivity values for some gas pairs (O₂/N₂ and CO₂/CH₄) are near the upper bound limits as suggested by Robeson. The initial gas permeability

measurements suggest a high affinity for carbon dioxide relative to other gases. With its high thermal stability and impressive Robeson values for the separation of gas pairs this polymer could also find use as a high temperature membrane.

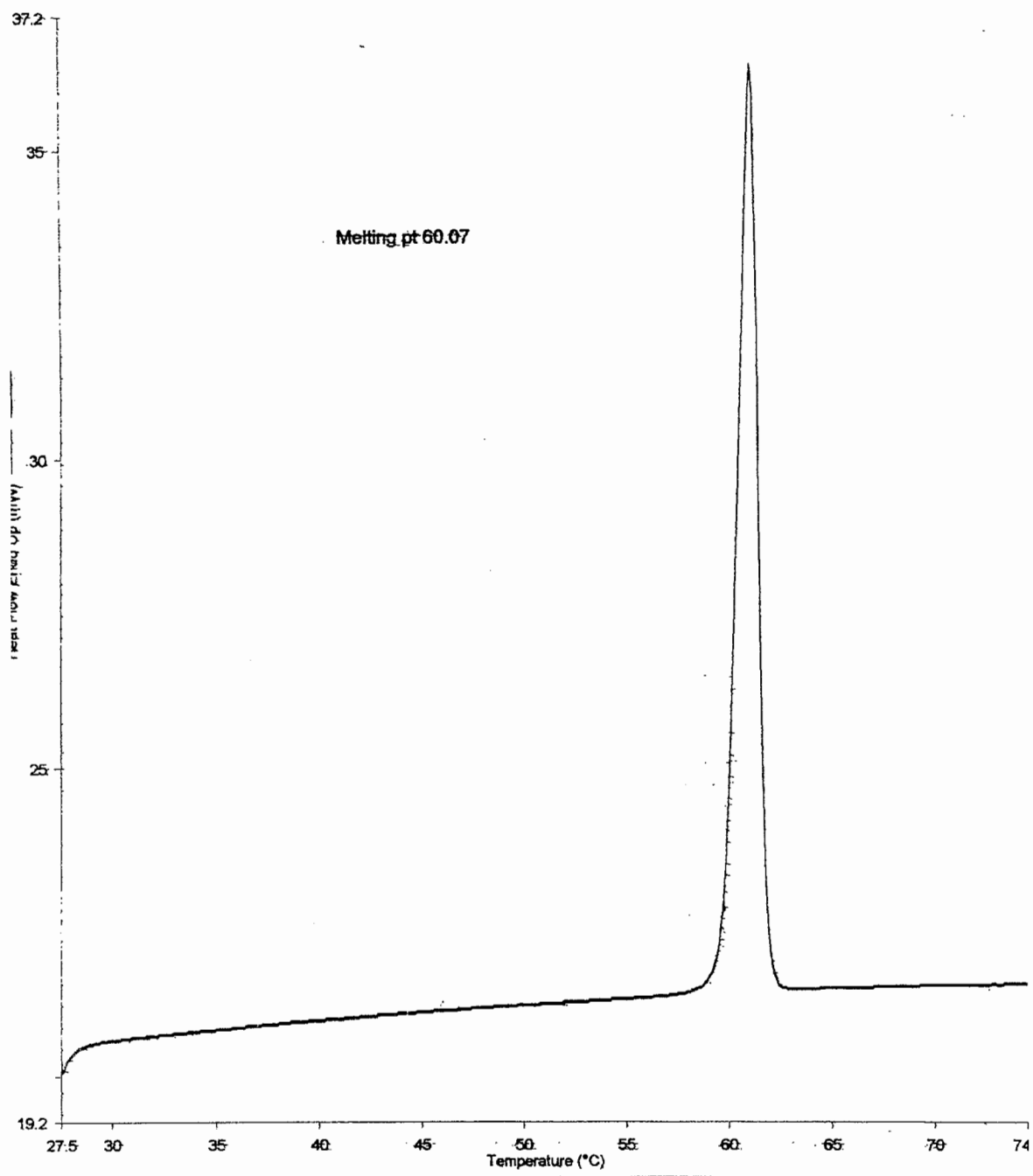
Acetylene crosslinking groups were successfully incorporated into the 6F polymer. These groups are critical to the industrial use of the polymer. With crosslinking capabilities, the polymer can be processed and then crosslinked. This would ensure chemical inertness. This last feature of the 6F polymer makes it even more desirable to the electronics industry. It could conceivably be used as a photoresist.

Poly[biphenyl-4,4'-diyl(1-phenyl-2,2,2-trifluoroethane-1,1-diyl)] also had impressive thermal properties. Even with its lower molecular weight, its glass transition temperature and polymer decomposition temperatures are higher than the 6F polymer. However, because of its low molecular weight, films could not be formed. Without film formation, the gas permeability measurements could not be taken. The lower molecular weight also hindered testing for its flame retardance. It is anticipated, that with new synthetic methods being constantly developed that high molecular weight 3F polymer also will be synthesized. If high molecular weight could be achieved using the same chemistry that was used to incorporate crosslinking groups into the 6F polymer, it would have an excellent chance of being useful to the electronics industry.

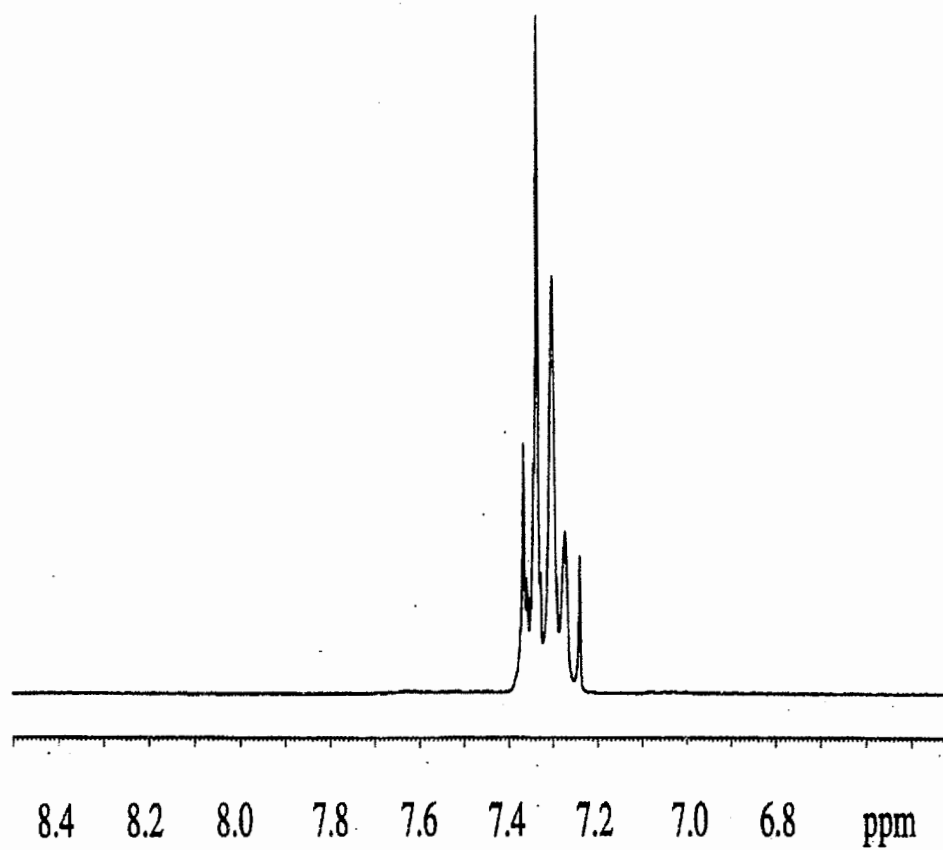
The initial success of the 6F polymer and the incorporation of a crosslinking group leads to many other possible polymer structures. A variety of perfluoroalkyl flexible linkages could be used to replace the HFIP group of the 6F polymer. This would allow for a

complete study of the enhancing effects of the trifluoromethyl group. In addition to this future work, HFIP styrenic derivatives could also be prepared and free radically polymerized. Finally, work on a solid support catalyst systems would enhance the feasibility of industrially producing these types of transition metal-catalyzed polymers.

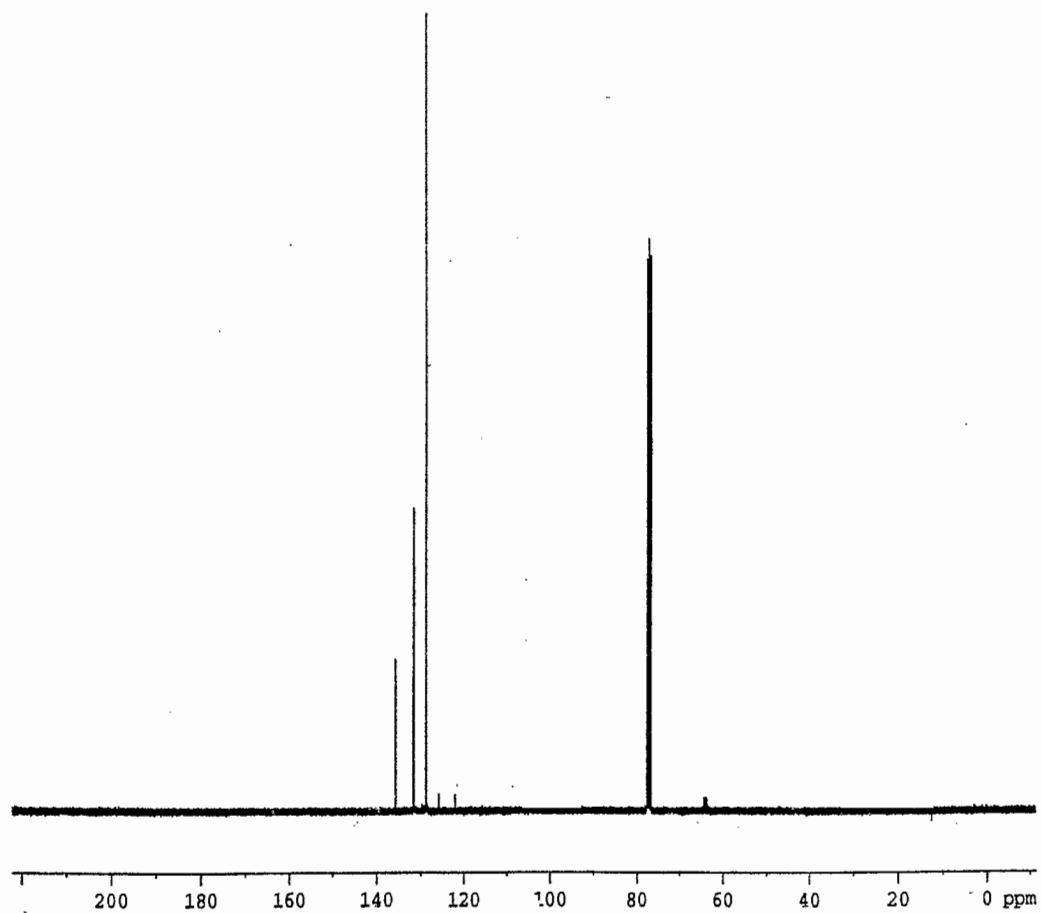
APPENDIX. SUPPORTING DATA



Melting point of 6F monomer



Proton NMR of 6F monomer



Carbon NMR of 6F polymer

Sample ID: 91H-095 Formula: C₁₅H₈F₆Cl₂

Crystallization solvent(s): _____

Theoretical weight percents (we can calculate these for you if you wish):

%C= 48.29 %H= 2.16 %N= _____ %S= _____

Number of runs requested 2. You are charged for each run. If you wish, save money and sample by just requesting one. For critical work you might want to request two or more runs.

Check here ☐ if you absolutely require %S. This is not the normal configuration of the instrument, and you may have to wait a couple of weeks for these results. Check here ☐ if you would like a CHN analysis prior to the CHNS analysis. You will be charged for each run.

Special combustion conditions (if you have information that would help us get better results on your sample, use this space, or attach the information to this form): _____

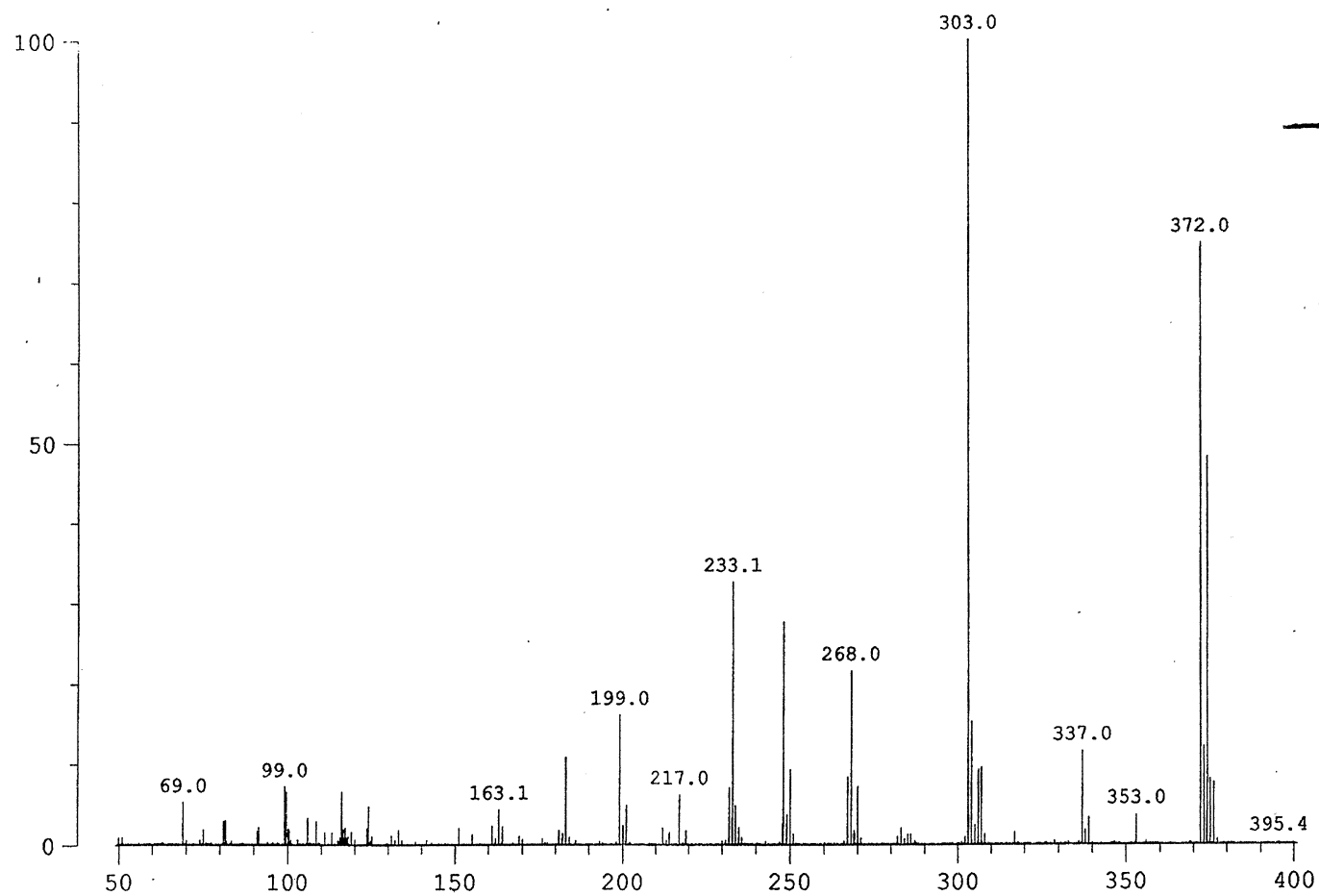
RATES: CHN = \$11.00 per run CHNS = \$15.50 per run

RESULTS

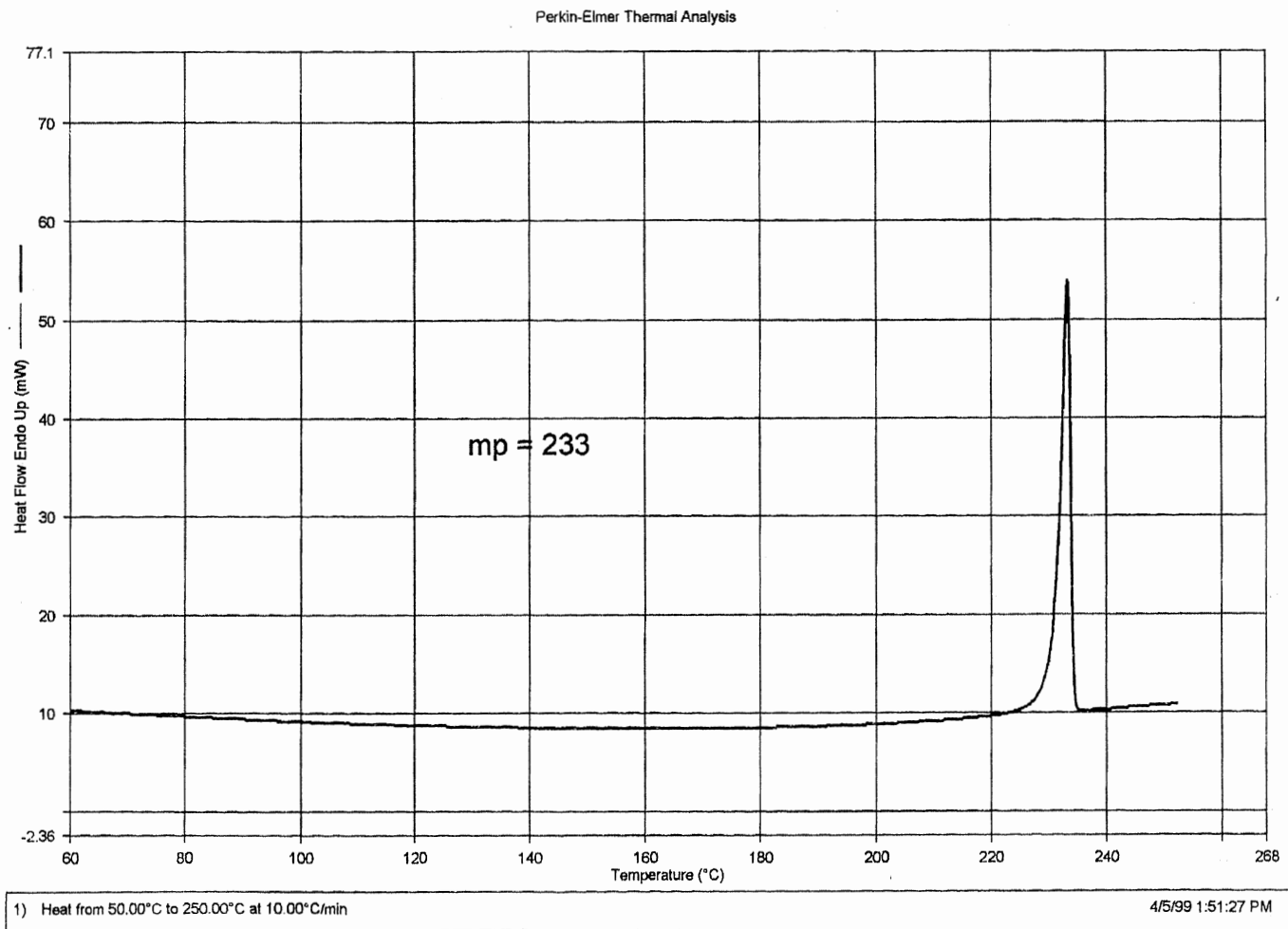
	#1	#2	#3	AVG
%C	<u>48.45</u>	<u>48.60</u>		<u>48.52</u>
%H	<u>2.13</u>	<u>2.14</u>		<u>2.14</u>
%N	<u>0</u>	<u>0</u>		<u>0</u>
%S				

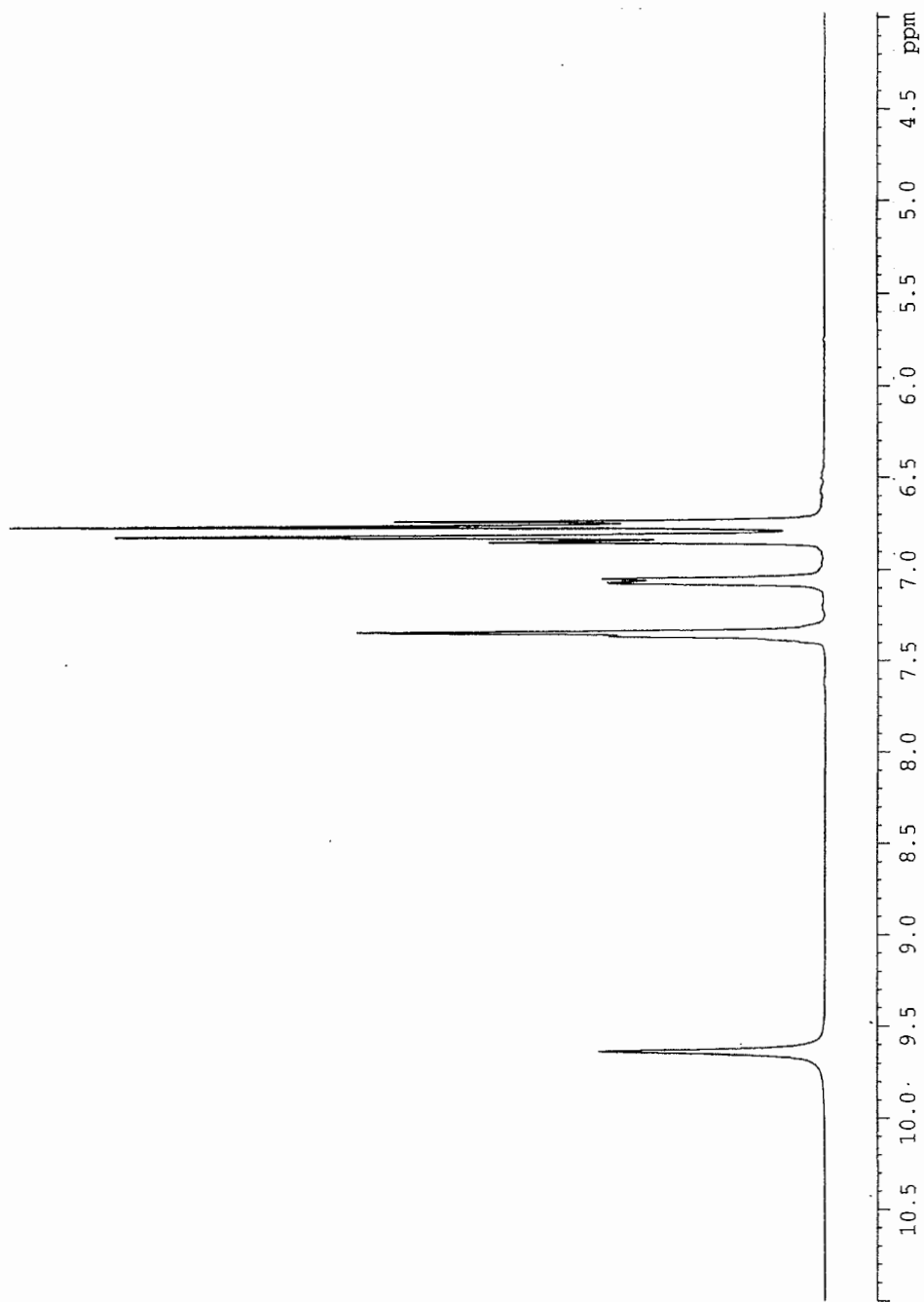
Elemental analysis of 6F monomer

HRMS of 6F monomer

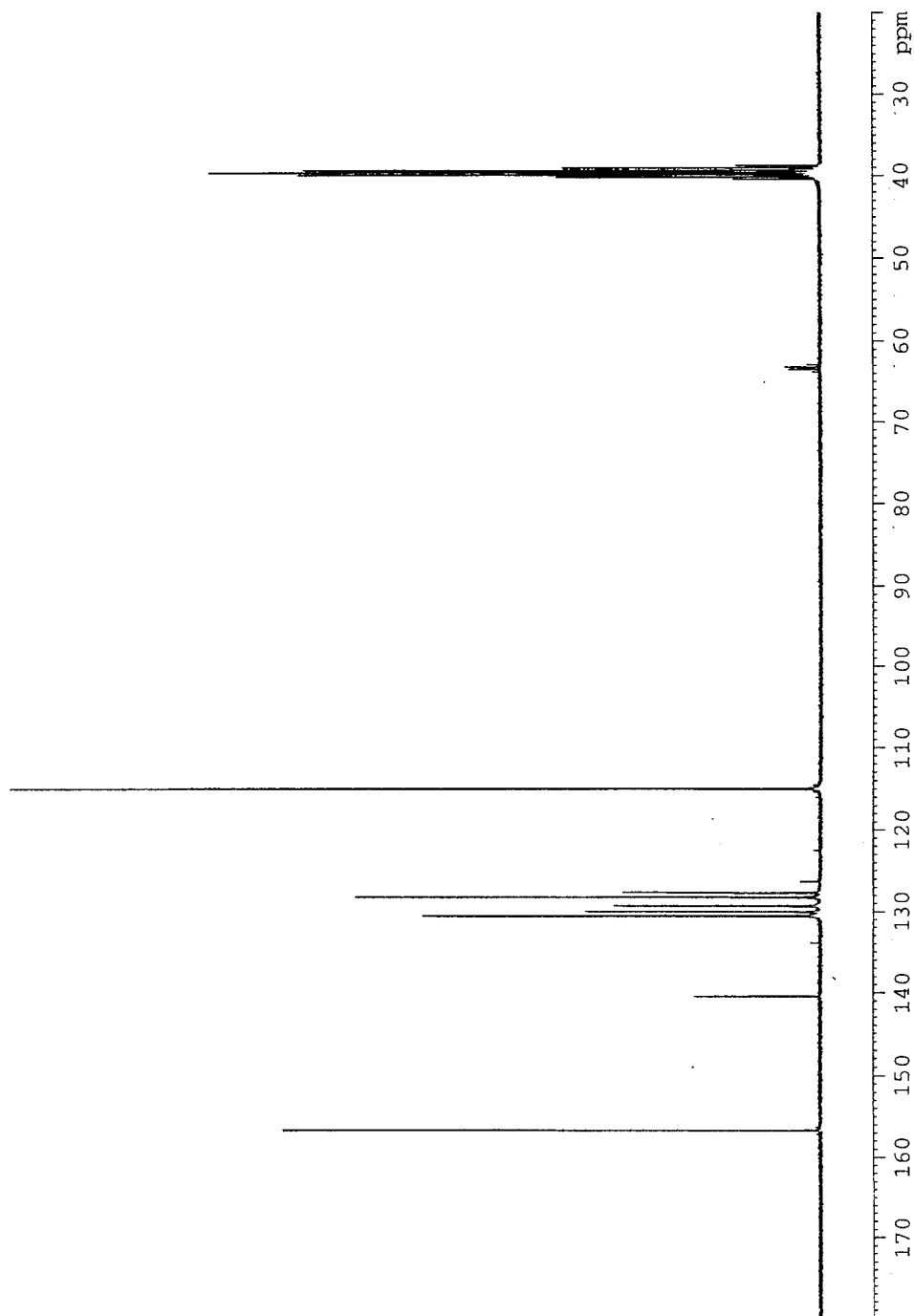


Melting point of 3F diol





Proton NMR of 3F diol



Carbon NMR of 3F diol

Elemental analysis of 3F diol

Sample ID: pah-124 Formula: C₂₀H₁₅O₂F₃

Crystallization solvent(s): CH₂Cl₂ (methylene chloride)

Theoretical weight percents (we can calculate these for you if you wish):

$\%C = 69.76$ $\%H = 4.3908$ $\%N =$ $\%S =$

Number of runs requested 2. You are charged for each run. If you wish, save money and sample by just requesting one. For critical work you might want to request two or more runs.

Check here ☐ if you absolutely require %S. This is not the normal configuration of the instrument, and you may have to wait a couple of weeks for these results. Check here ☐ if you would like a CHN analysis prior to the CHNS analysis. You will be charged for each run.

Special combustion conditions (If you have information that would help us get better results on your sample, use this space, or attach the information to this form): _____

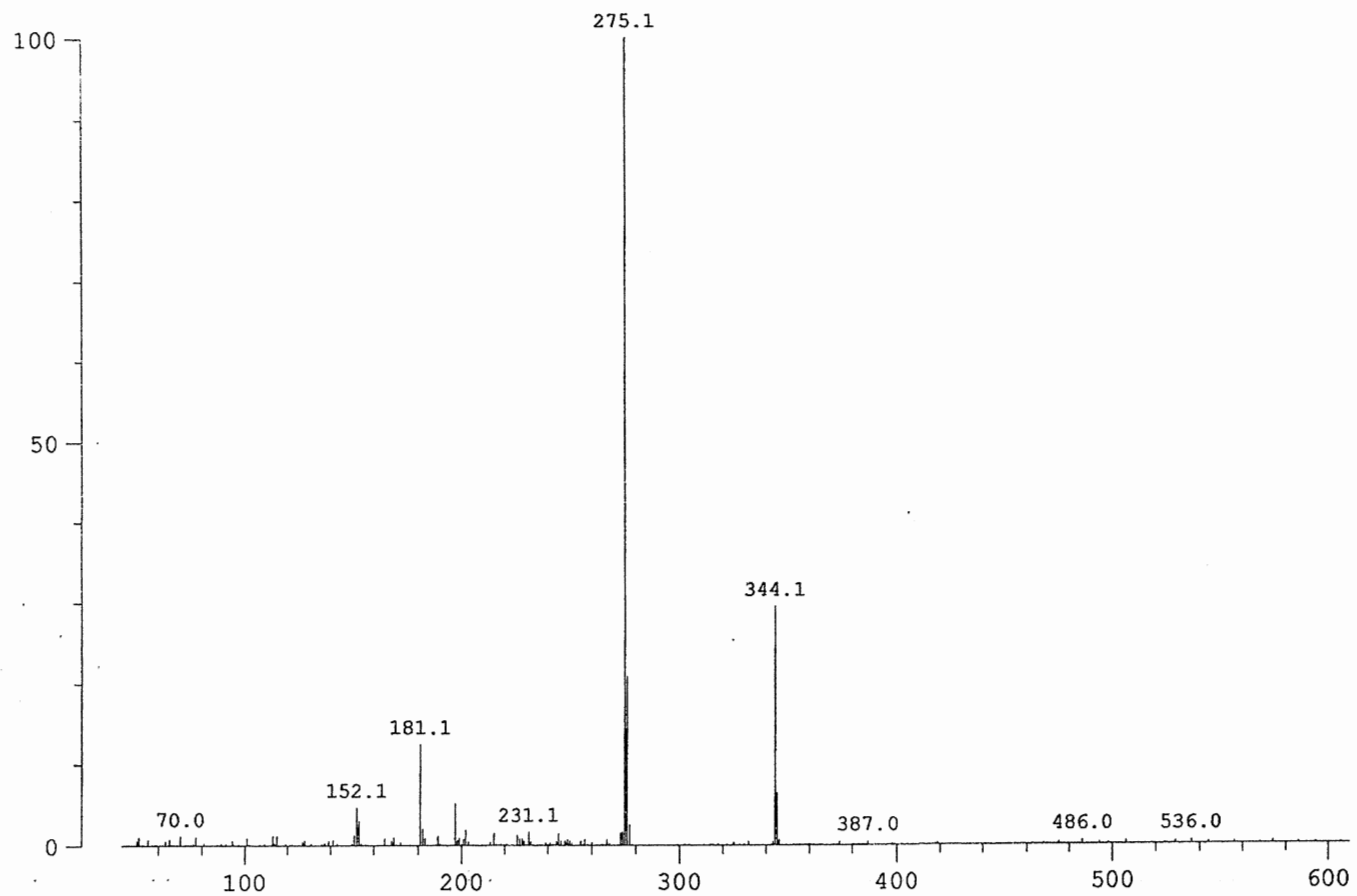
RATES: CHN = \$11.00 per run CHNS = \$15.50 per run

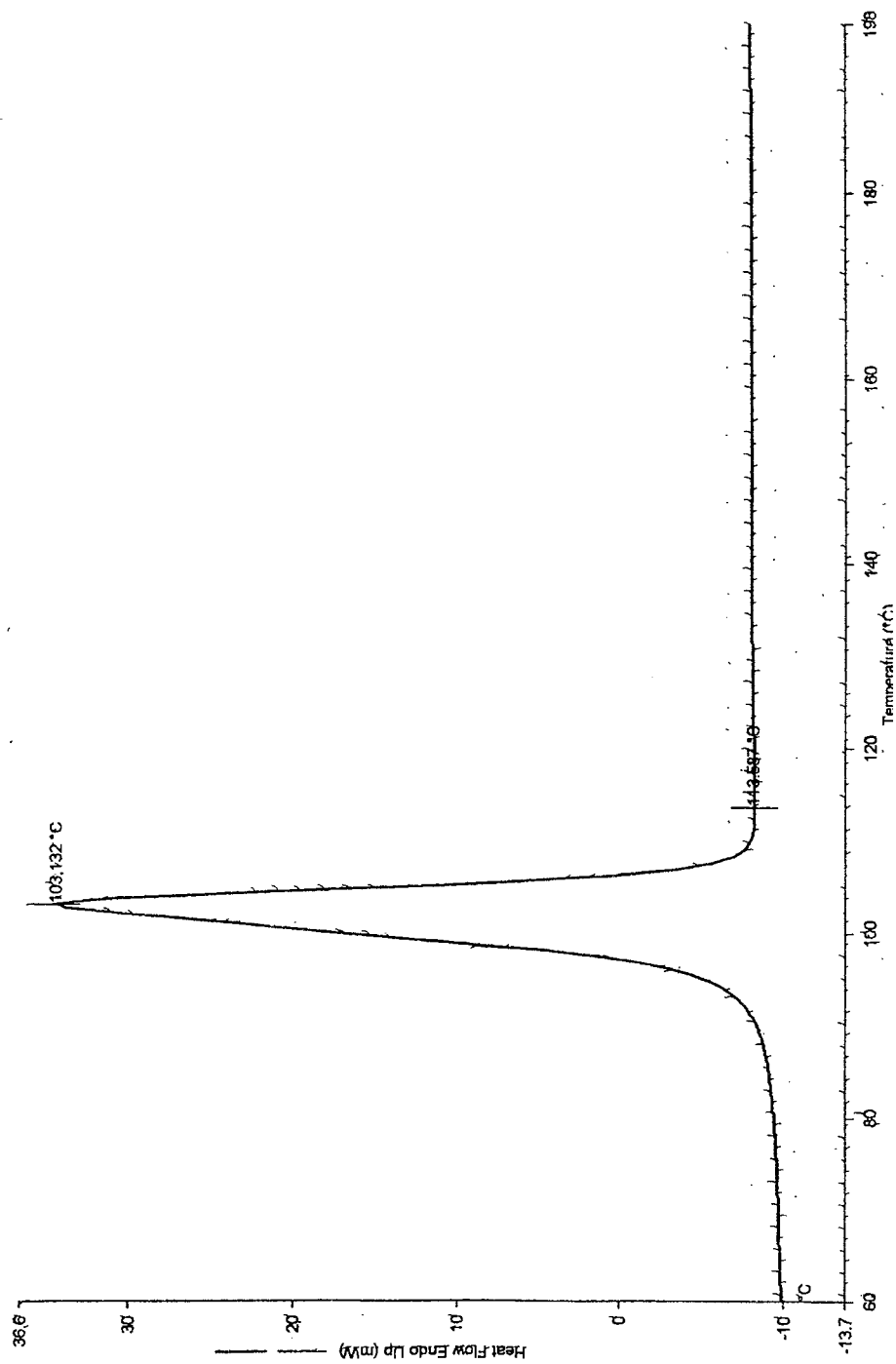
RESULTS

	#1	#2	#3	AVG
%C	69.69	69.71		69.70
%H	4.56	4.54		4.55
%N	0.02	0.02		
%S				

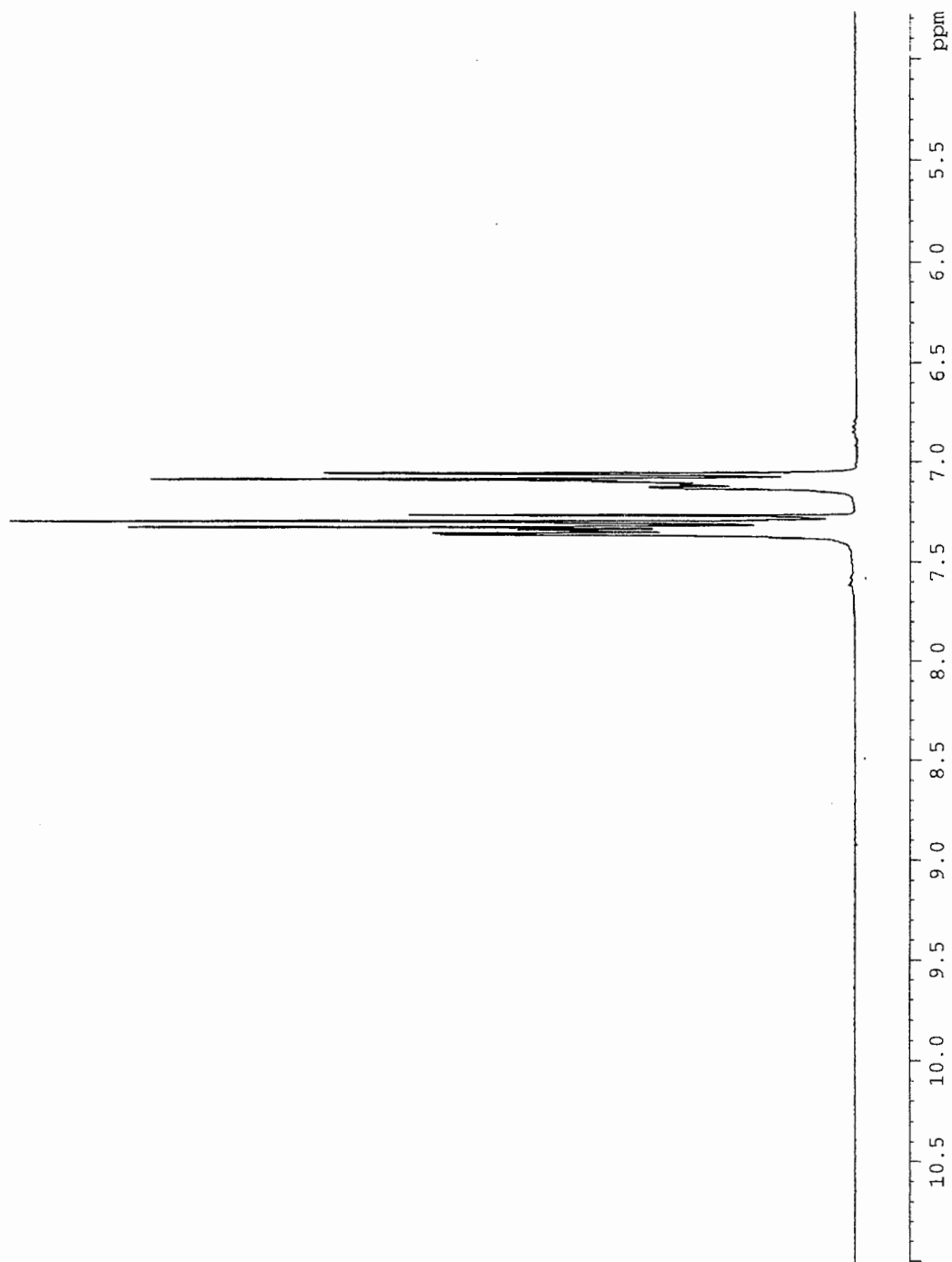
Elemental analysis of 3F diol

HRMS of 3F diol

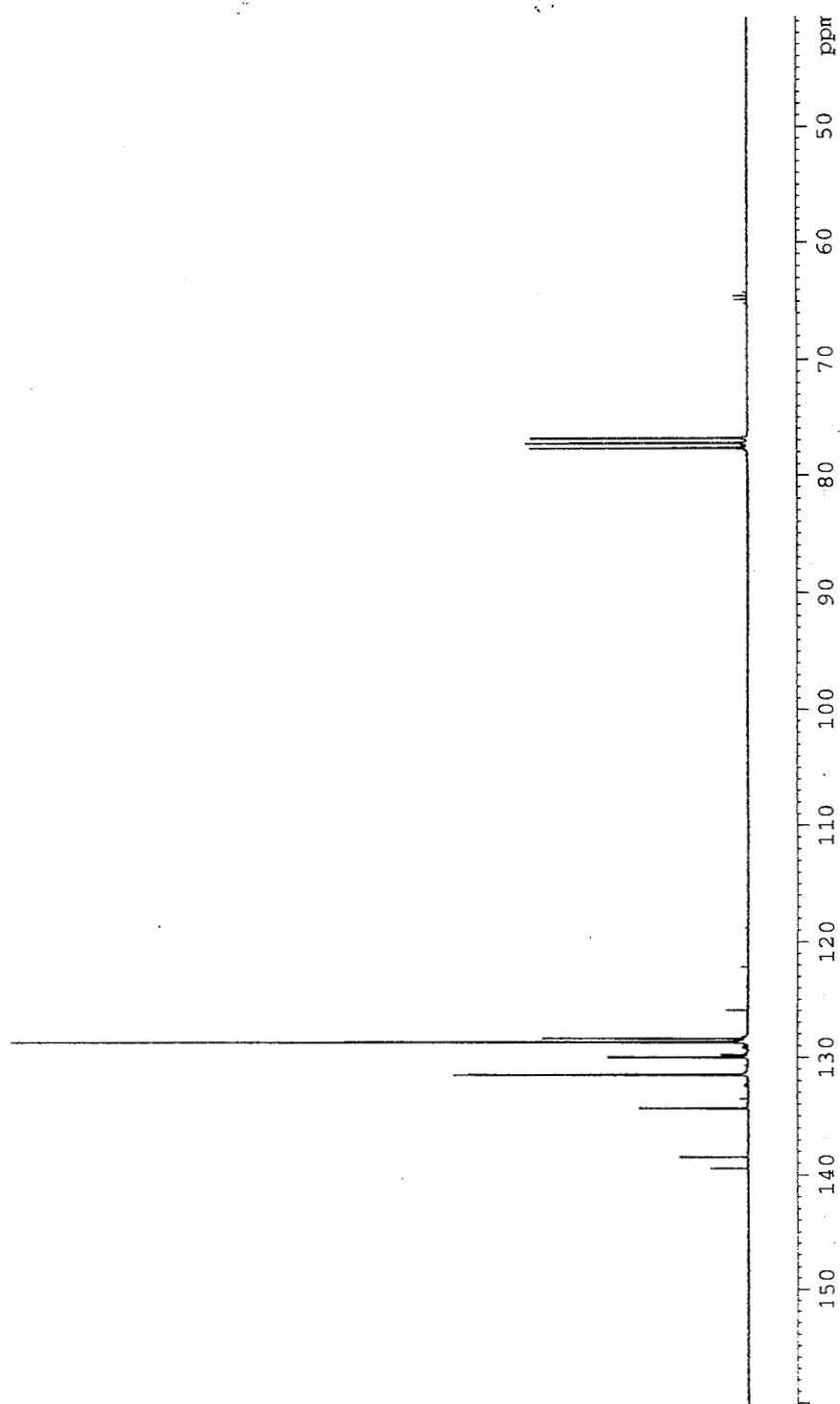




Melting point of 3F monomer



Proton NMR of 3F monomer



Carbon NMR of 3F monomer

Sample ID: pan-126 Formula: C₂₀H₁₃Cl₂F₃

Crystallization solvent(s): hexanes

Theoretical weight percents (we can calculate these for you if you wish):

%C= 63.01 %H= 3.4371 %N= _____ %S= _____

Number of runs requested 2. You are charged for each run. If you wish, save money and sample by just requesting one. For critical work you might want to request two or more runs.

Check here ☐ if you absolutely require %S. This is not the normal configuration of the instrument, and you may have to wait a couple of weeks for these results. Check here ☐ if you would like a CHN analysis prior to the CHNS analysis. You will be charged for each run.

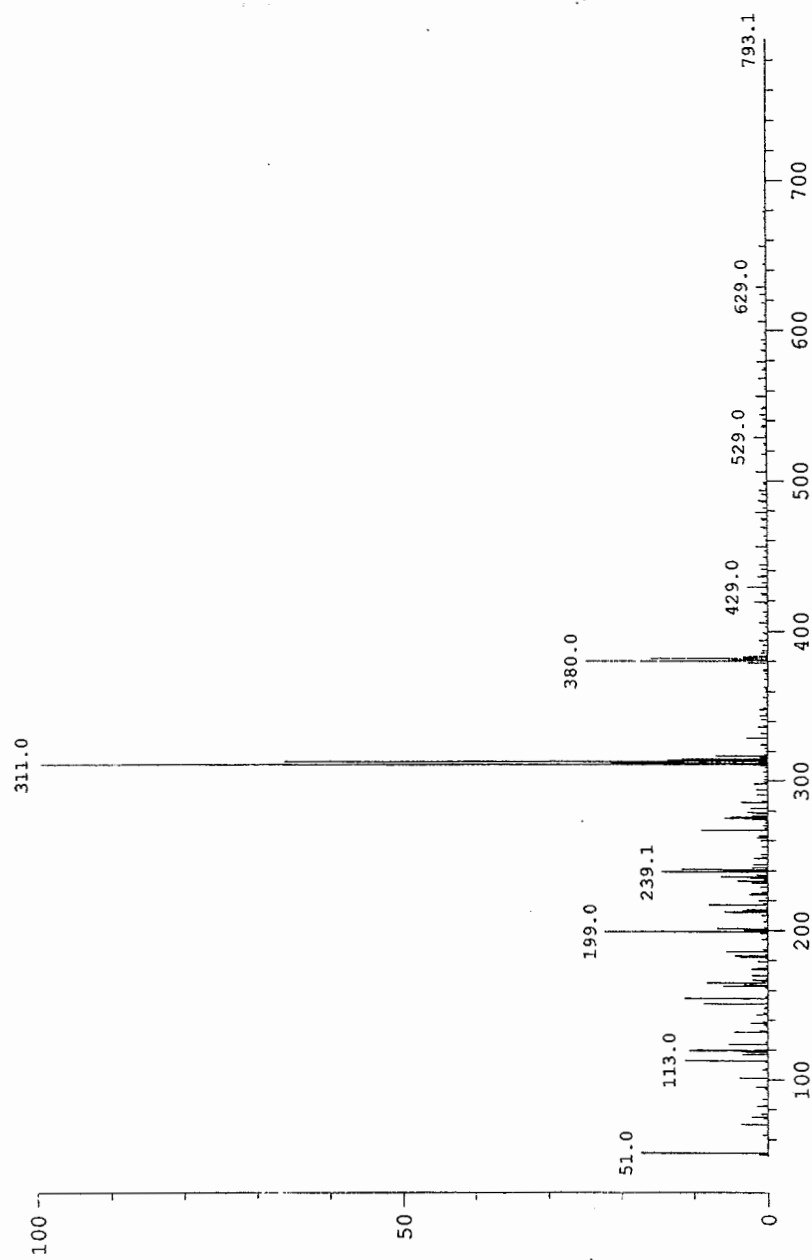
Special combustion conditions (if you have information that would help us get better results on your sample, use this space, or attach the information to this form): _____

RATES: CHN = \$11.00 per run CHNS = \$15.50 per run

RESULTS

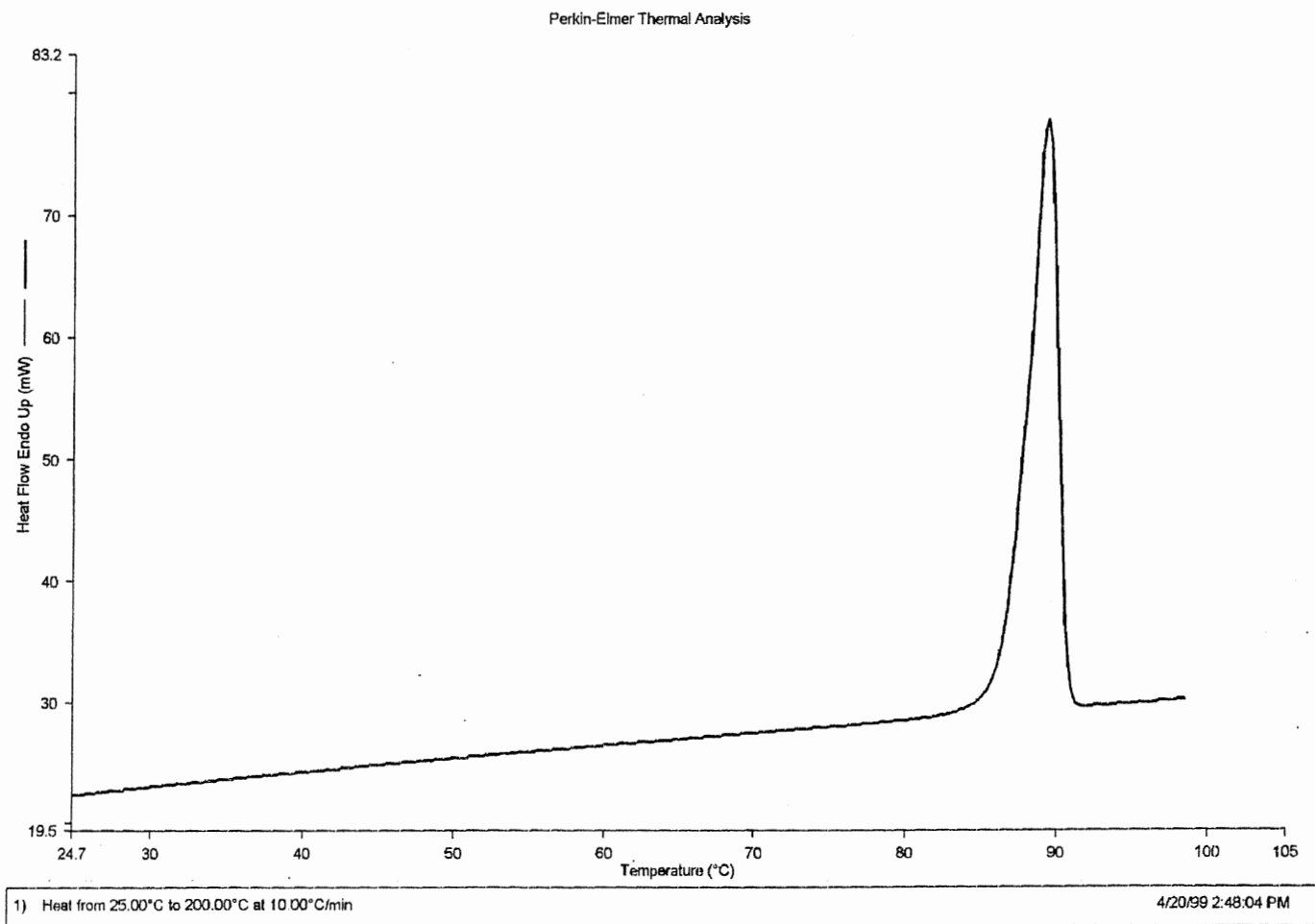
	#1	#2	#3	AVG
%C	61.75	61.13		61.54 ?
%H	3.76	3.86		3.81
%N	0.01	0.02		0.01
%S				

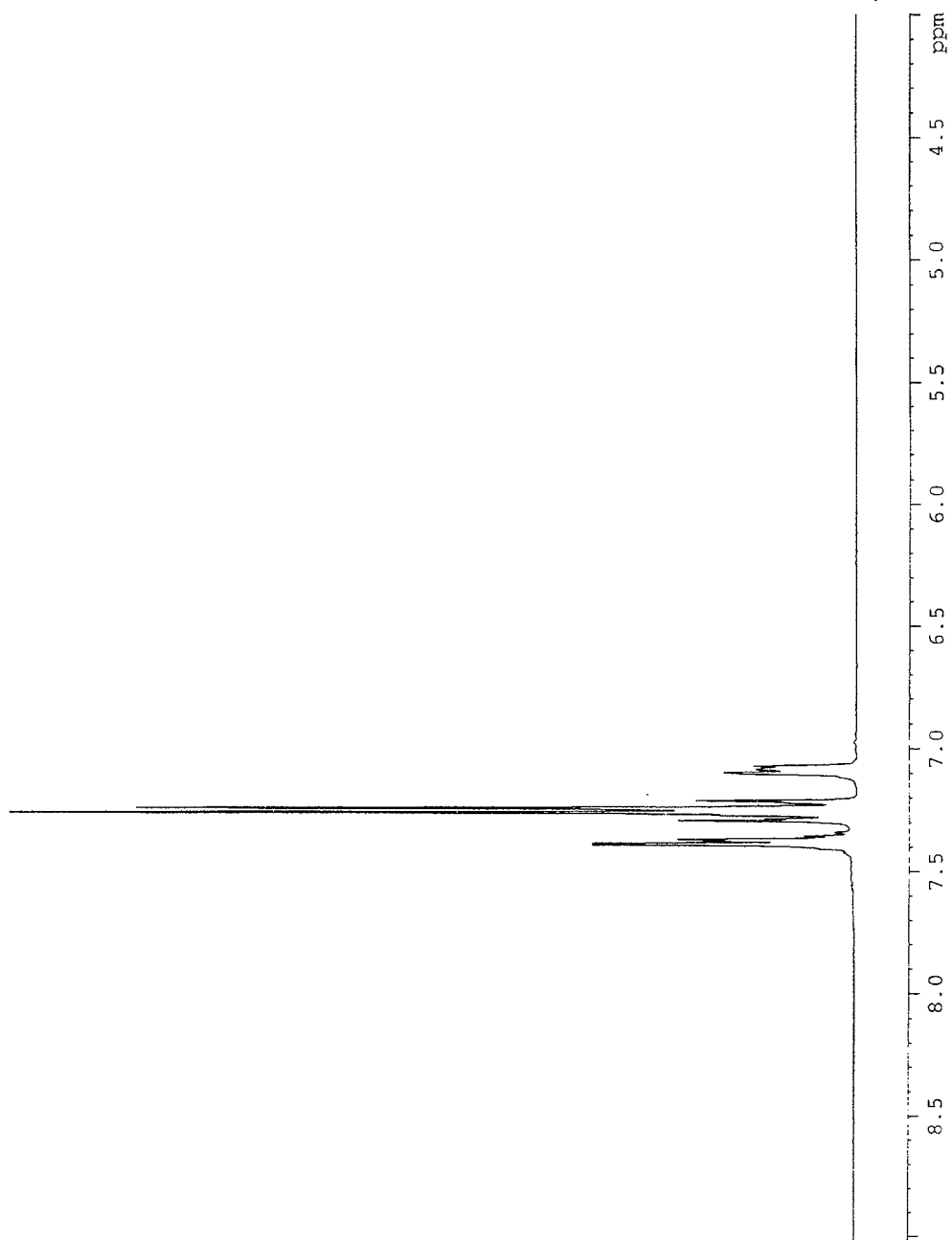
Elemental analysis of 3F monomer



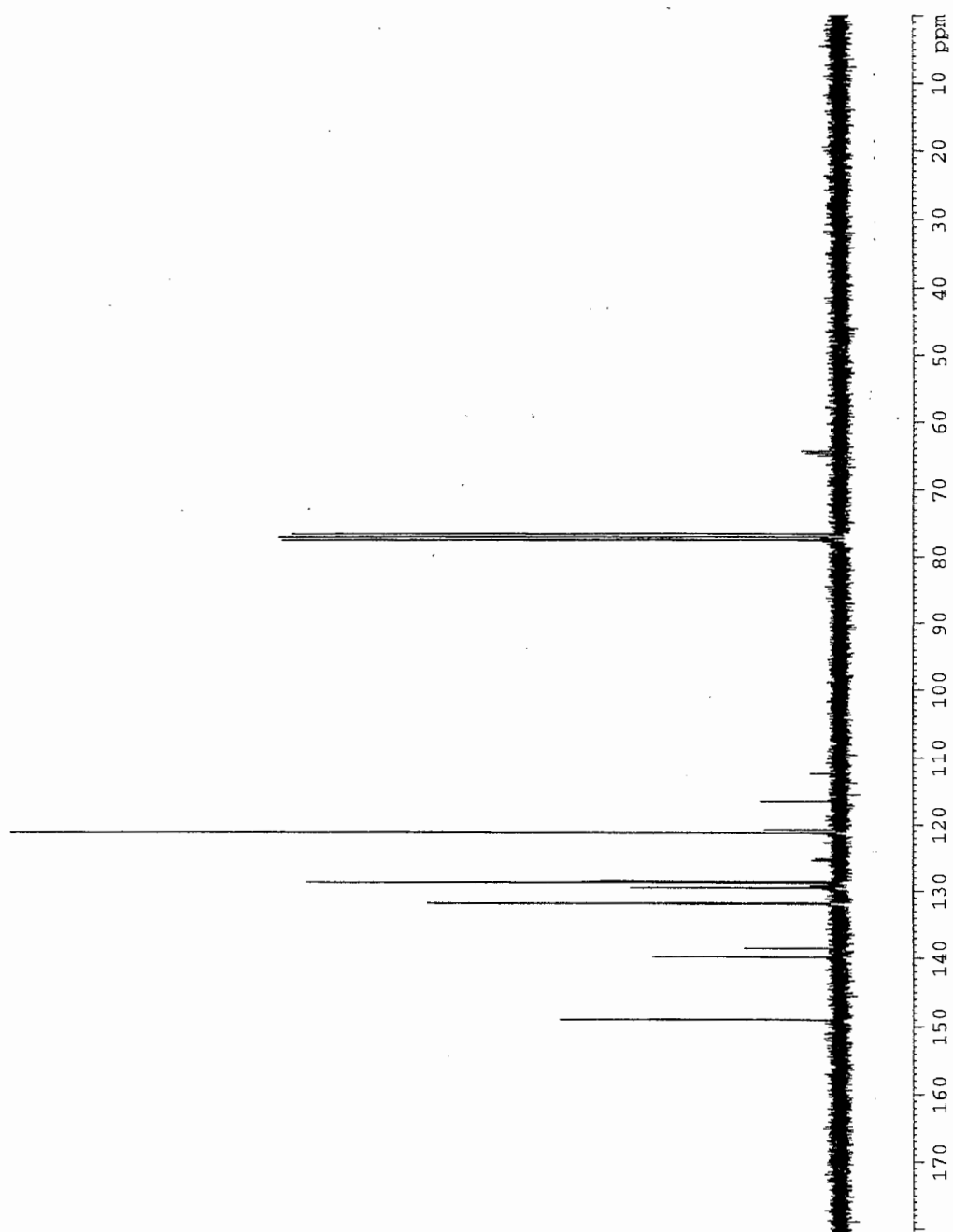
HRMS of 3F monomer

Melting point of 3F triflate

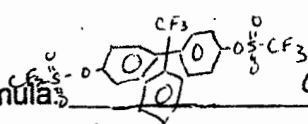




Proton NMR of 3F triflate



Carbon NMR of 3F triflate

Sample ID: pan3-066 Formula:  C₂₂H₁₃O₆S₂F₉

Crystallization solvent(s): ethanol

Theoretical weight percents (we can calculate these for you if you wish):

%C= 43.43 %H= 2.15 %N= _____ %S= _____

Number of runs requested 2. You are charged for each run. If you wish, save money and sample by just requesting one. For critical work you might want to request two or more runs.

Check here ☐ if you absolutely require %S. This is not the normal configuration of the instrument, and you may have to wait a couple of weeks for these results. Check here ☐ if you would like a CHN analysis prior to the CHNS analysis. You will be charged for each run.

Special combustion conditions (if you have information that would help us get better results on your sample, use this space, or attach the information to this form): _____

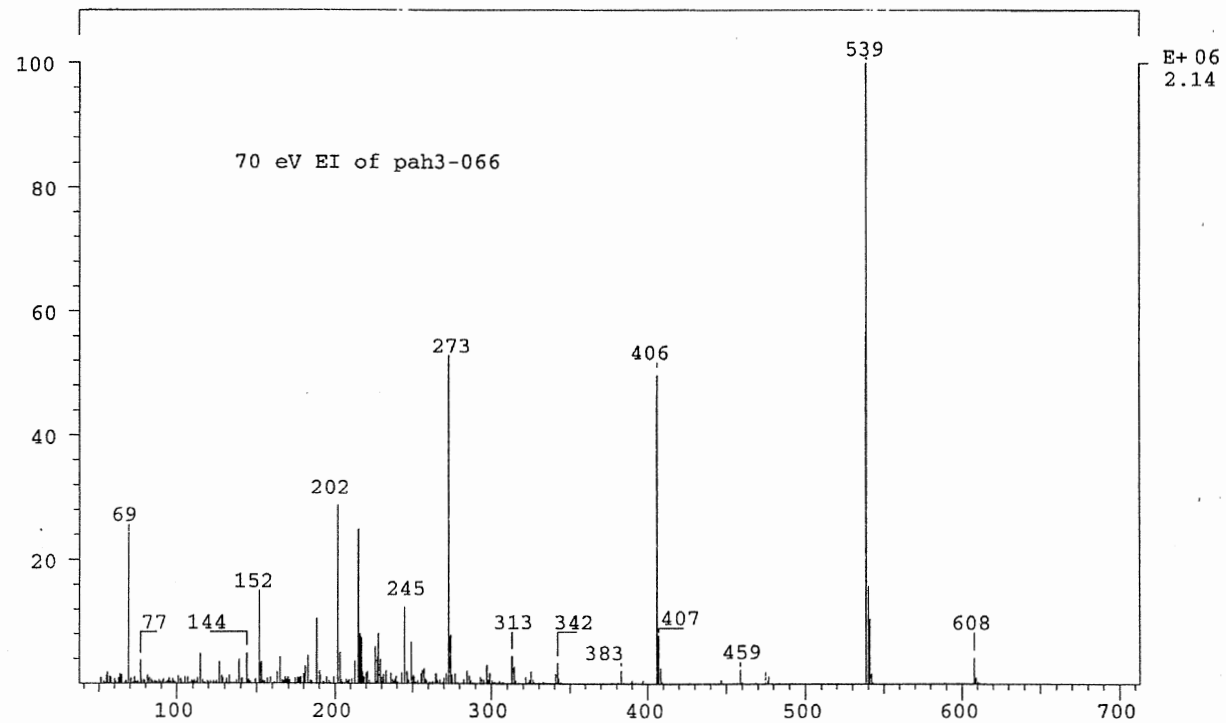
RATES: CHN = \$11.00 per run CHNS = \$15.50 per run

RESULTS				
	#1	#2	#3	AVG
%C	<u>43.44</u>	<u>43.44</u>		<u>43.44</u>
%H	<u>2.41</u>	<u>2.30</u>		<u>2.36</u>
%N				
%S				

Elemental analysis of 3F triflate

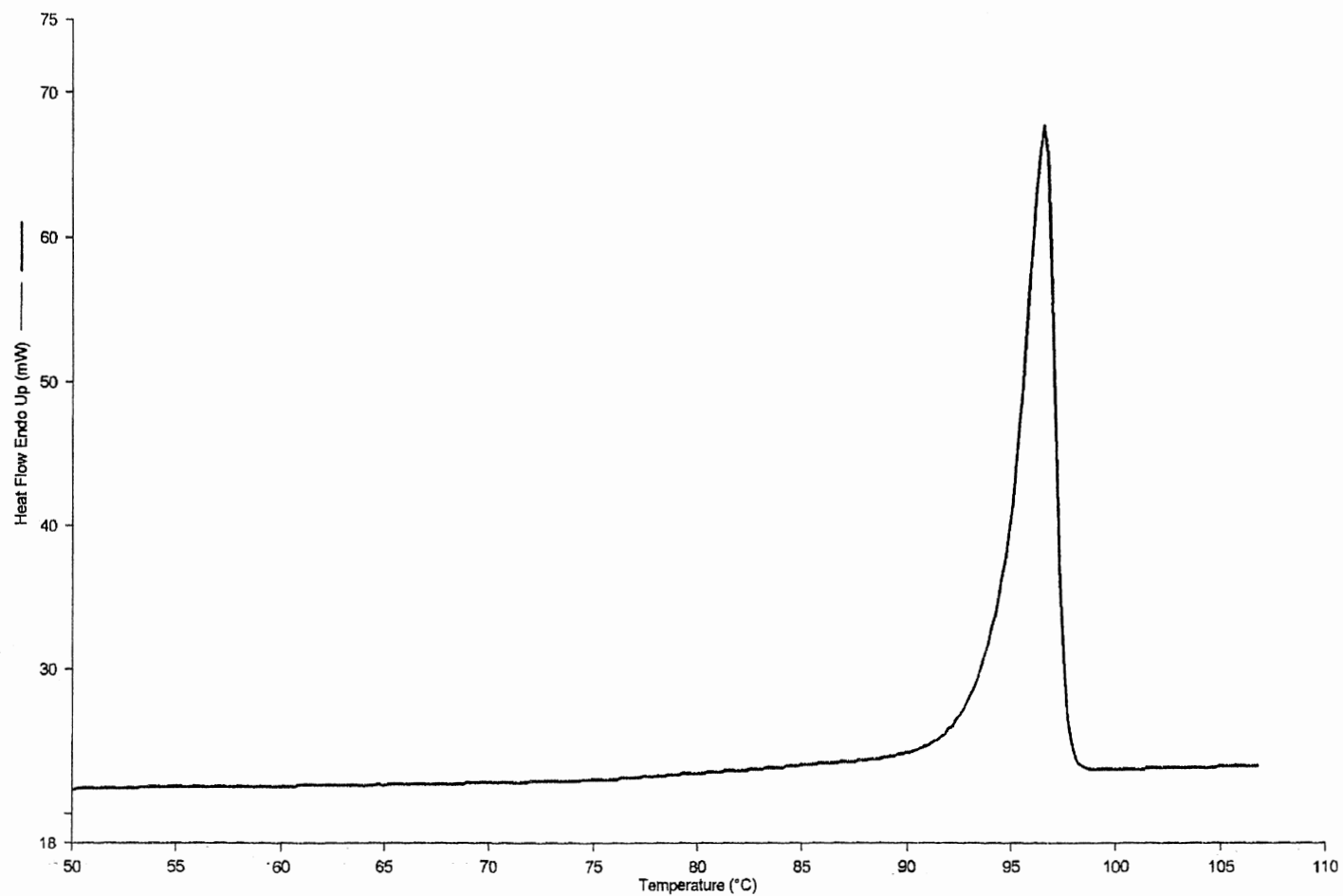
HRMS of 3F triflate

Peak: 1000.00 mmu



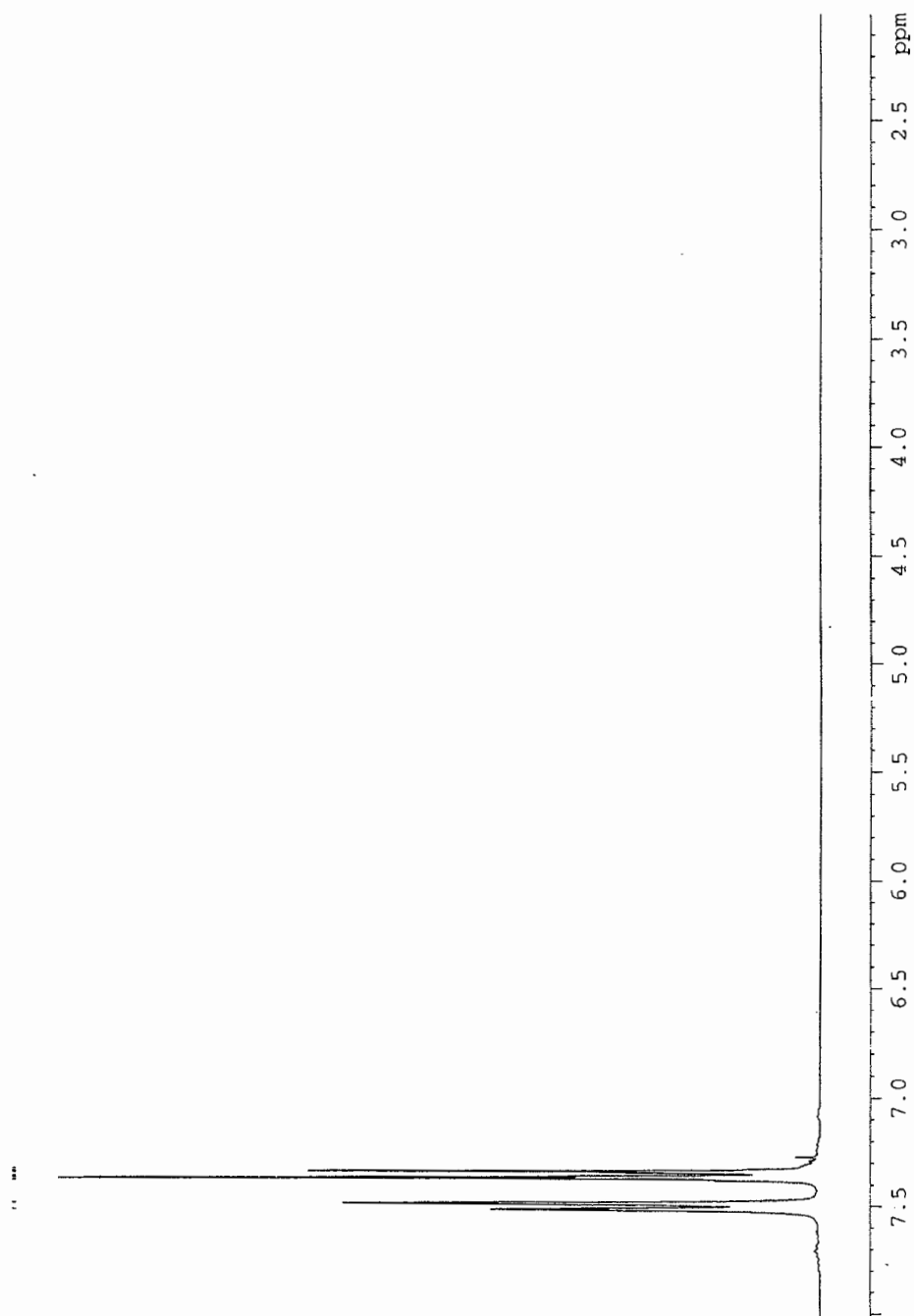
Melting point of 6F triflate

Perkin-Elmer Thermal Analysis

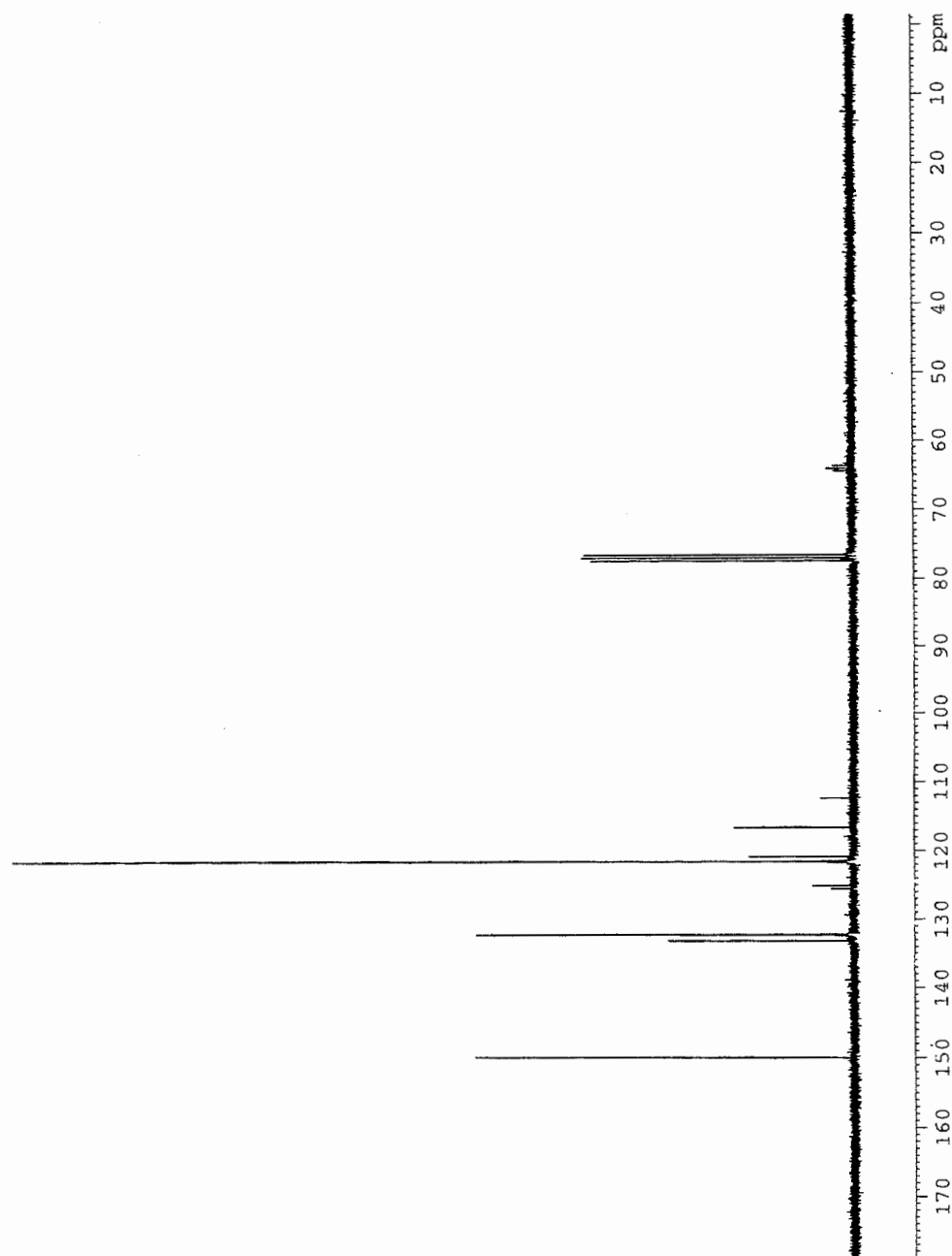


1) Heat from 50.00°C to 250.00°C at 10.00°C/min

4/7/99 8:50:10 AM



Proton NMR of 6F triflate



Carbon NMR of 6F triflate

Sample ID: Cal 13-068 Formula: $\text{C}_{17}\text{H}_8\text{O}_6\text{S}_2\text{F}_{12}$

Crystallization solvent(s): Ethanol

Theoretical weight percents (we can calculate these for you if you wish):

%C= 34.01 %H= 1.34 %N= %S=

Number of runs requested 2. You are charged for ⁴ each run. If you wish, save money and sample by just requesting one. For critical work you might want to request two or more runs.

Check here ☐ if you absolutely require %S. This is not the normal configuration of the instrument, and you may have to wait a couple of weeks for these results. Check here ☐ if you would like a CHN analysis prior to the CHNS analysis. You will be charged for each run.

Special combustion conditions (if you have information that would help us get better results on your sample, use this space, or attach the information to this form): _____

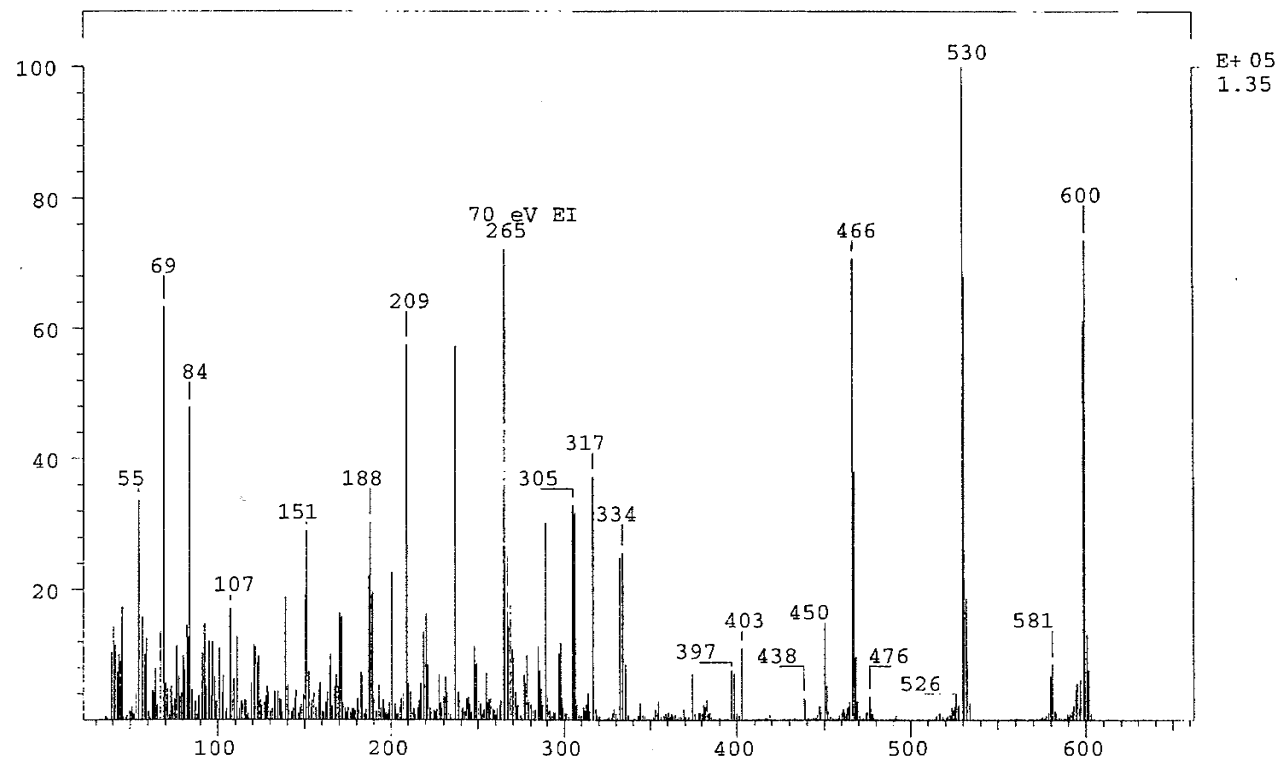
RATES: CHN = \$11.00 per run CHNS = \$15.50 per run

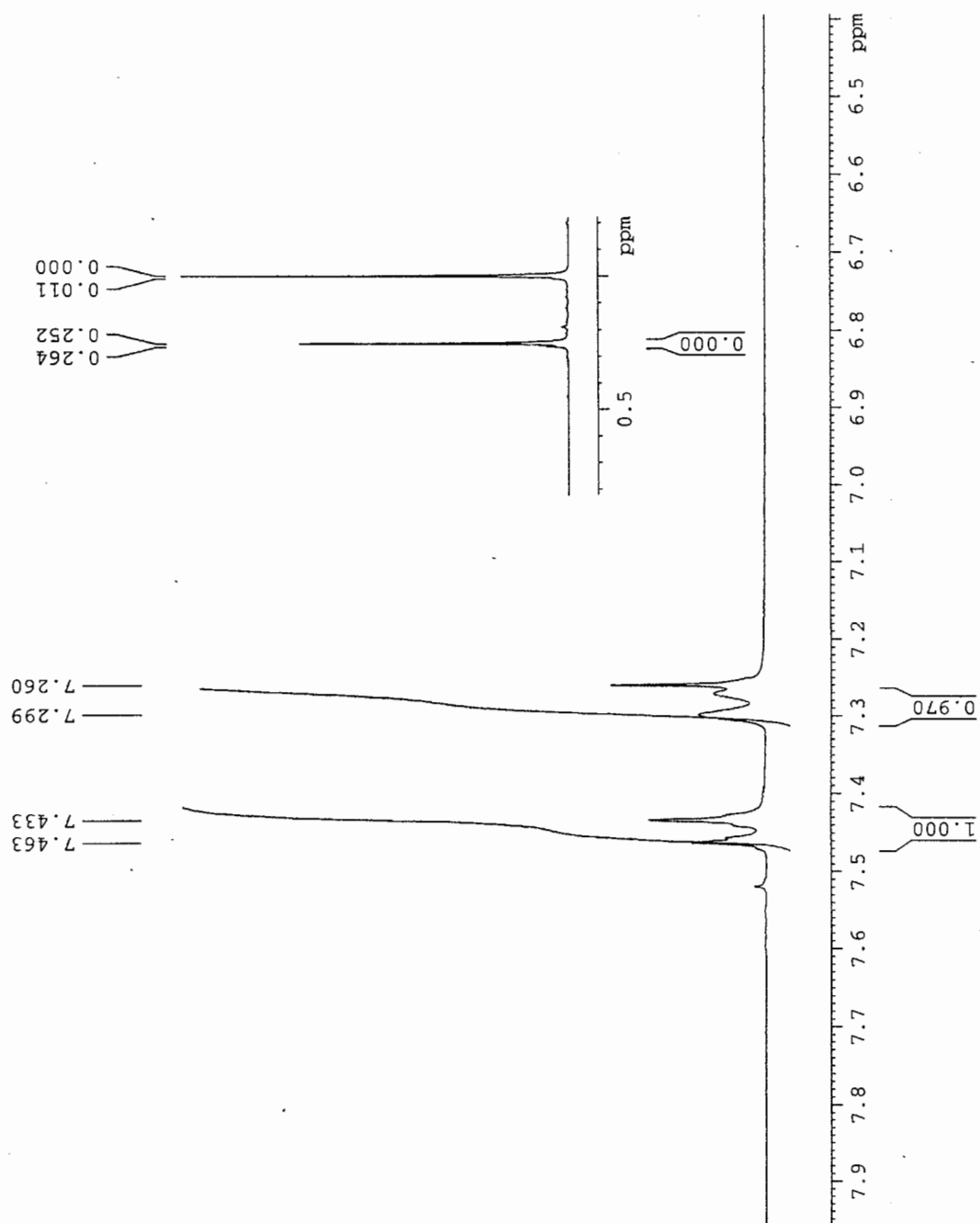
RESULTS

	#1	#2	#3	AVG
%C	33.89	33.69		33.84
%H	1.49	1.43		1.46
%N				
%S				

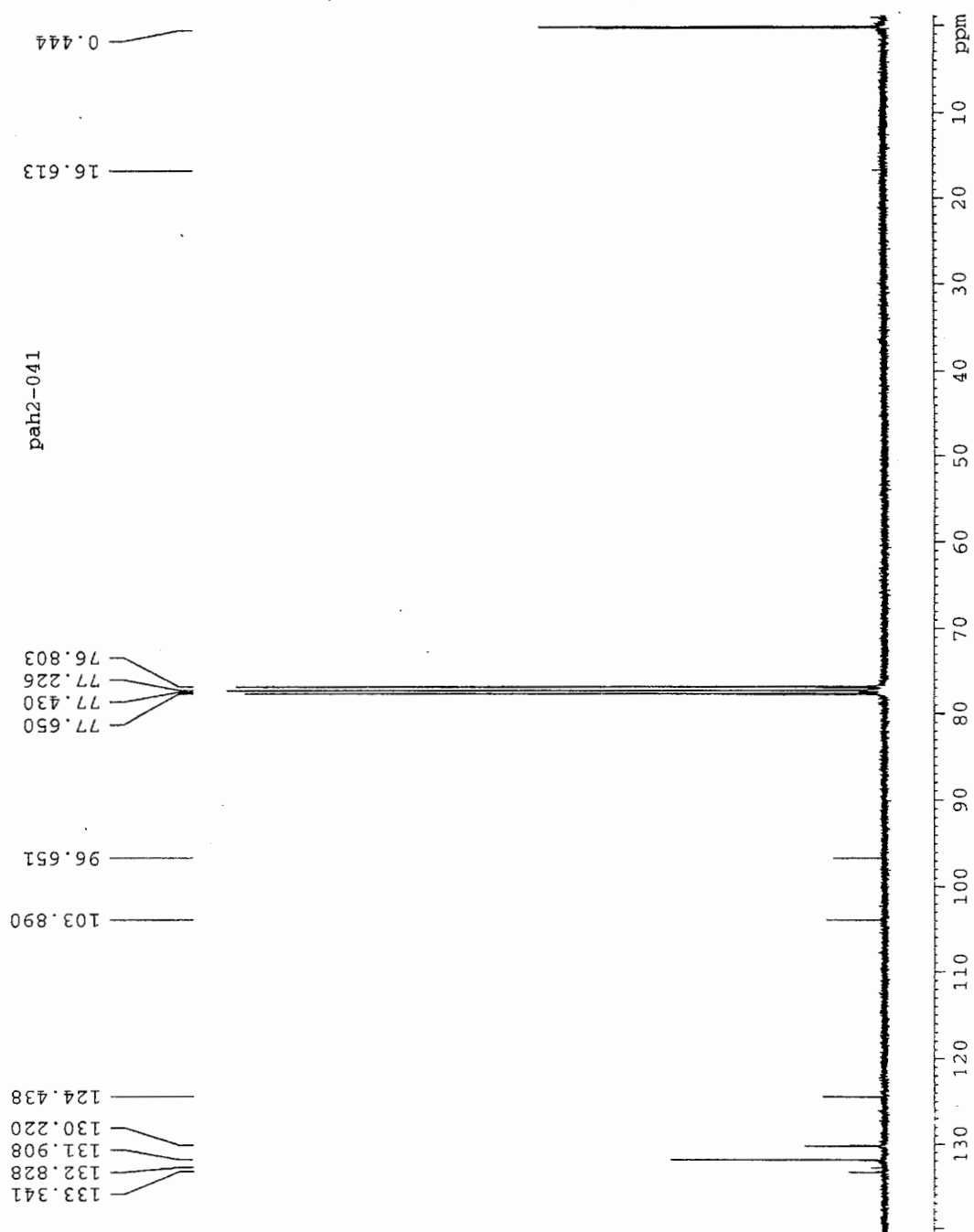
Elemental analysis of 6F triflate

HRMS of 6F triflate

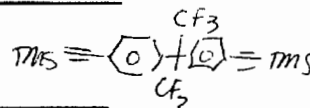




Proton NMR of protected crosslinking 6F monomer



Carbon NMR of protected crosslinking 6F monomer

Lab no. 502-041 PHONE. 4-1122Date: 5/23/00Sample ID: 502-041 Formula: C₂₅H₂₆F₆Si₂Crystallization solvent(s): hexane

Theoretical weight percents (we can calculate these for you if you wish):

%C= 60.46 %H= 5.28 %N= _____ %S= _____Number of runs requested 2. You are charged for each run. The default is two.

Check here ☐ if you absolutely require %S. This is not the normal configuration of the instrument, and you may have to wait a couple of weeks for these results. Check here ☐ if you would like a CHN analysis prior to the CHNS analysis. You will be charged for each run.

Special combustion conditions (if you have literature references or other specific information that would help get better results on your sample, use this space, or attach the information to this form): _____

RATES: CHN = \$11.00 per run CHNS = \$15.50 per run

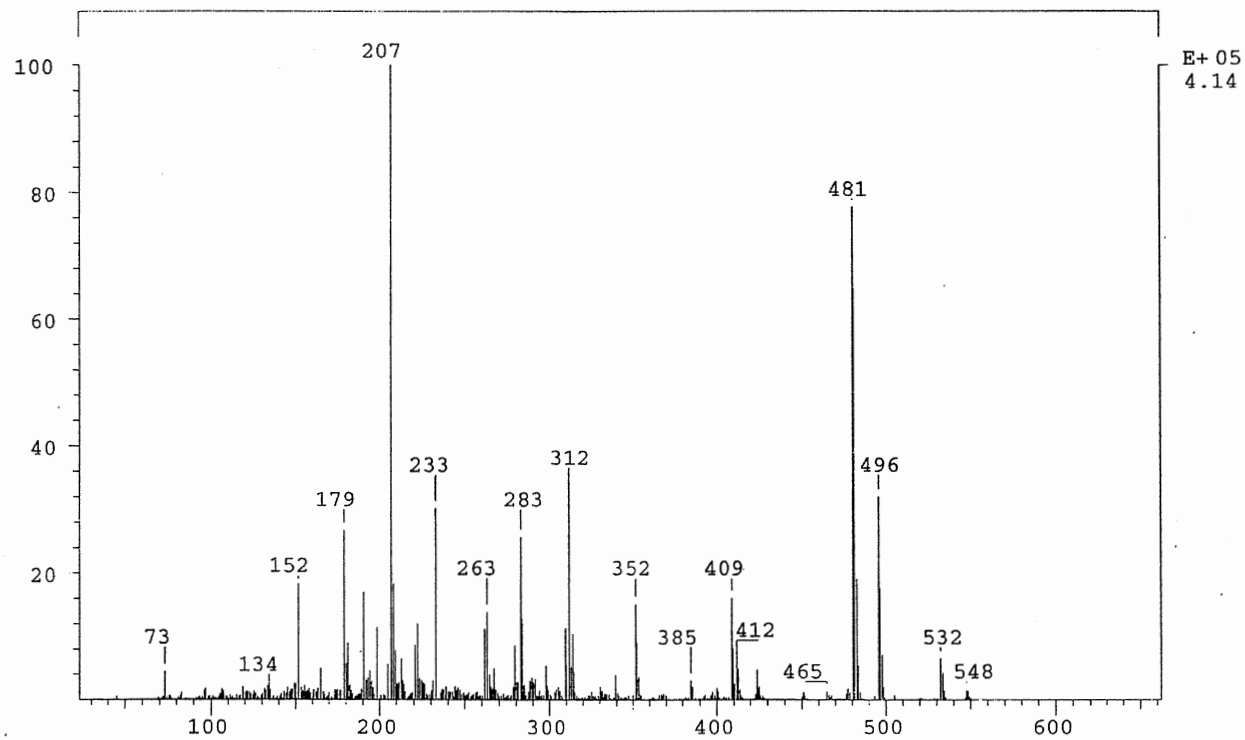
RESULTS

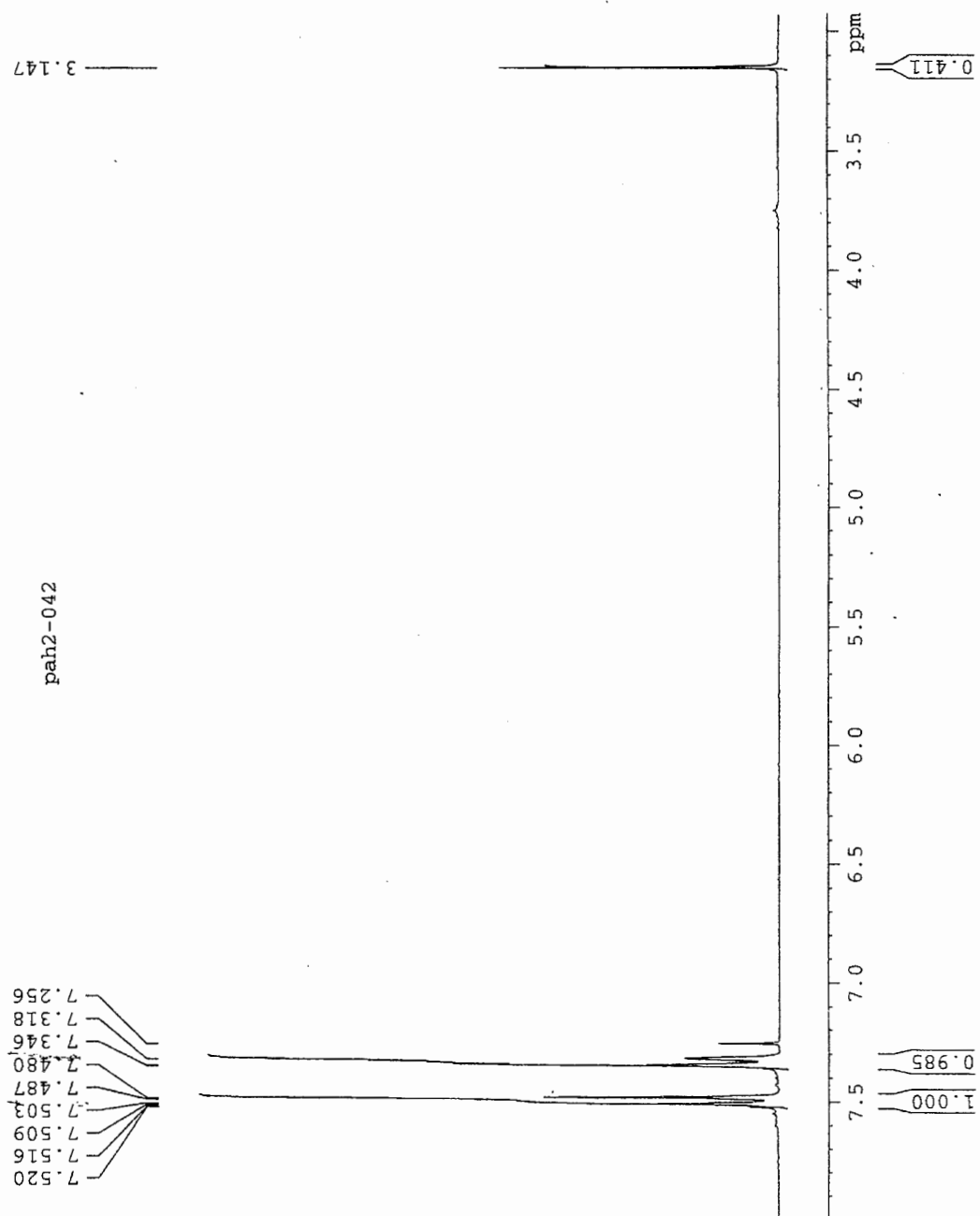
	#1	#2	#3	#4	AVG
%C	<u>60.49</u>	<u>60.36</u>			
%H	<u>5.41</u>	<u>5.63</u>			
%N	<u>-</u>	<u>-</u>			
%S	<u>0.37 ?</u>	<u>0.39 ?</u>			

Elemental analysis of protected crosslinking 6F monomer

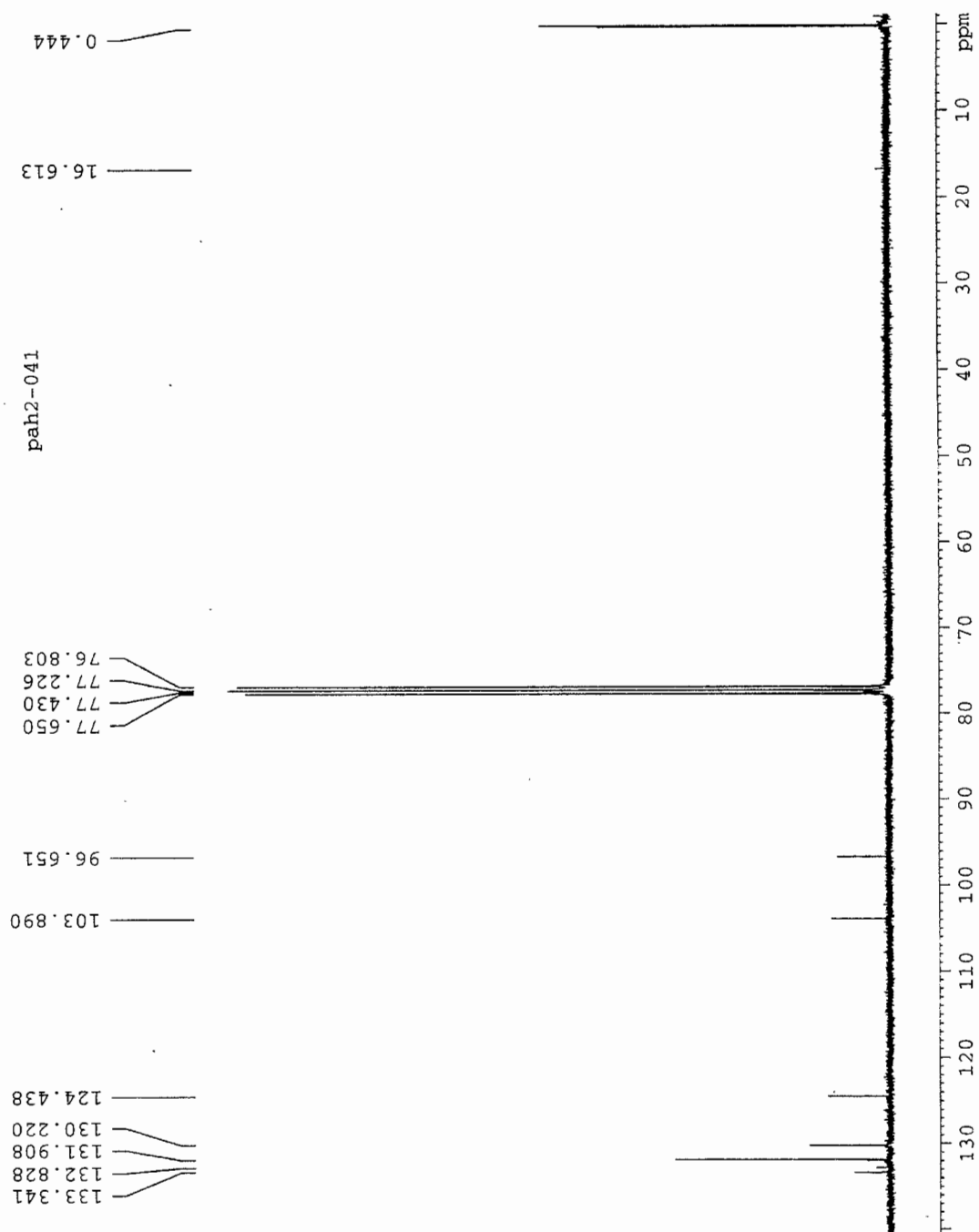
HRMS of protected crosslinking 6F monomer

Peak: 1000.00 mmu

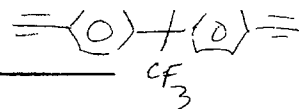




Proton NMR of crosslinking 6F monomer



Carbon NMR of crosslinking 6F monomer

Sample ID: peh2-044 Formula: C₁₉H₁₀F₆Crystallization solvent(s): hexane

Theoretical weight percents (we can calculate these for you if you wish):

%C= 64.78 %H= 2.86 %N= _____ %S= _____Number of runs requested 2. You are charged for each run. The default is two.

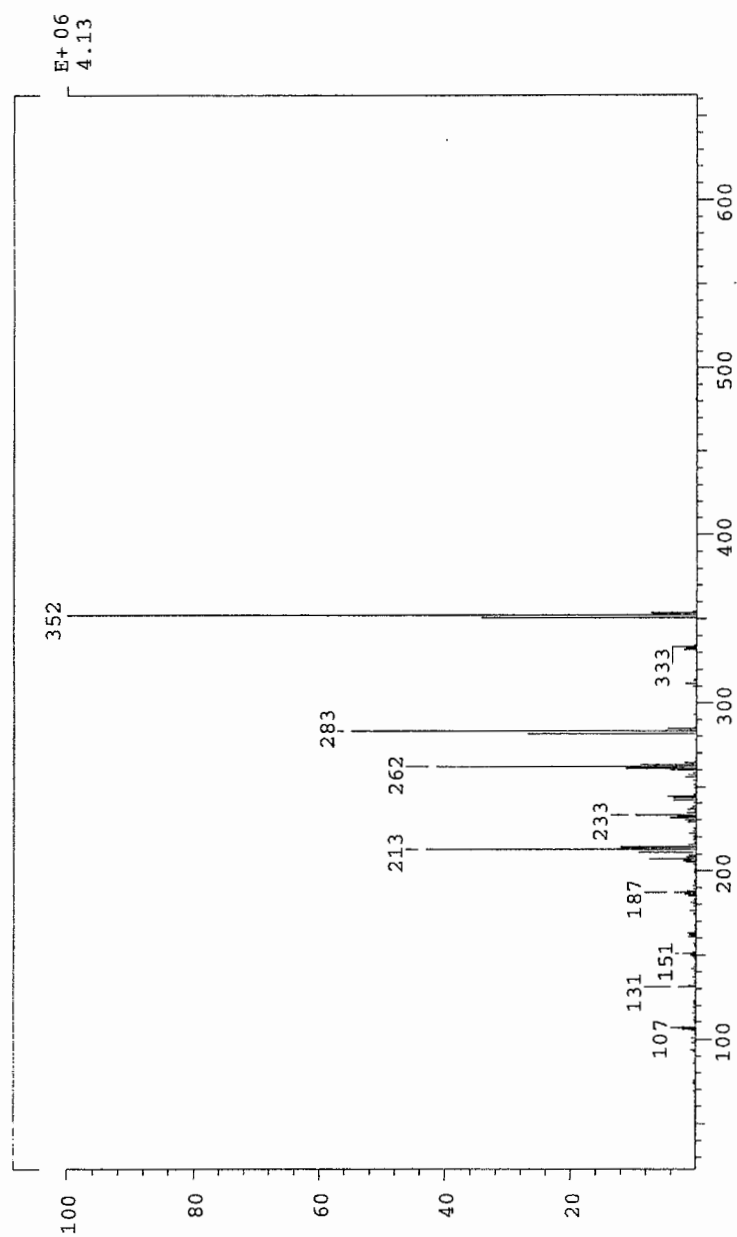
Check here ☐ if you absolutely require %S. This is not the normal configuration of the instrument, and you may have to wait a couple of weeks for these results. Check here ☐ if you would like a CHN analysis prior to the CHNS analysis. You will be charged for each run.

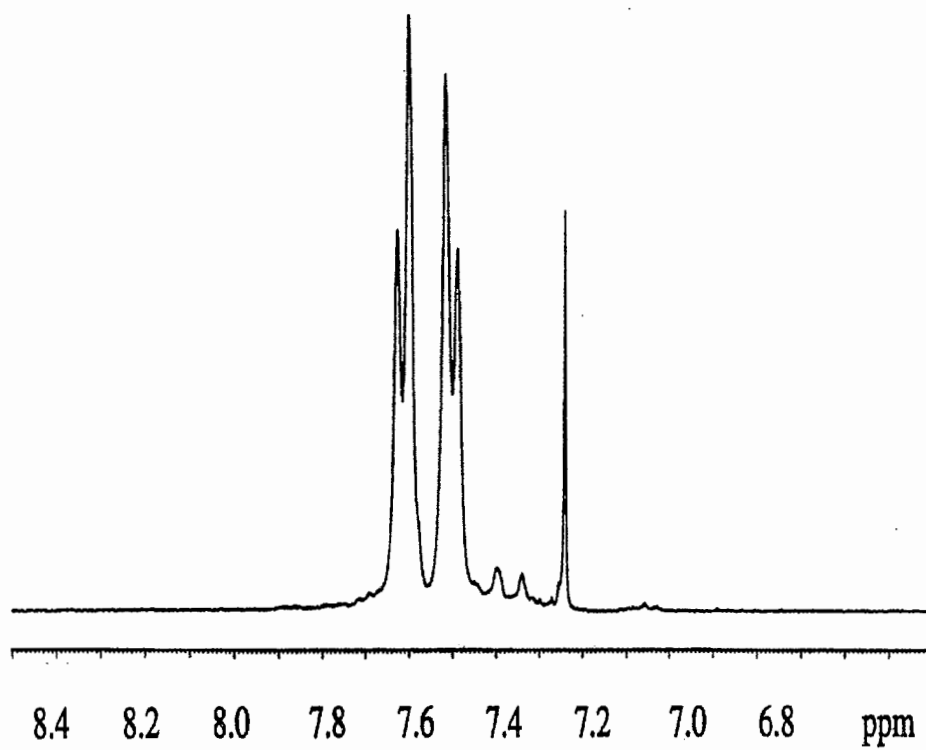
Special combustion conditions (if you have literature references or other specific information that would help us get better results on your sample, use this space, or attach the information to this form): _____

RATES: CHN = \$11.00 per run CHNS = \$15.50 per run

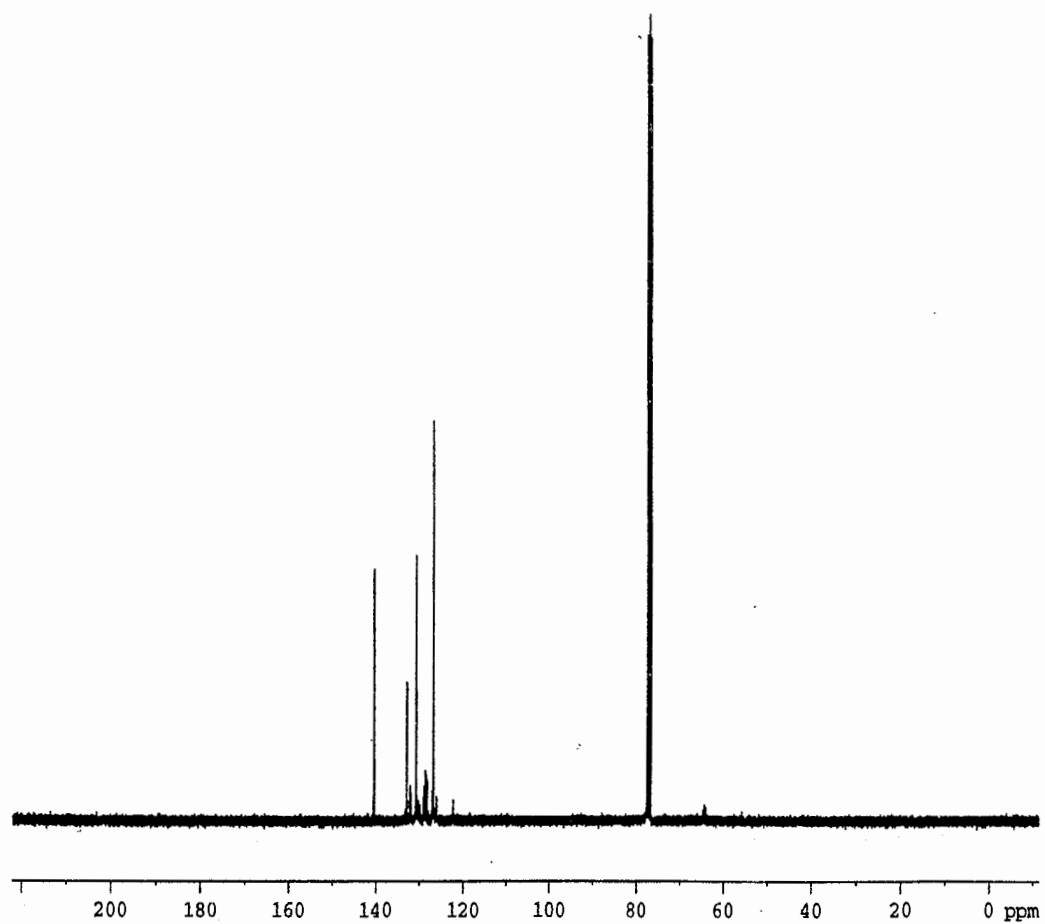
	RESULTS				
	#1	#2	#3	#4	AVG
%C	64.65	64.77			
%H	3.50	3.96			
%N	-	-			
%S	1.32 ??	2.96 !?			

Elemental analysis of crosslinking 6F monomer



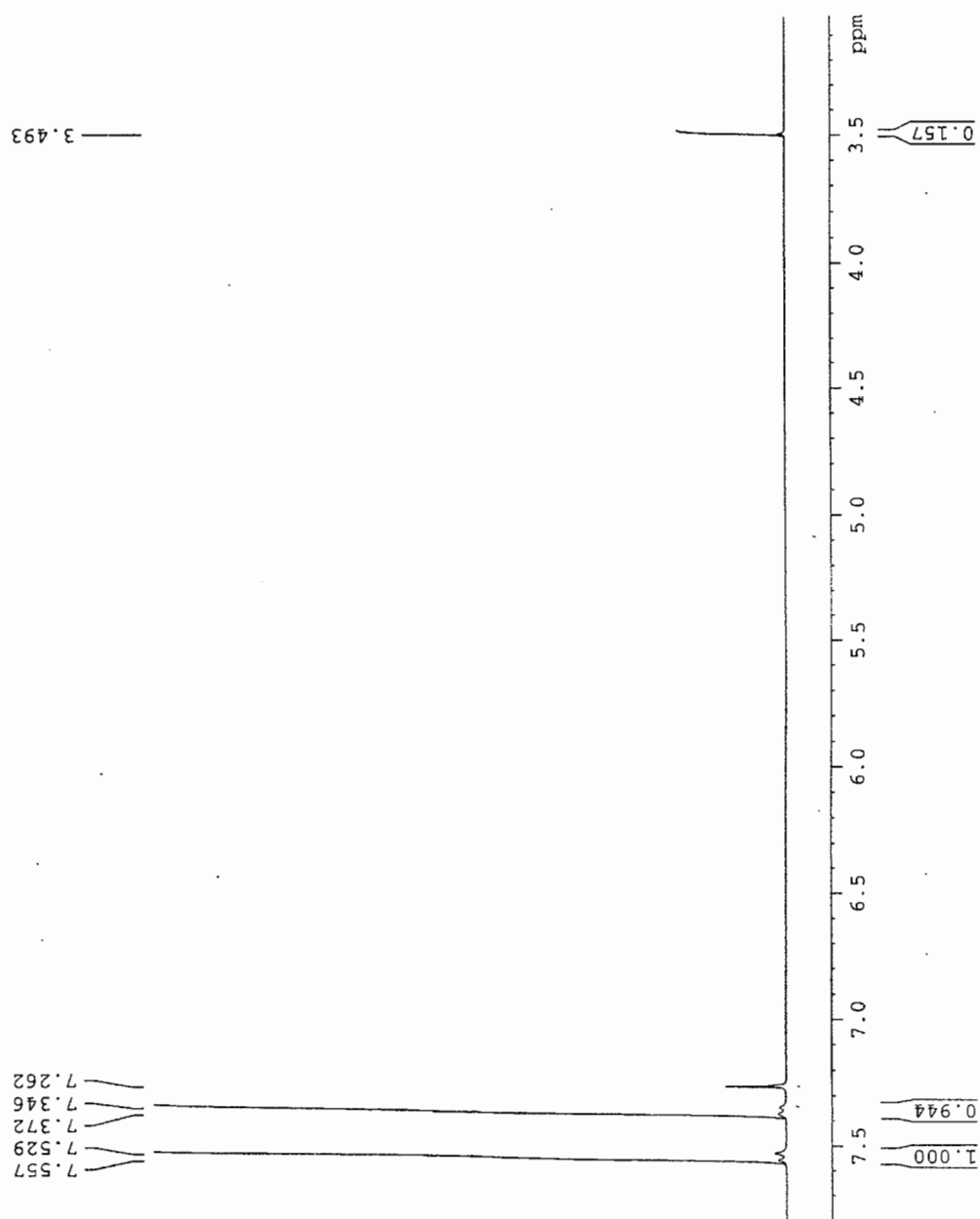


Proton NMR of 6F polymer



Carbon NMR of 6F polymer

Elemental analysis of 6F polymer



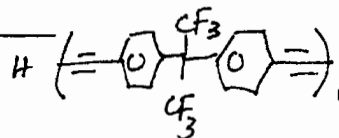
Proton NMR of crosslinking 6F polymer

Sample ID: Lab 2-045 Formula: C₁₉H₁₀F₆

Crystallization solvent(s): _____

Theoretical weight percents (we can calculate these for you if you wish):

%C= 64.78 %H= 2.86 %N= _____ %S= _____



Number of runs requested 2. You are charged for each run. The default is two.

Check here ~~if~~ if you absolutely require %S. This is not the normal configuration of the instrument, and you may have to wait a couple of weeks for these results. Check here _____ if you would like a CHN analysis prior to the CHNS analysis. You will be charged for each run.

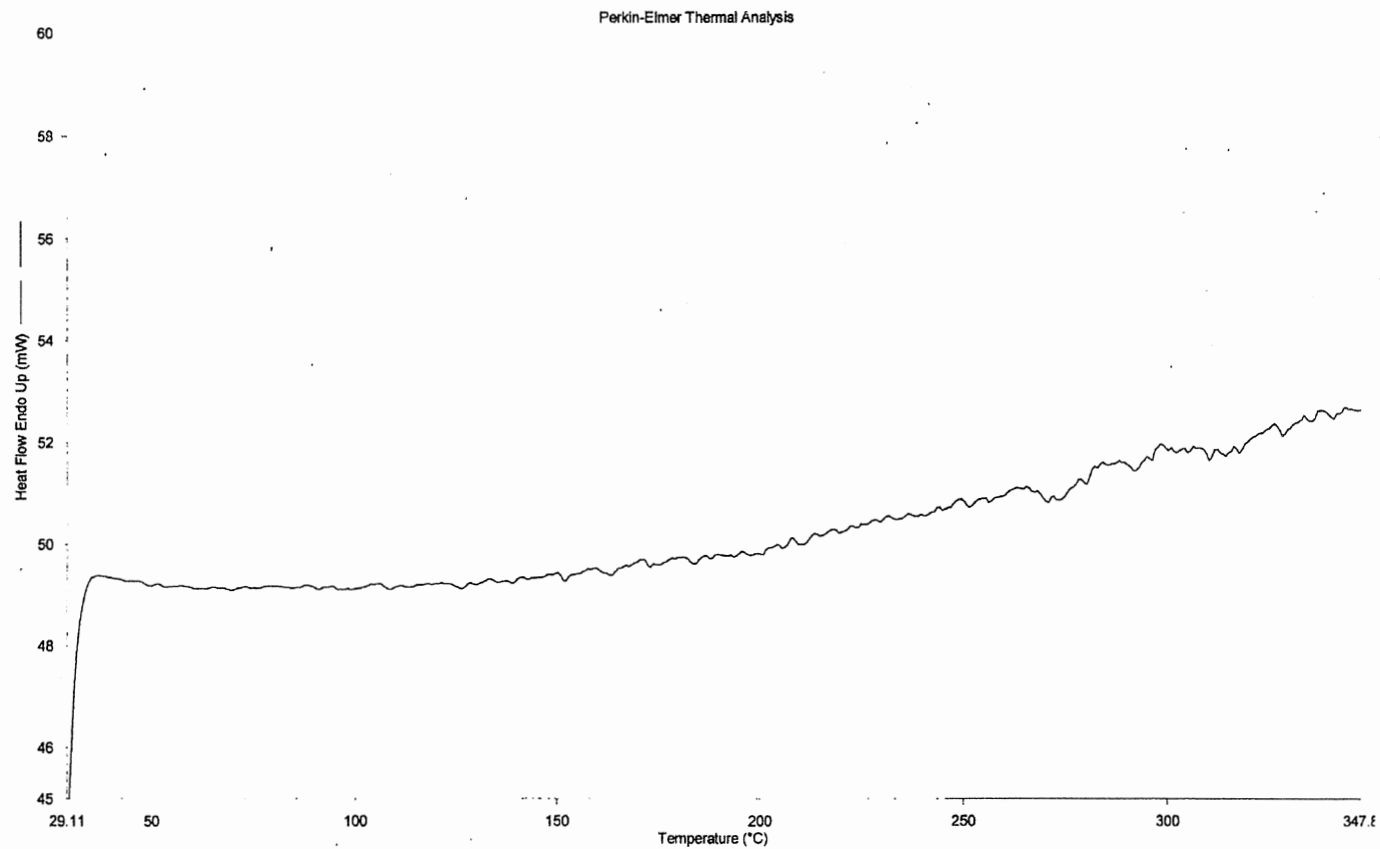
Special combustion conditions (if you have literature references or other specific information that would help us get better results on your sample, use this space, or attach the information to this form): _____

RATES: CHN = \$11.00 per run CHNS = \$15.50 per run

RESULTS					
	#1	#2	#3	#4	AVG
%C	58.56	58.97			
%H	3.26	3.07			
%N	1.47	1.34			
%S					

Elemental analysis of crosslinking 6F polymer

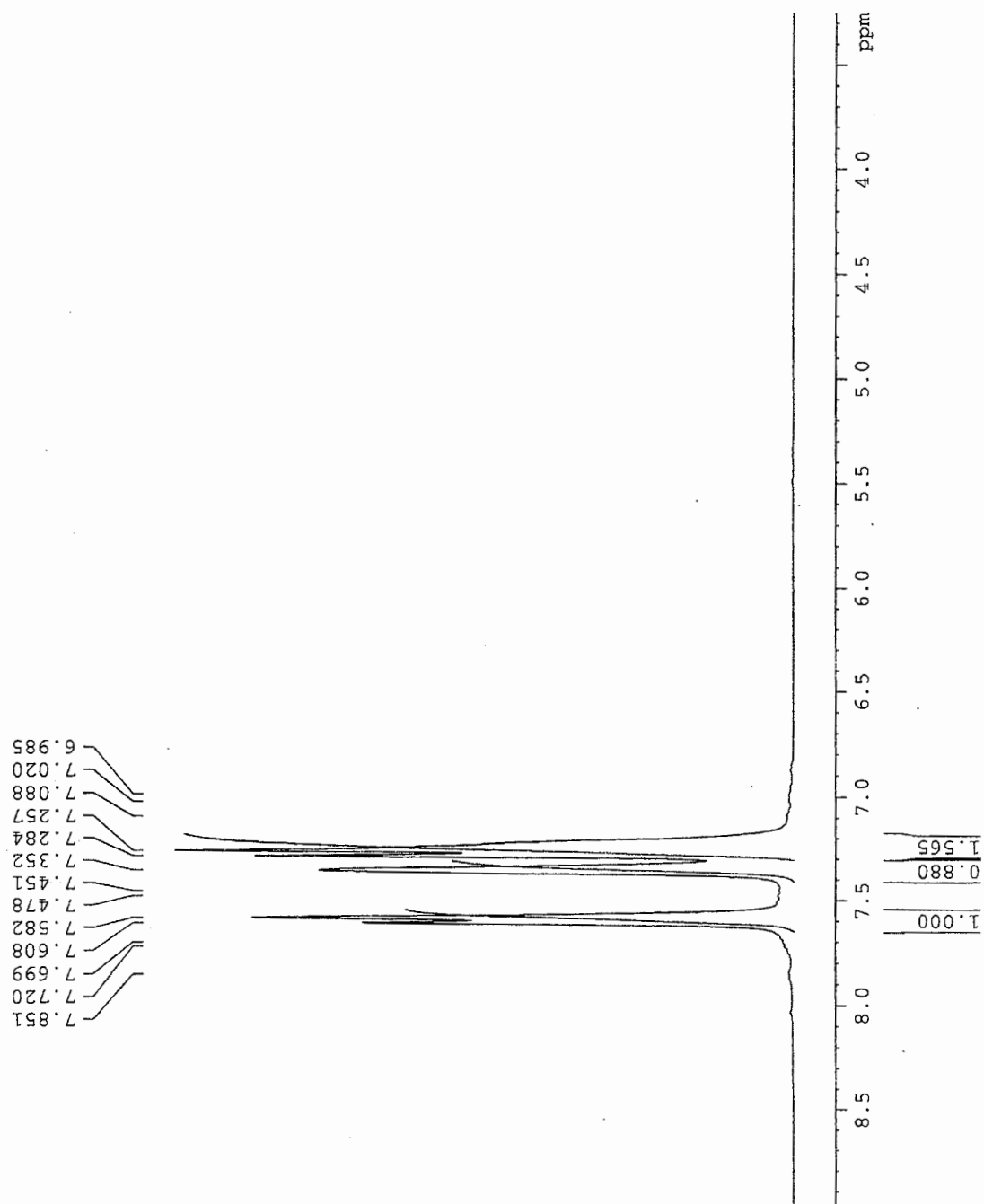
DSC of crosslinking 6F polymer



1) Heat from 25.00°C to 350.00°C at 20.00°C/min
2) Cool from 350.00°C to 25.00°C at 40.00°C/min

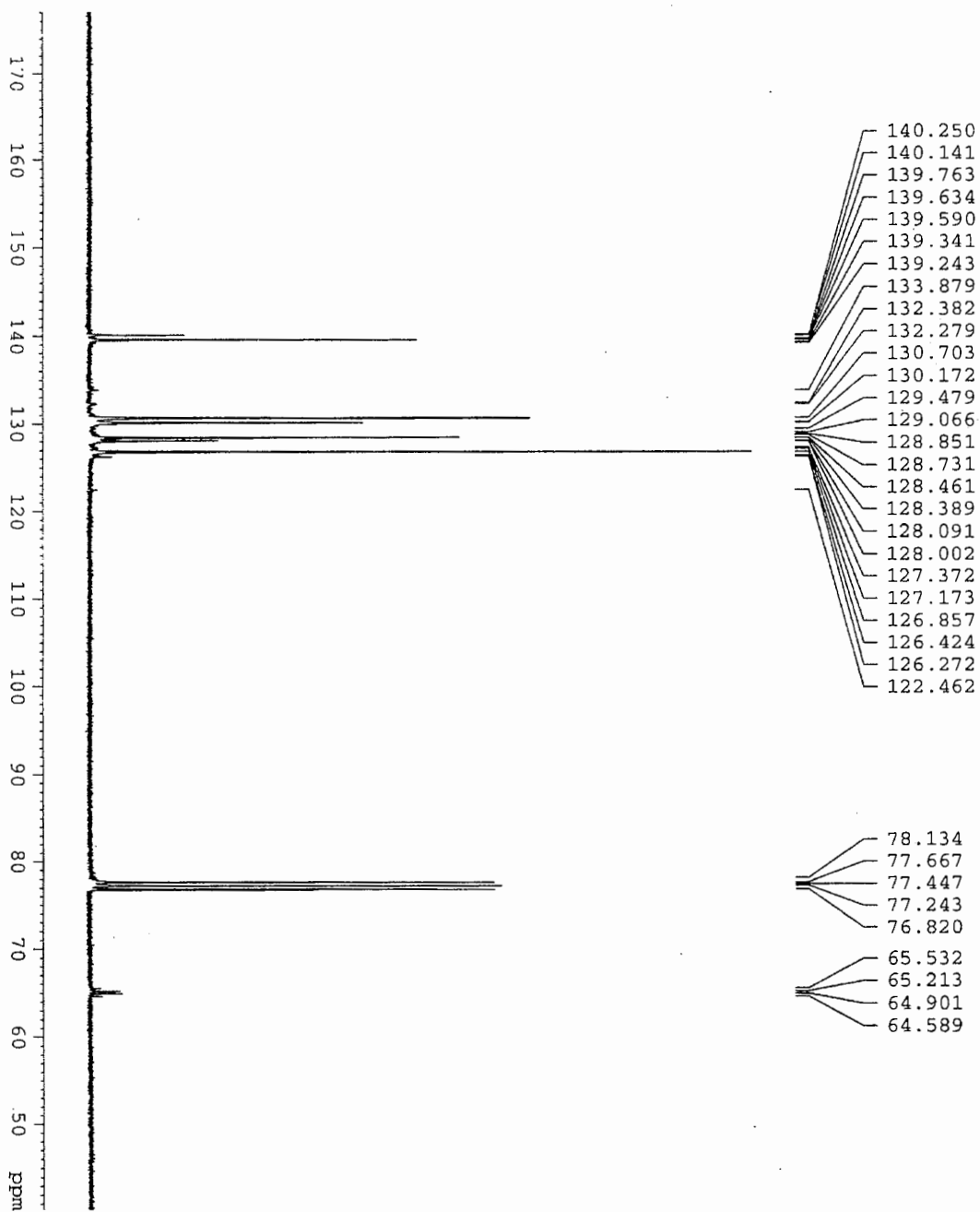
3) Hold for 1.0 min at 25.00°C
4) Heat from 25.00°C to 350.00°C at 20.00°C/min

6/16/00 11:21:24 AM



Proton NMR of 3F polymer

Carbon NMR of 3F polymer



Sample ID: PAH2-006 Formula: C₂₀H₁₃F₃ polymer

Crystallization solvent(s): _____

Theoretical weight percents (we can calculate these for you if you wish):

%C= 77.41 %H= 4.22 %N= _____ %S= _____

Number of runs requested 2. You are charged for each run. The default is two.

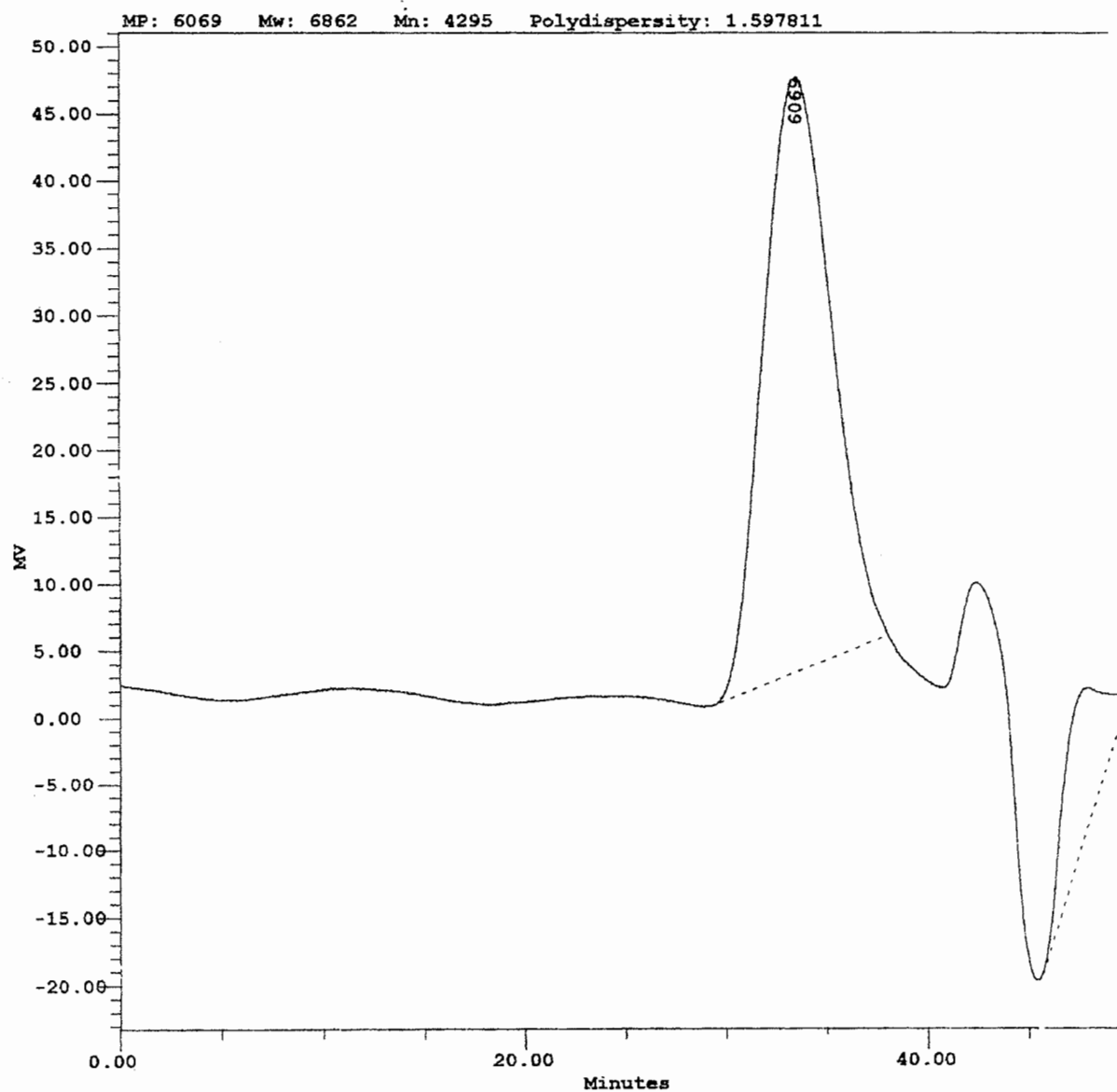
Check here ☐ if you absolutely require %S. This is not the normal configuration of the instrument, and you may have to wait a couple of weeks for these results. Check here ☐ if you would like a CHN analysis prior to the CHNS analysis. You will be charged for each run.

Special combustion conditions (if you have literature references or other specific information that would help us get better results on your sample, use this space, or attach the information to this form): _____

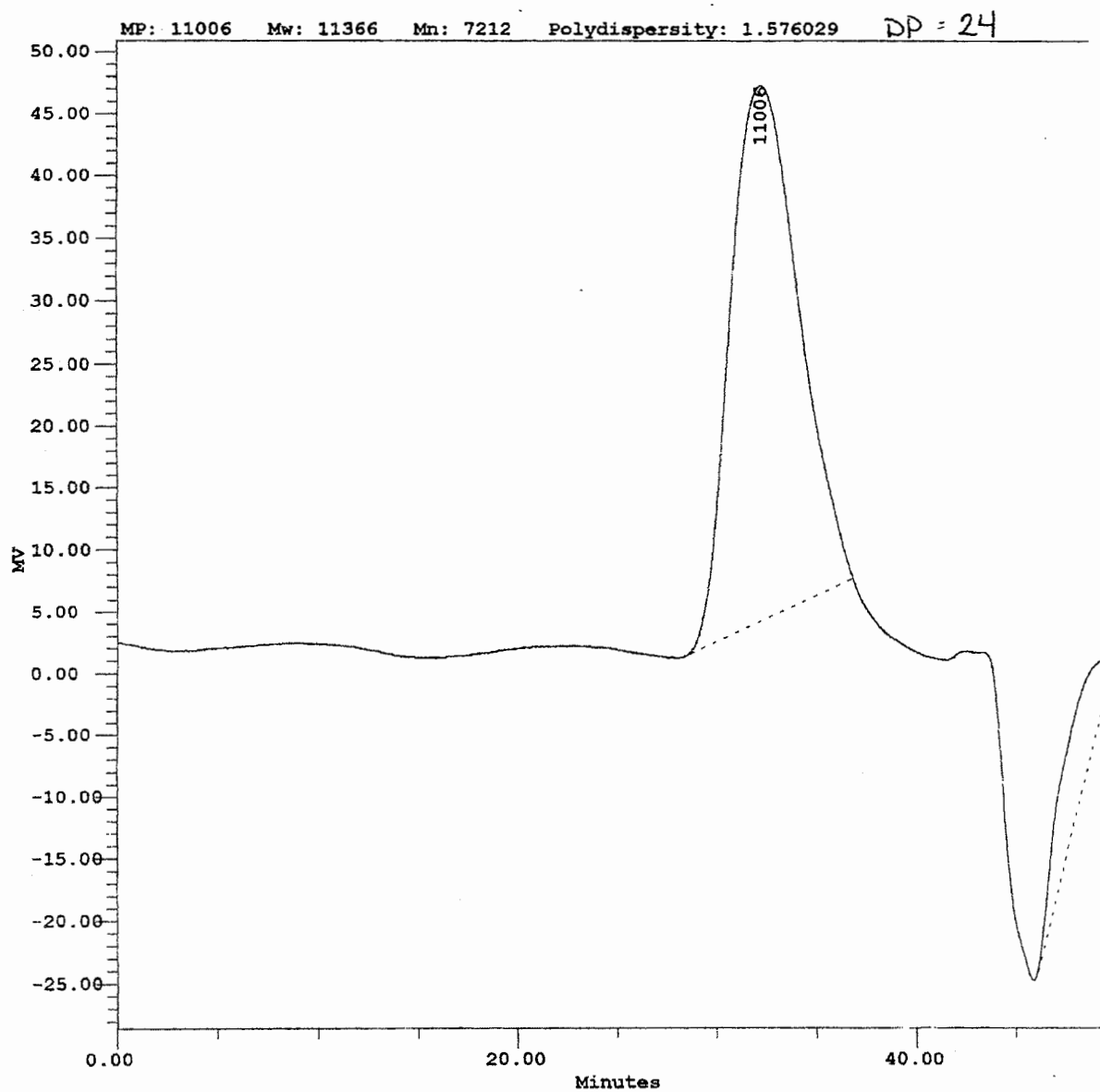
RATES: CHN = \$11.00 per run CHNS = \$15.50 per run

RESULTS				
	#1	#2	#3	#4
%C	76.44	76.55		
%H	4.47	4.48		
%N	0.31	0.27		
%S				
				AVG
				76.645
				4.475

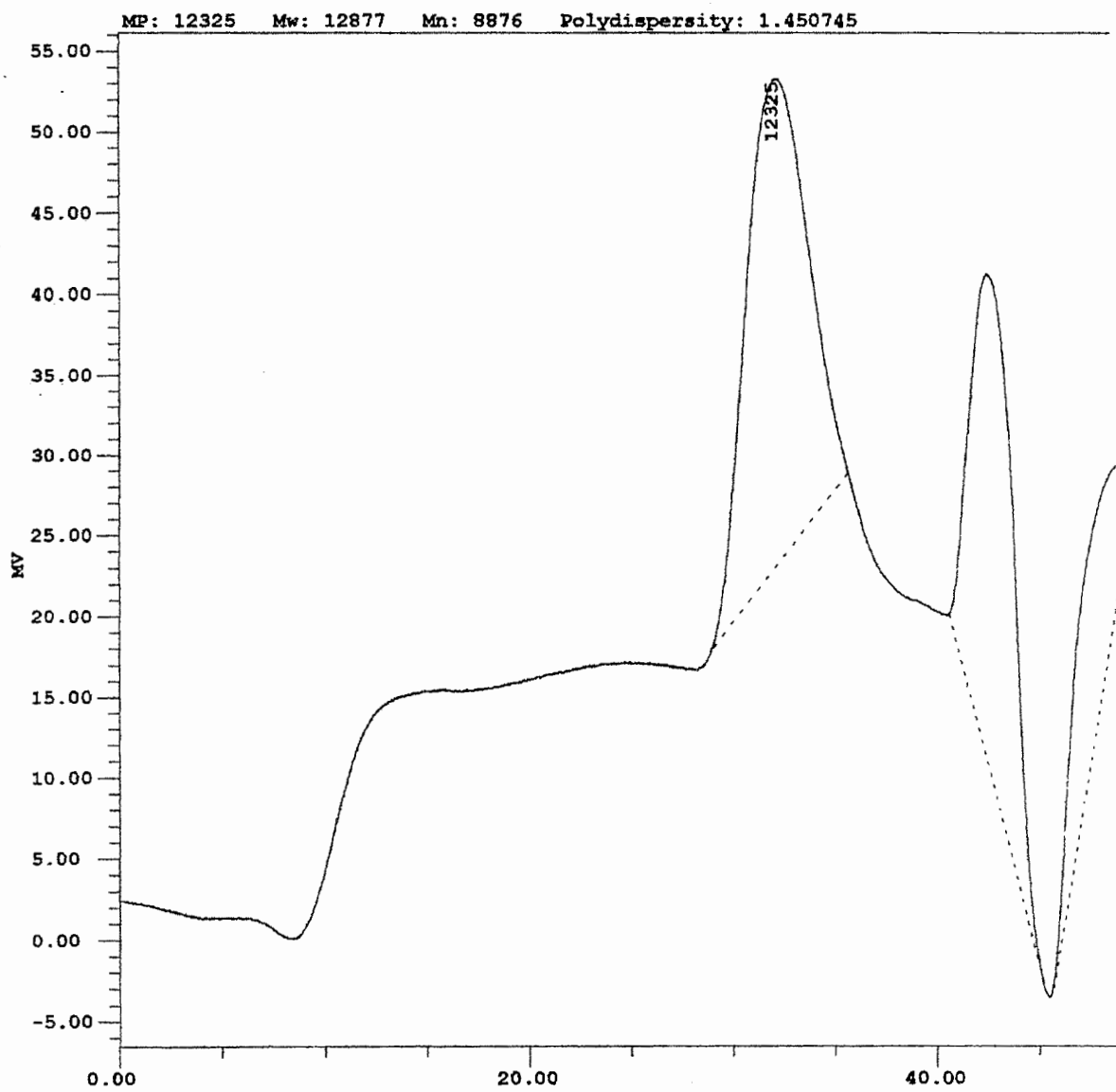
Elemental analysis of 3F polymer



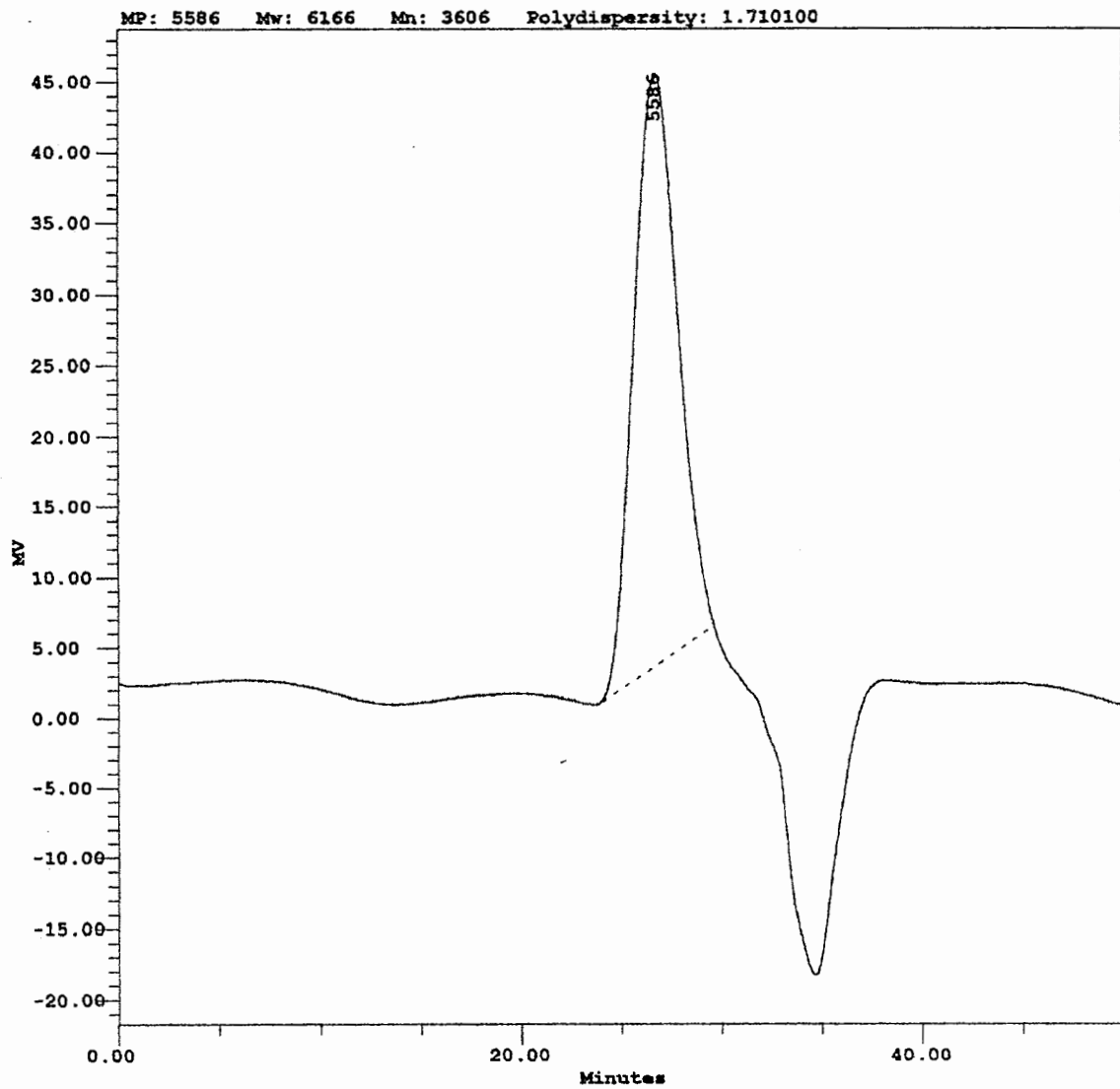
Entry 1



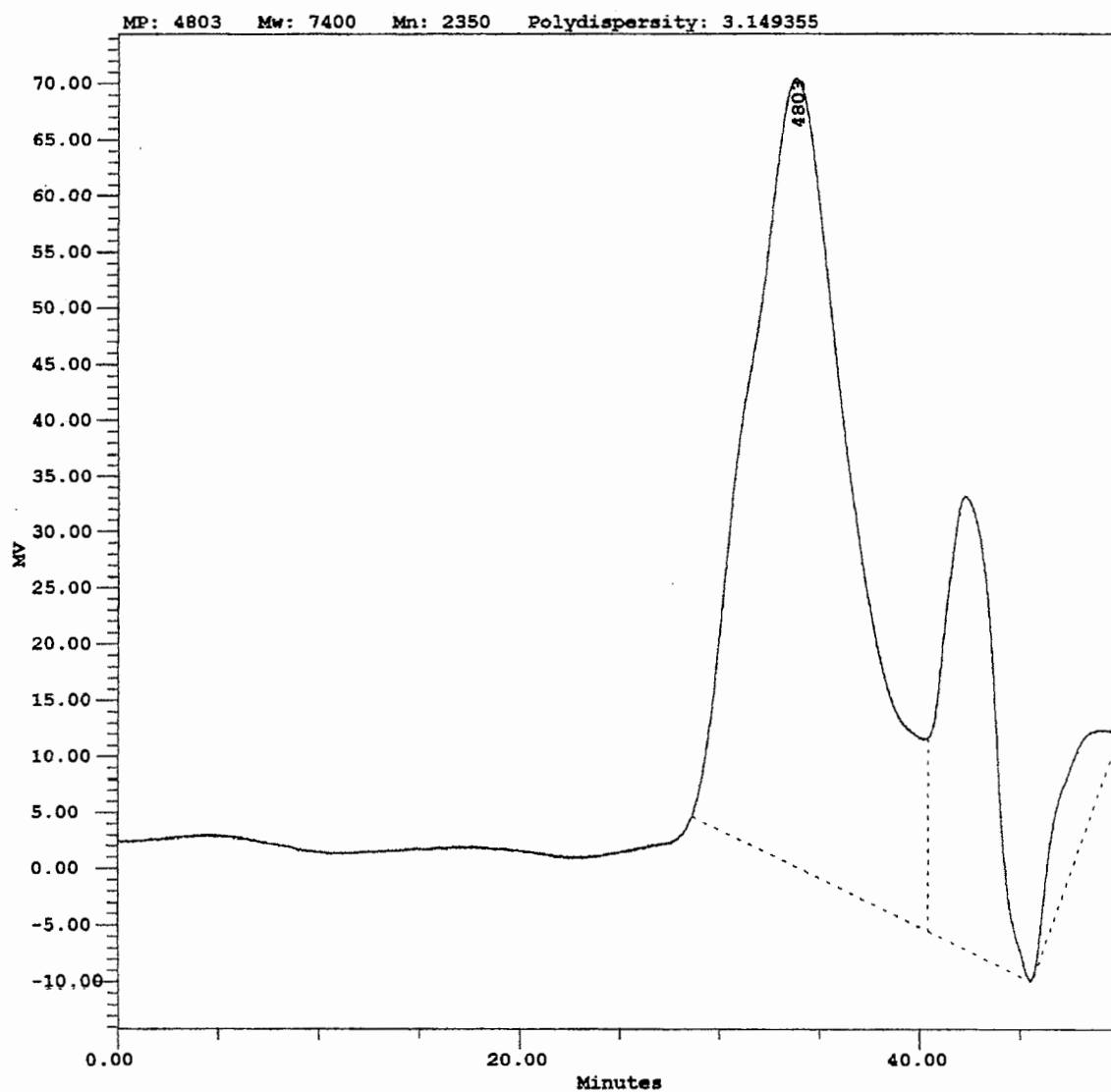
Entry 2



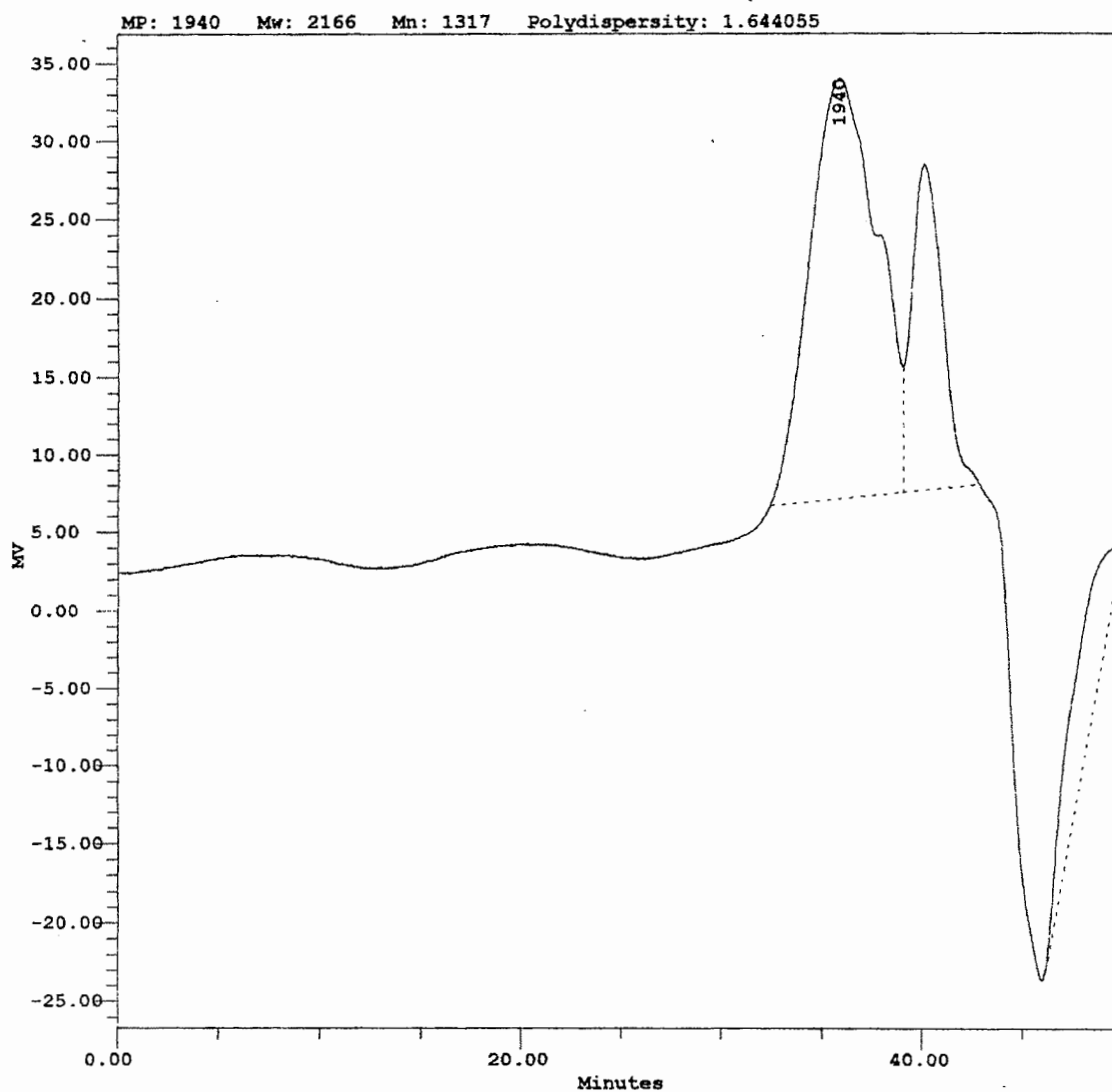
Entry 3



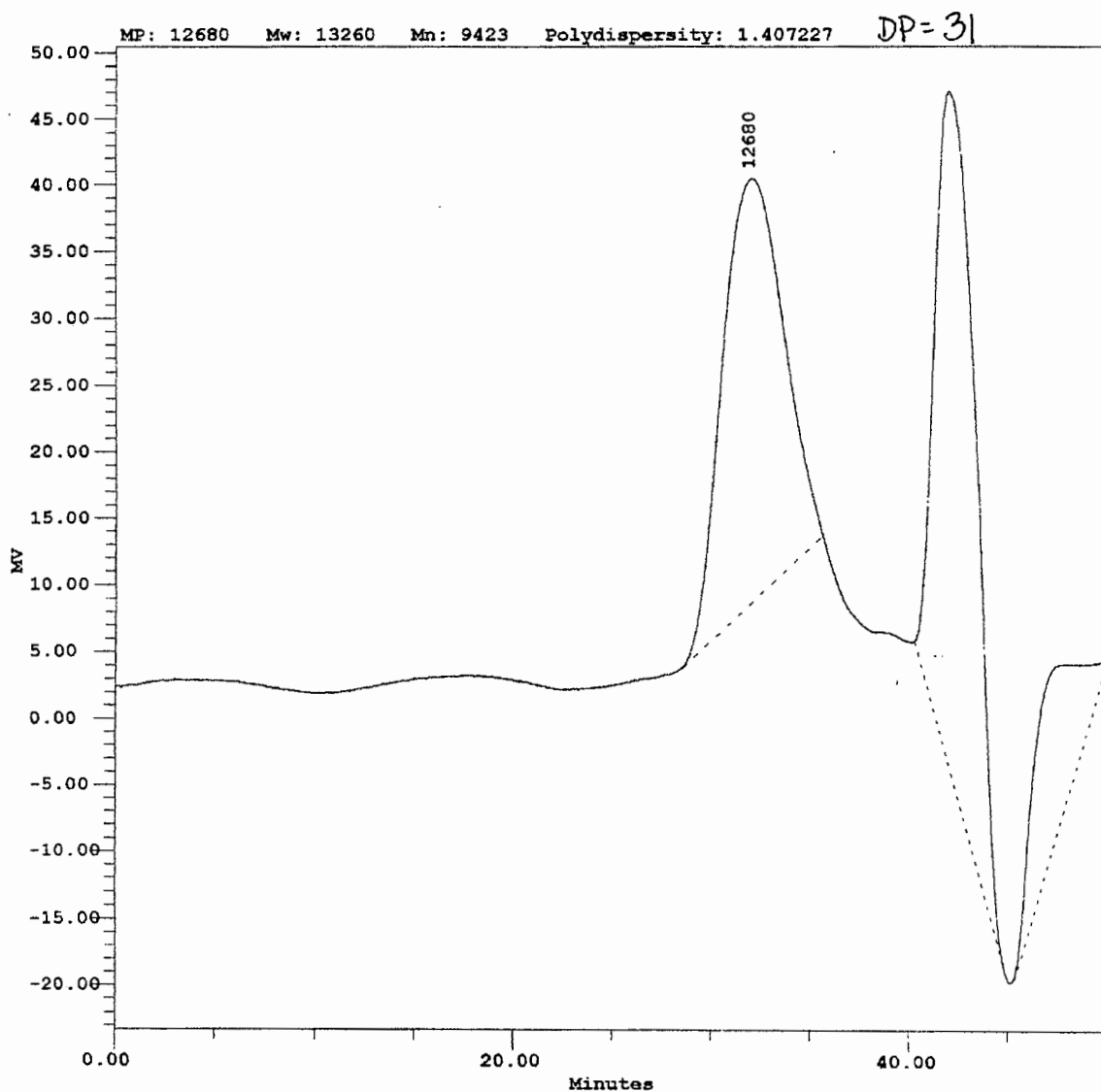
Entry 4



Entry 5

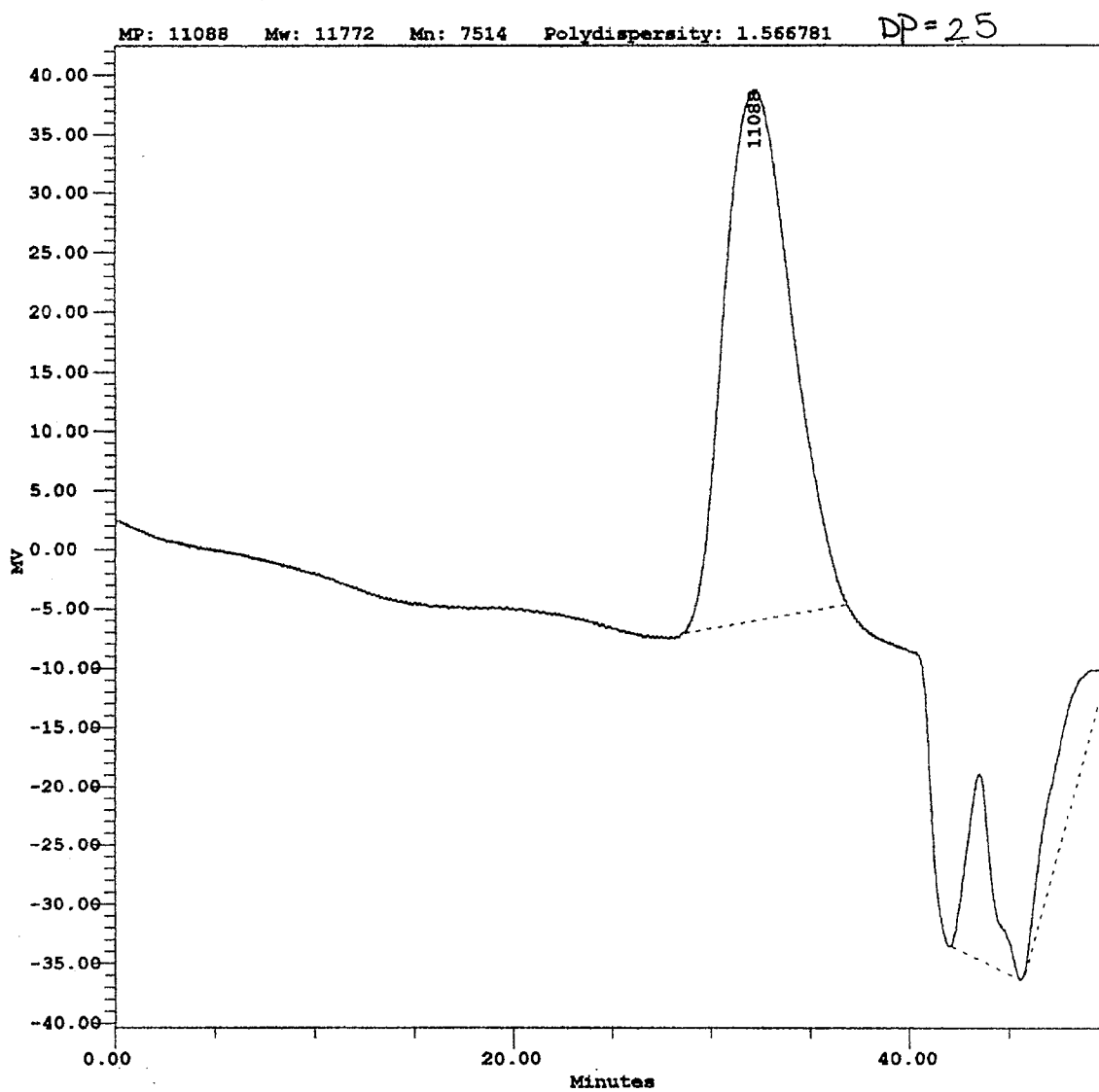


Entry 6



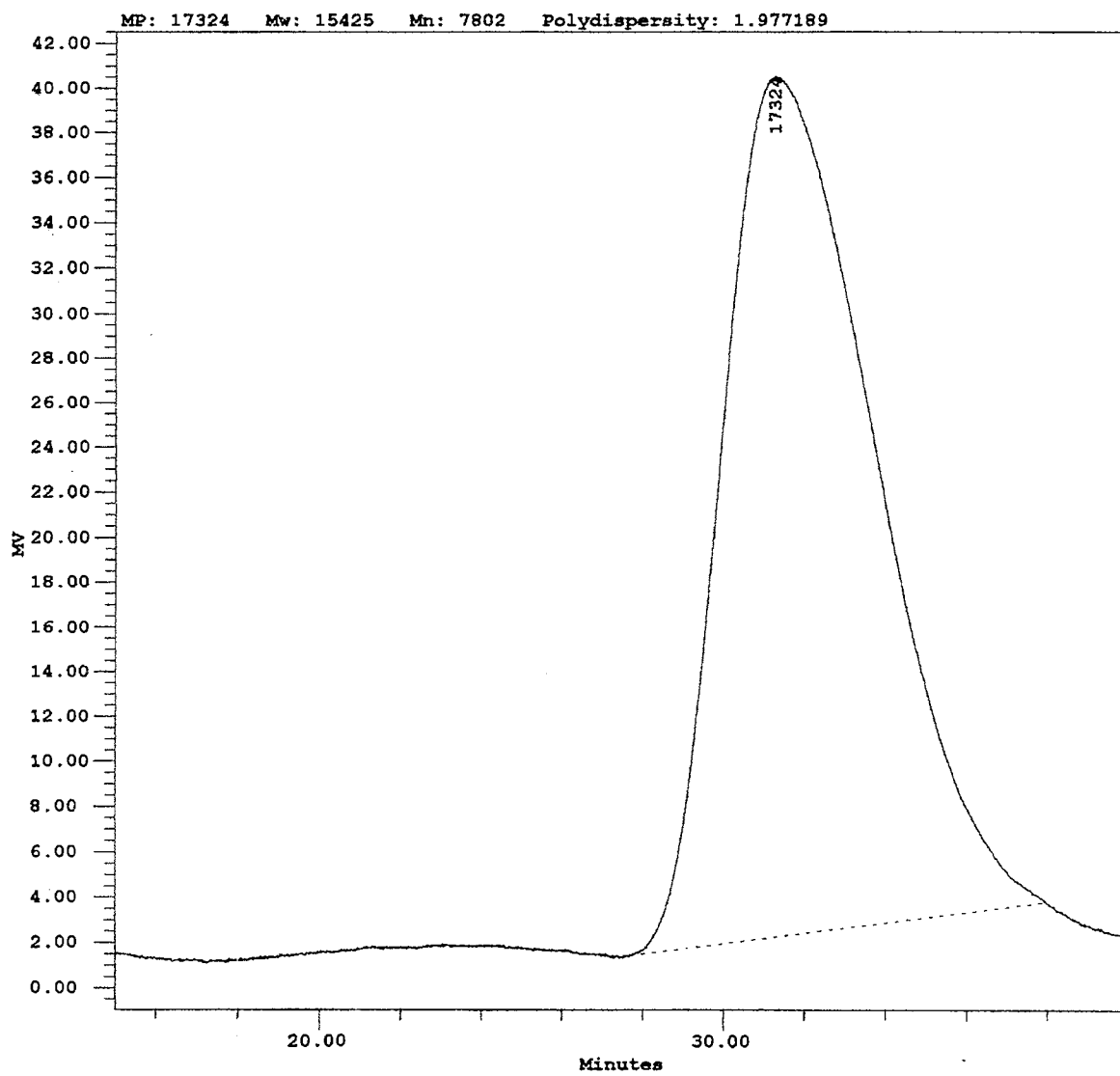
MALLS - No Data

Entry 7

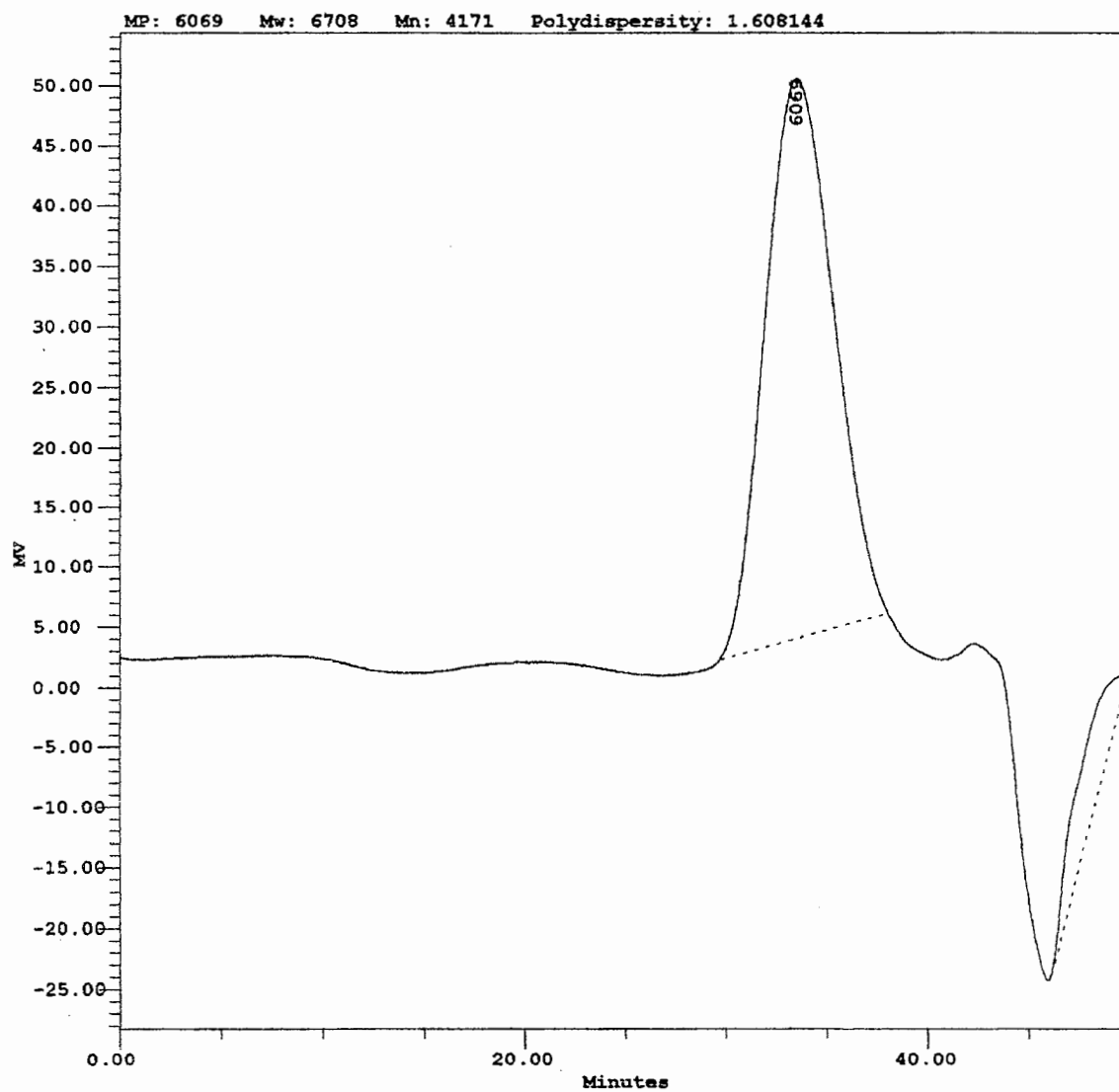


MALLS M_n 9942
" " 19970

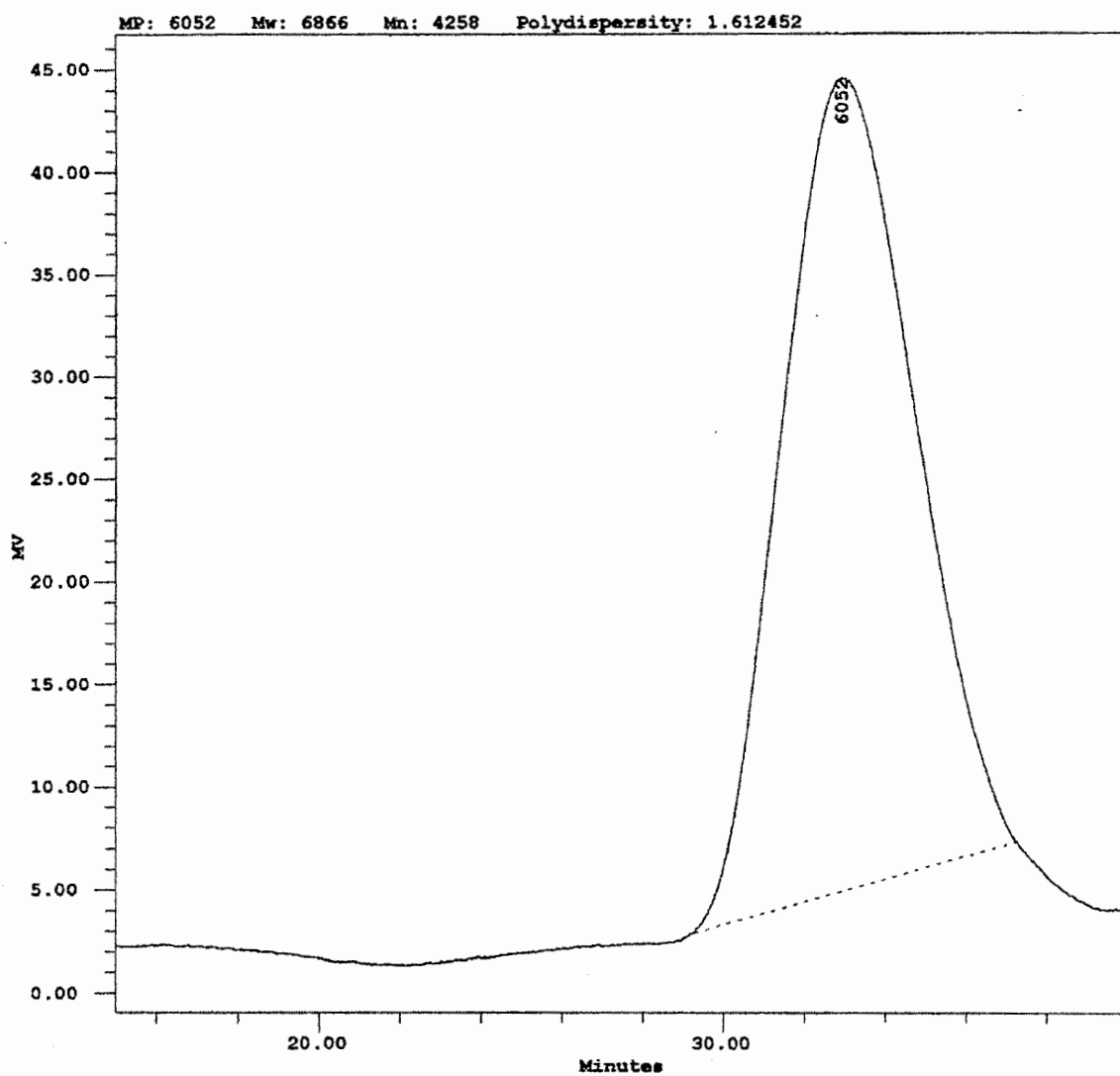
Entry 8



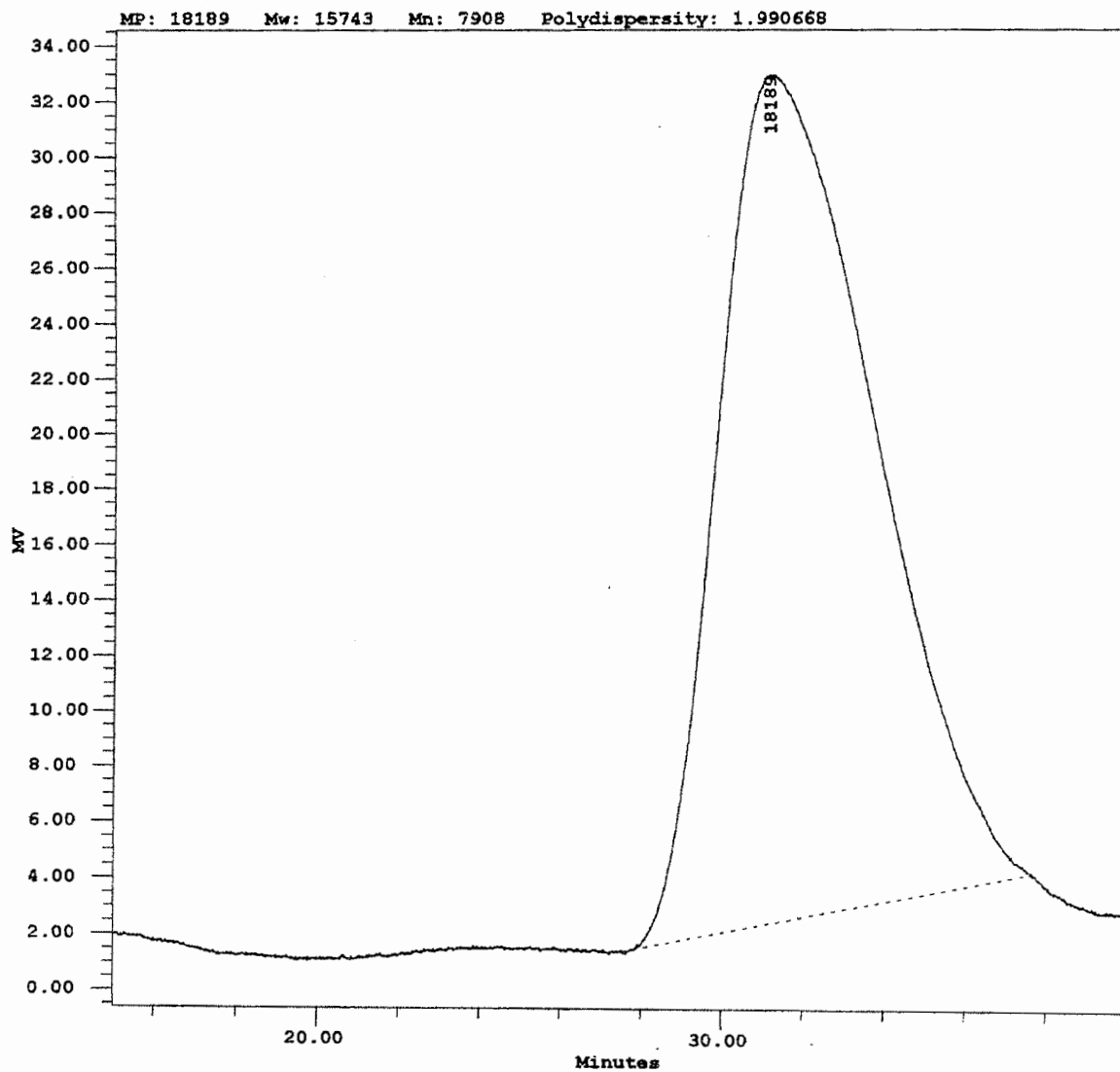
Entry 9



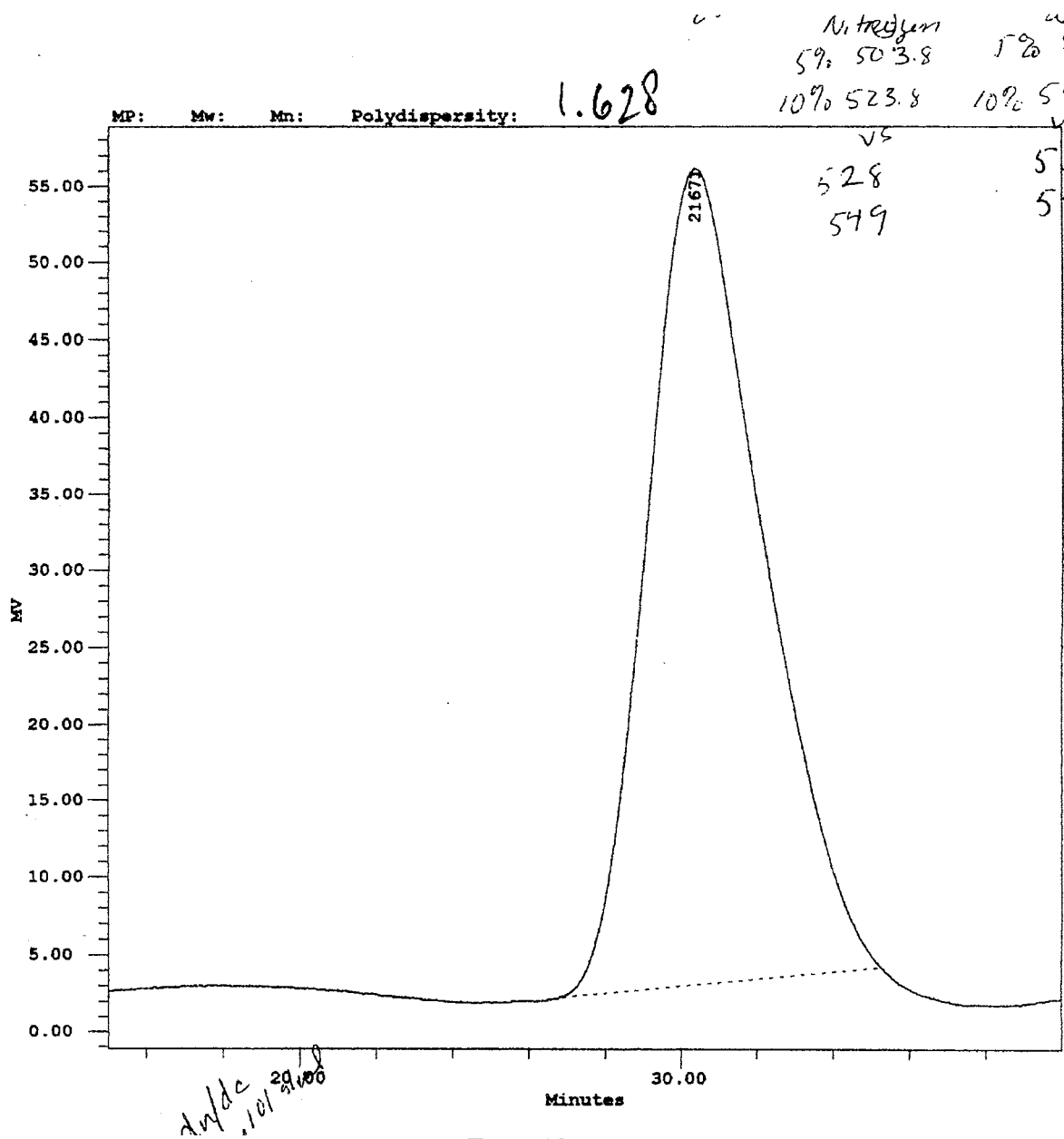
Entry 10

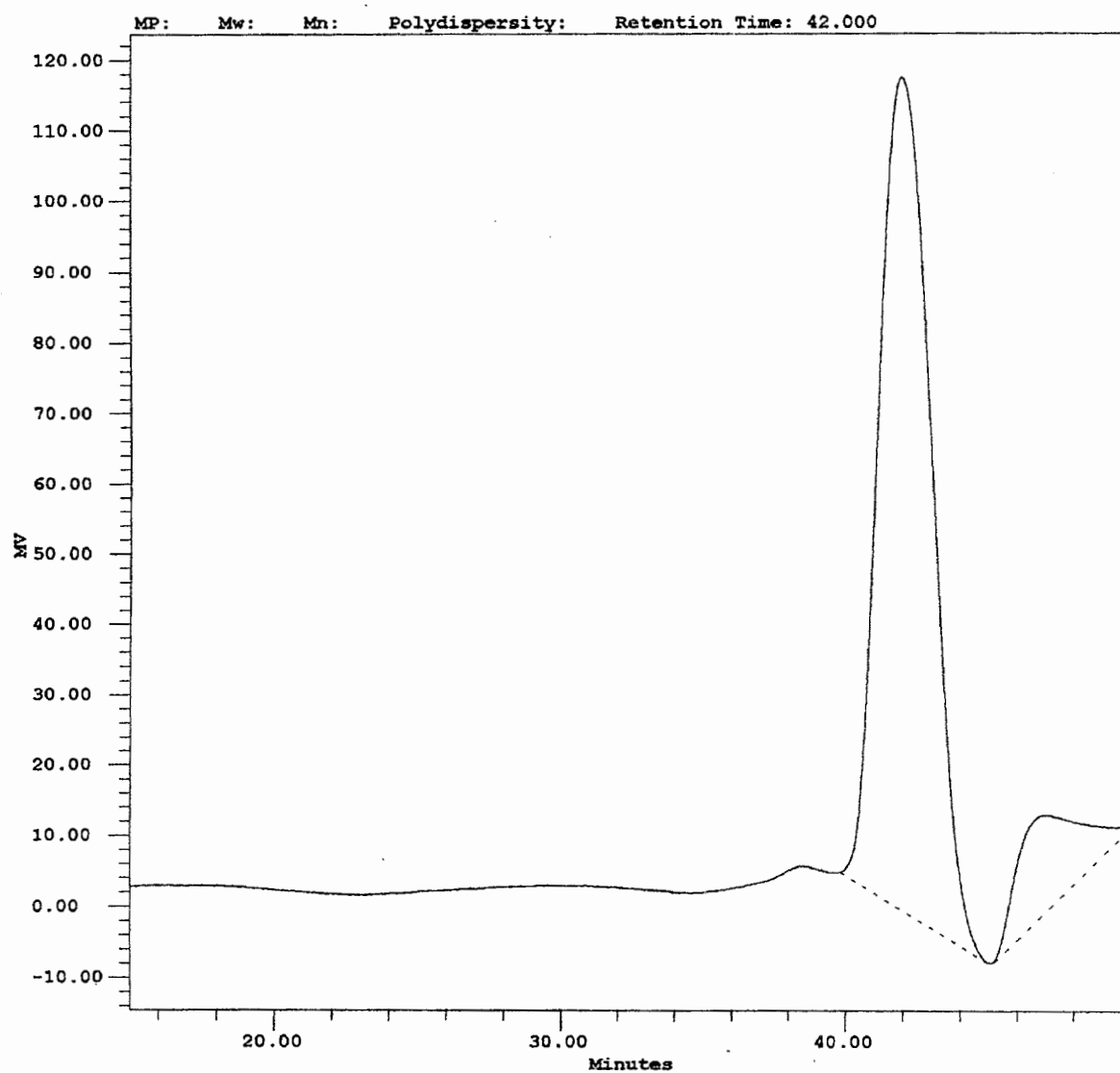


Entry 11

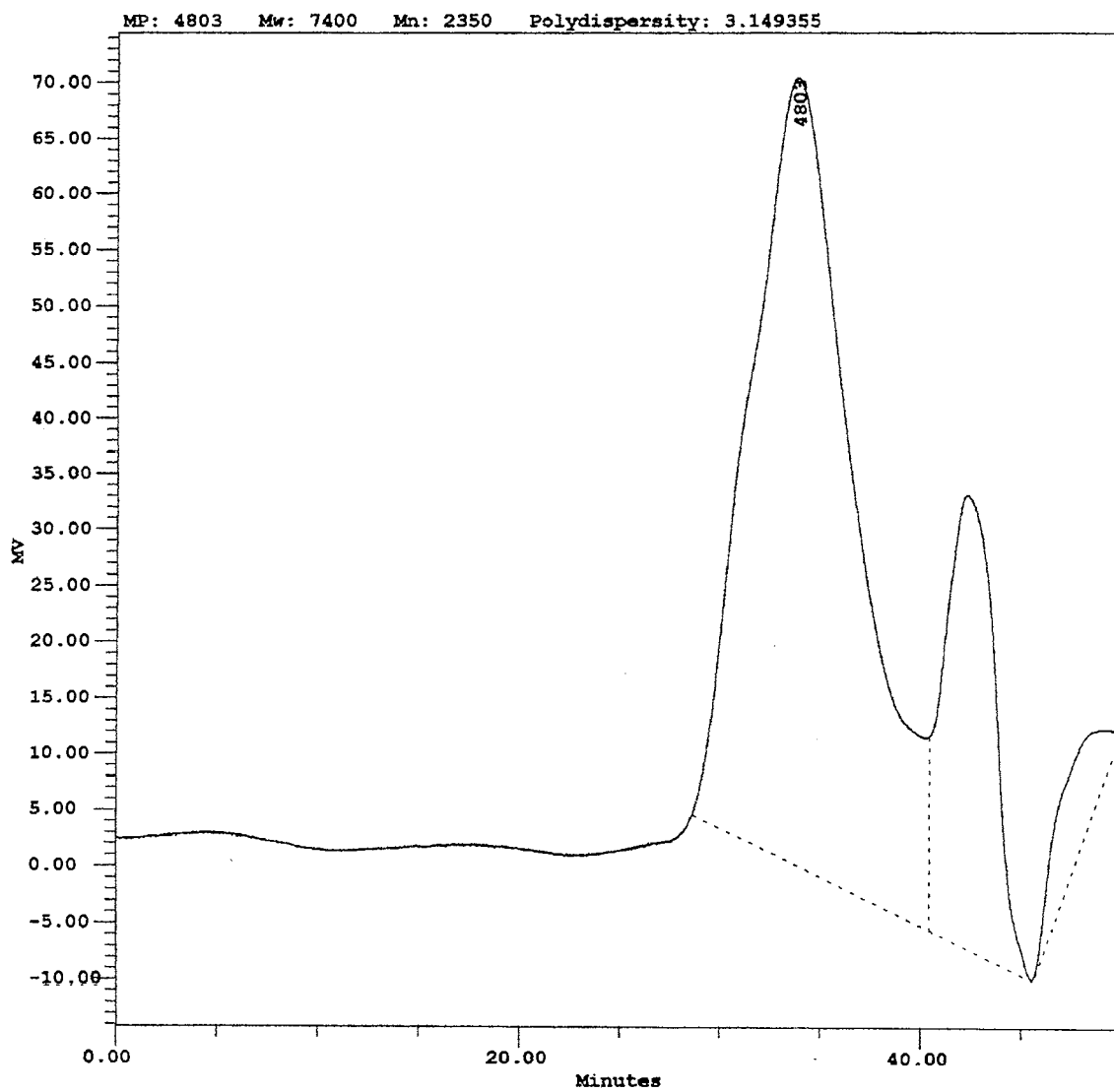


Entry 12

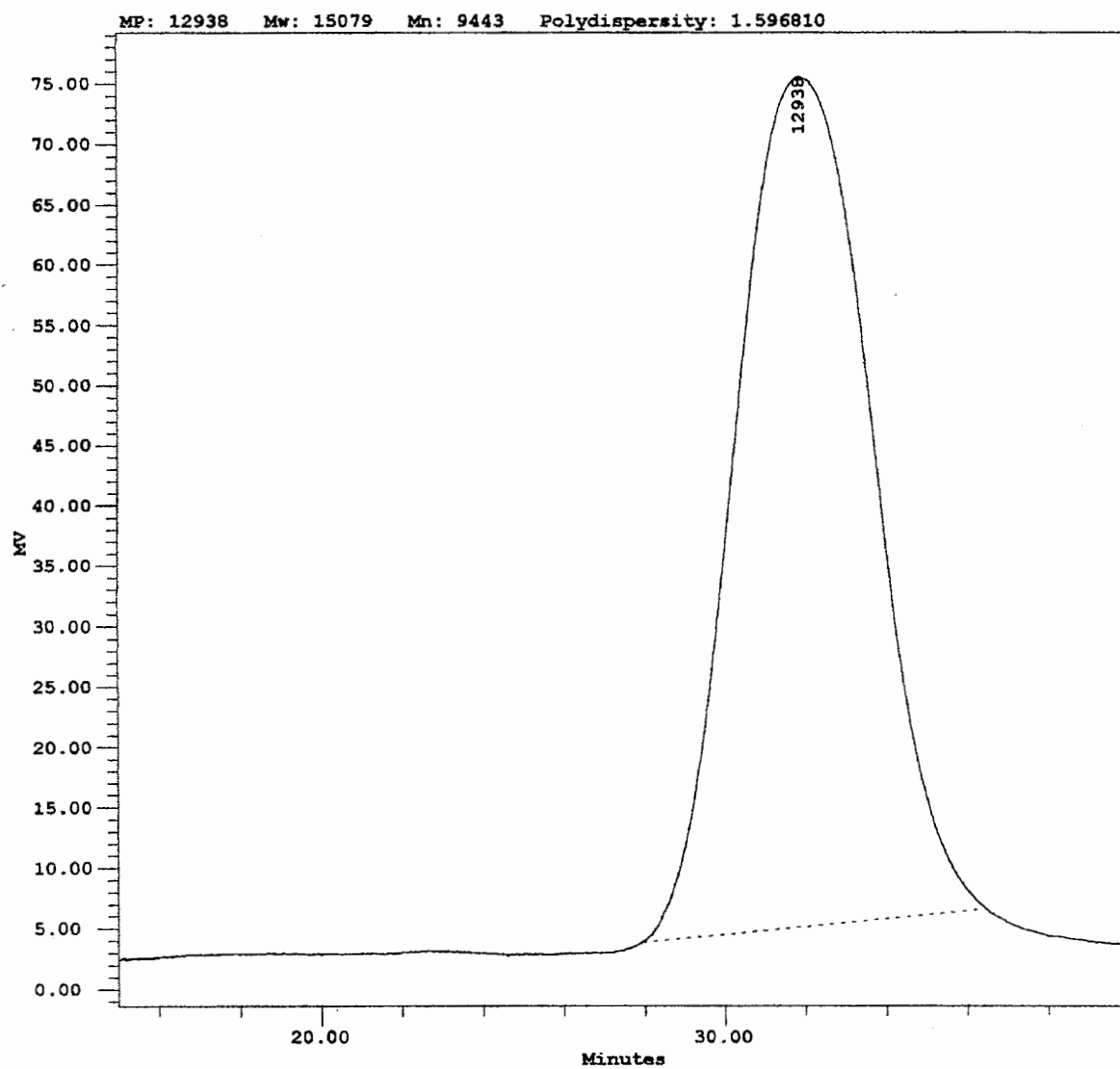




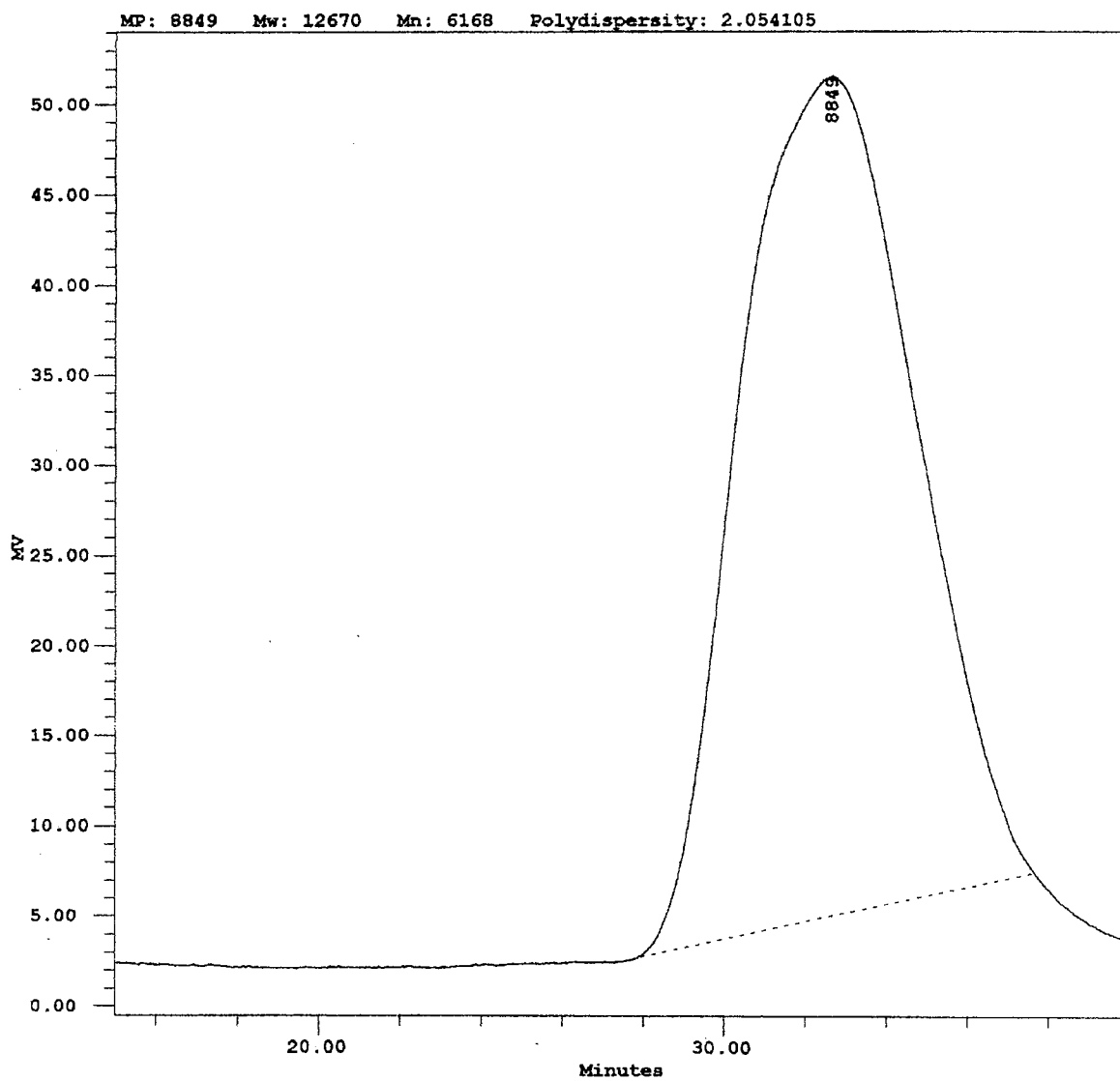
Entry 14



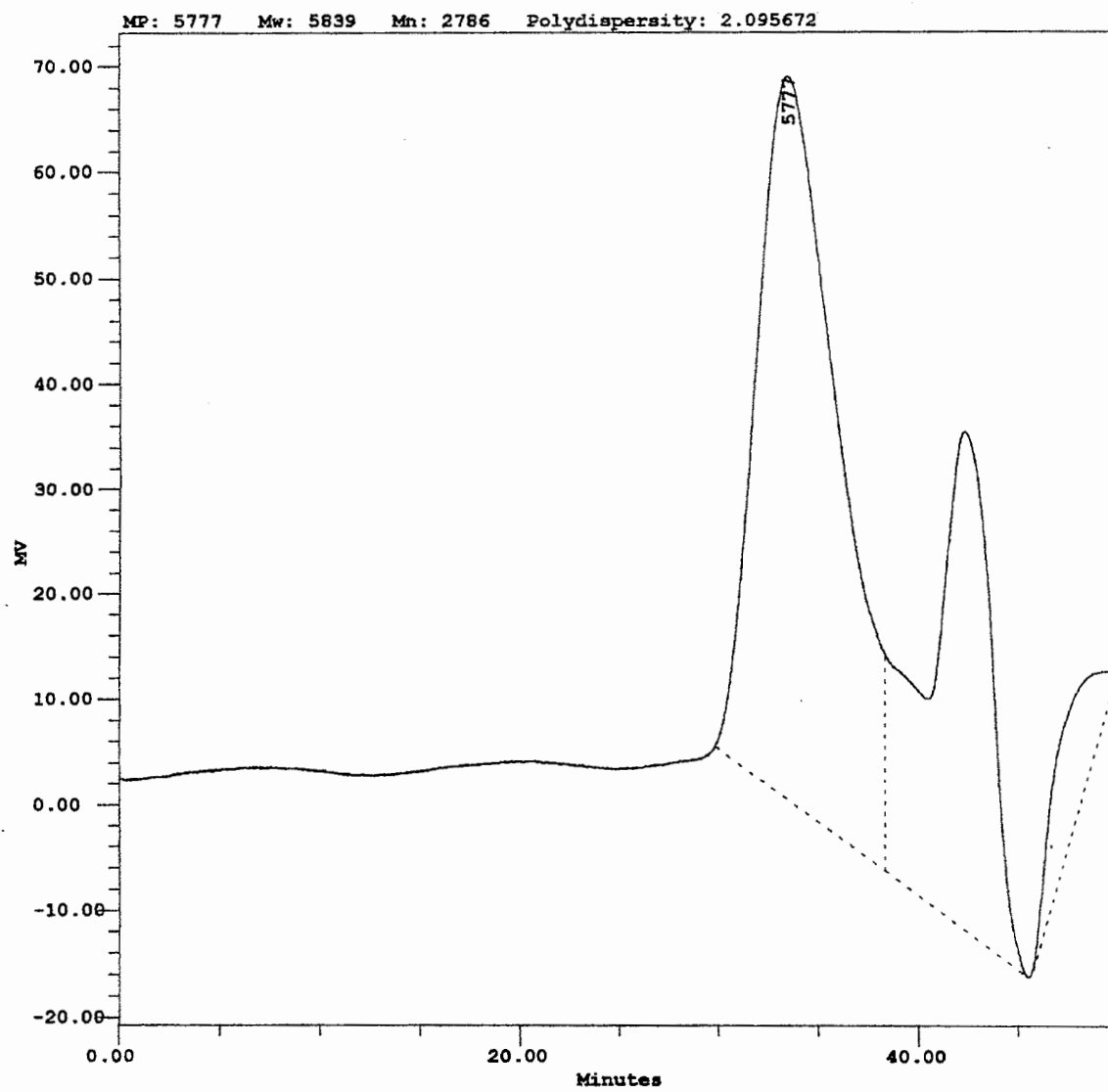
Entry 15



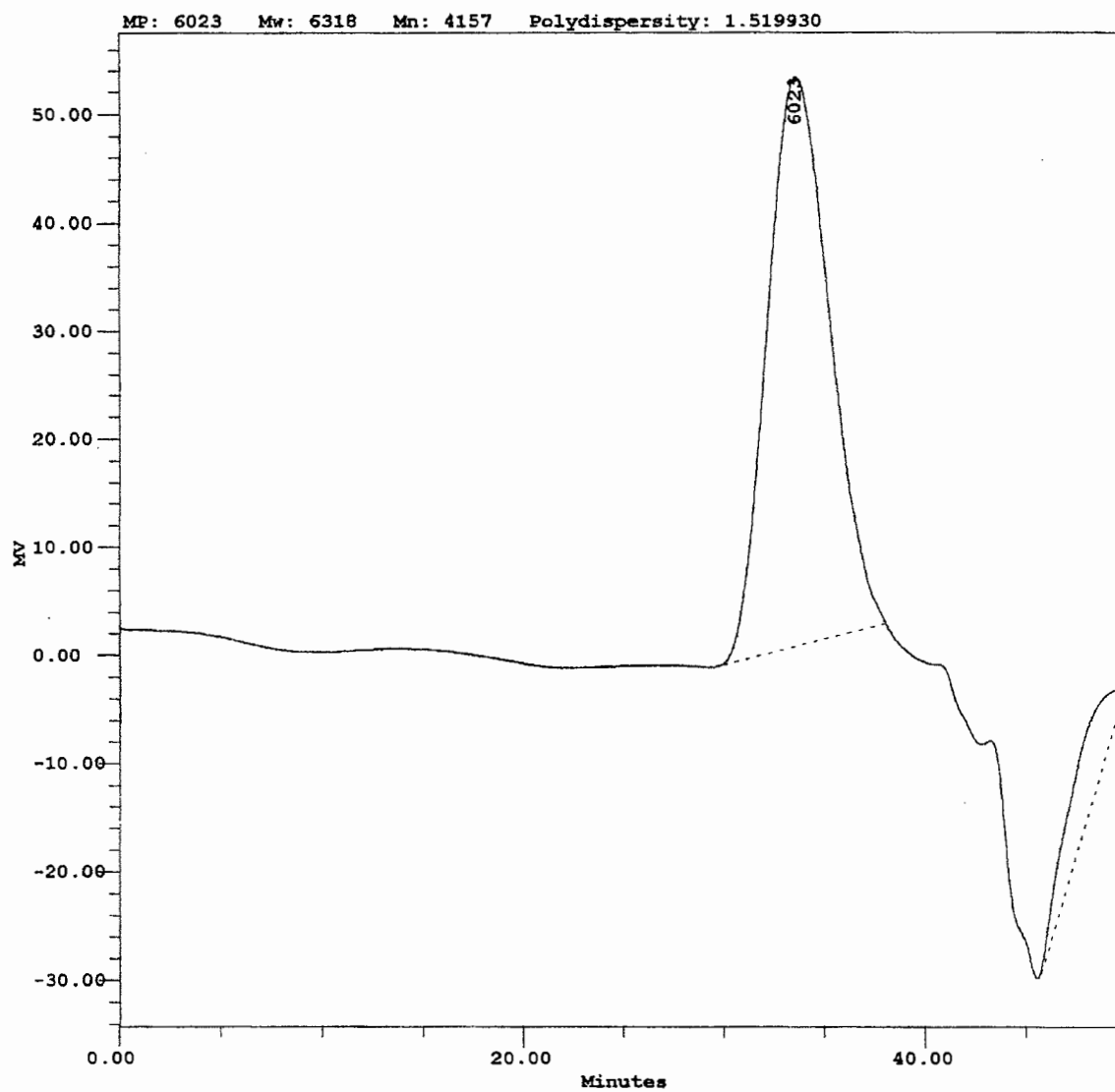
Entry 16



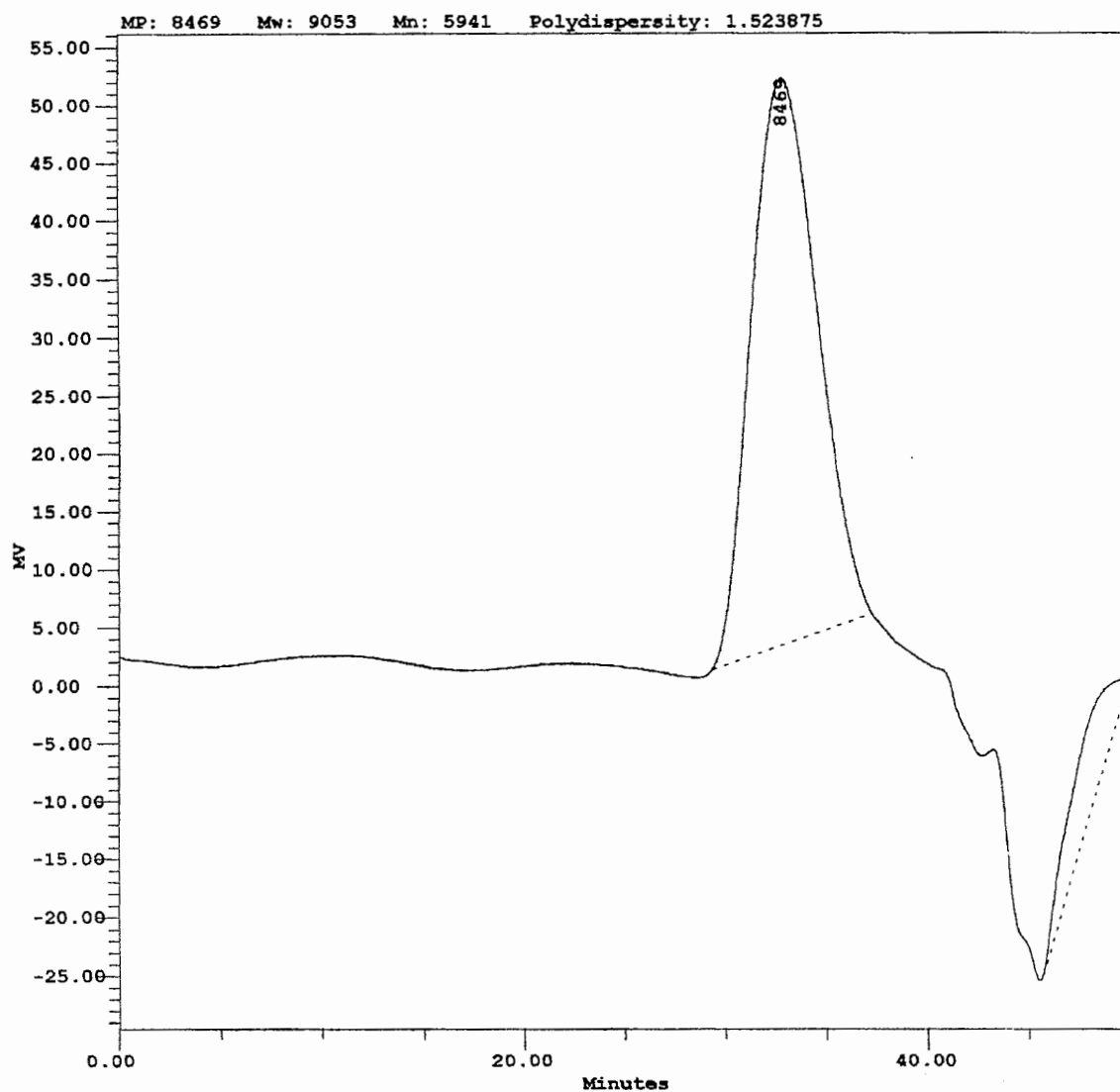
Entry 17



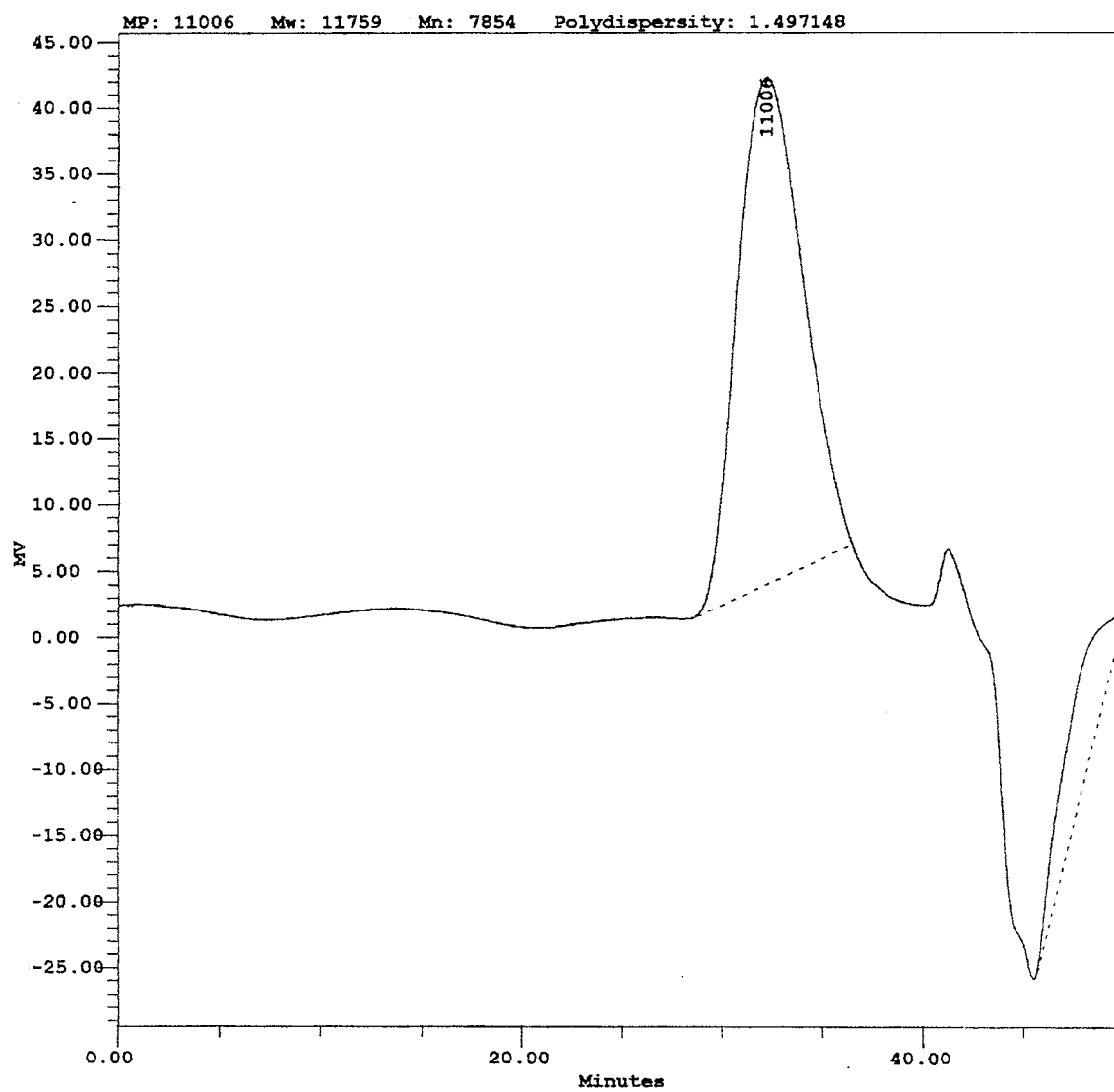
Entry 18



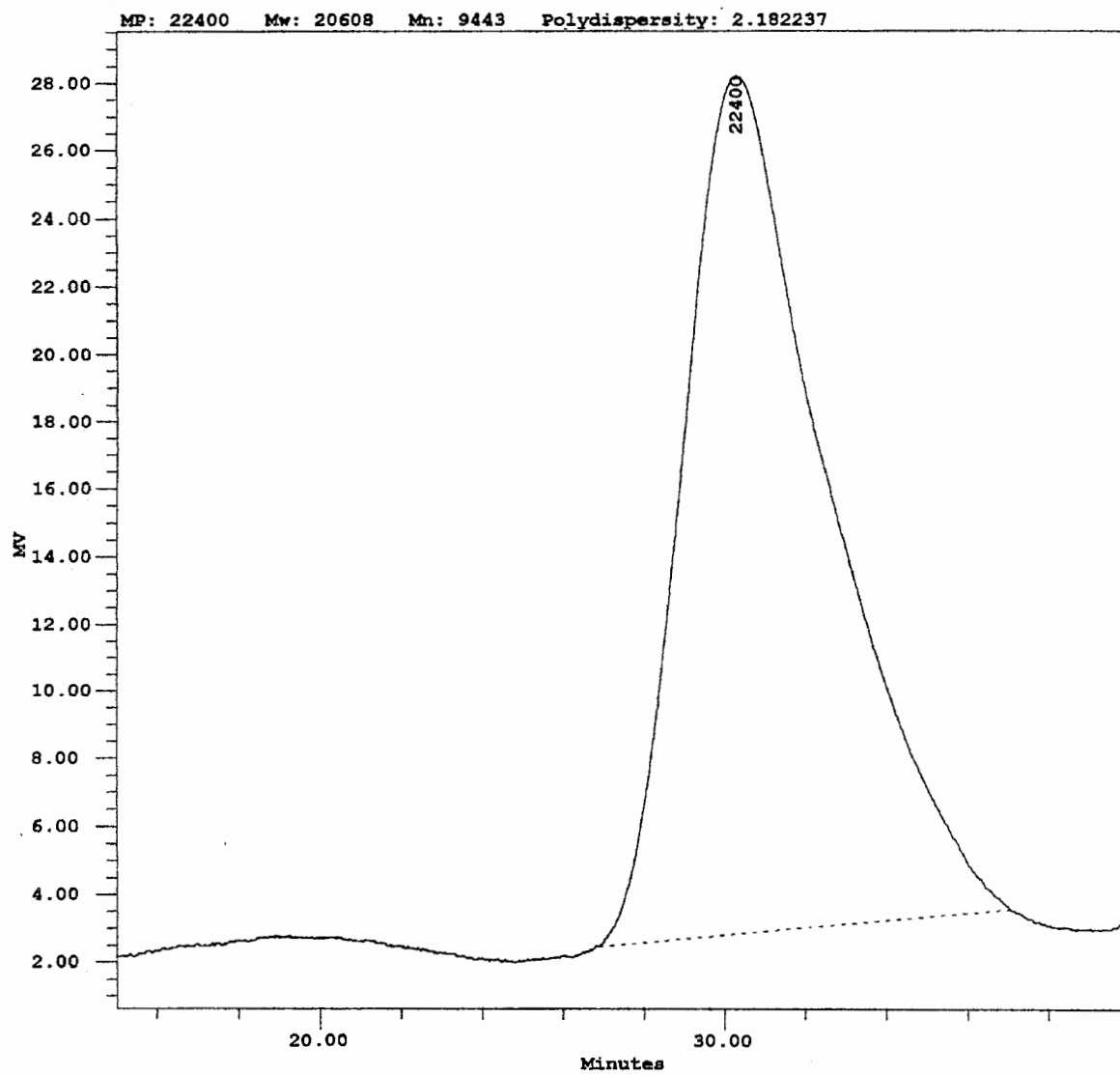
Entry 19



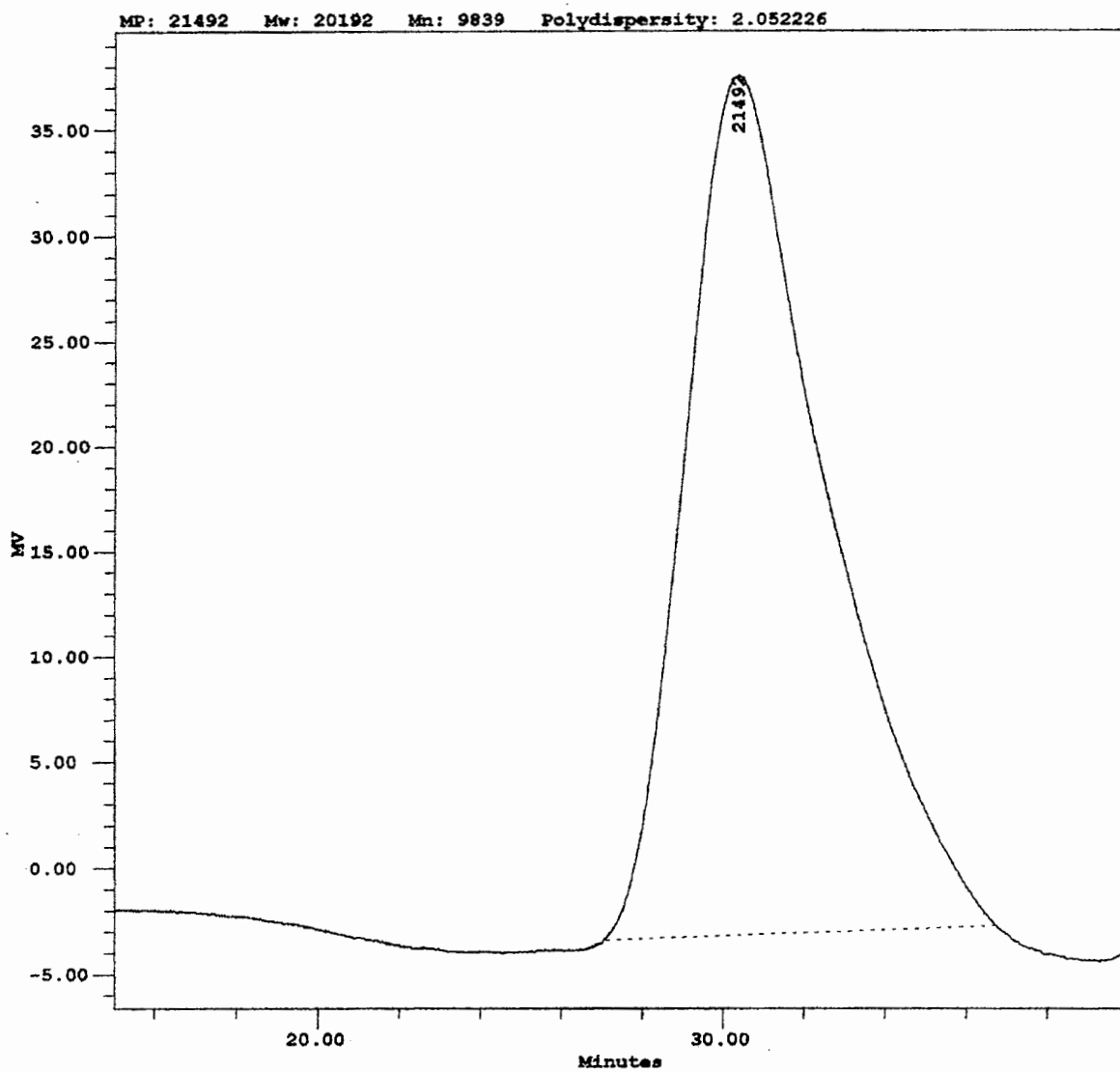
Entry 20



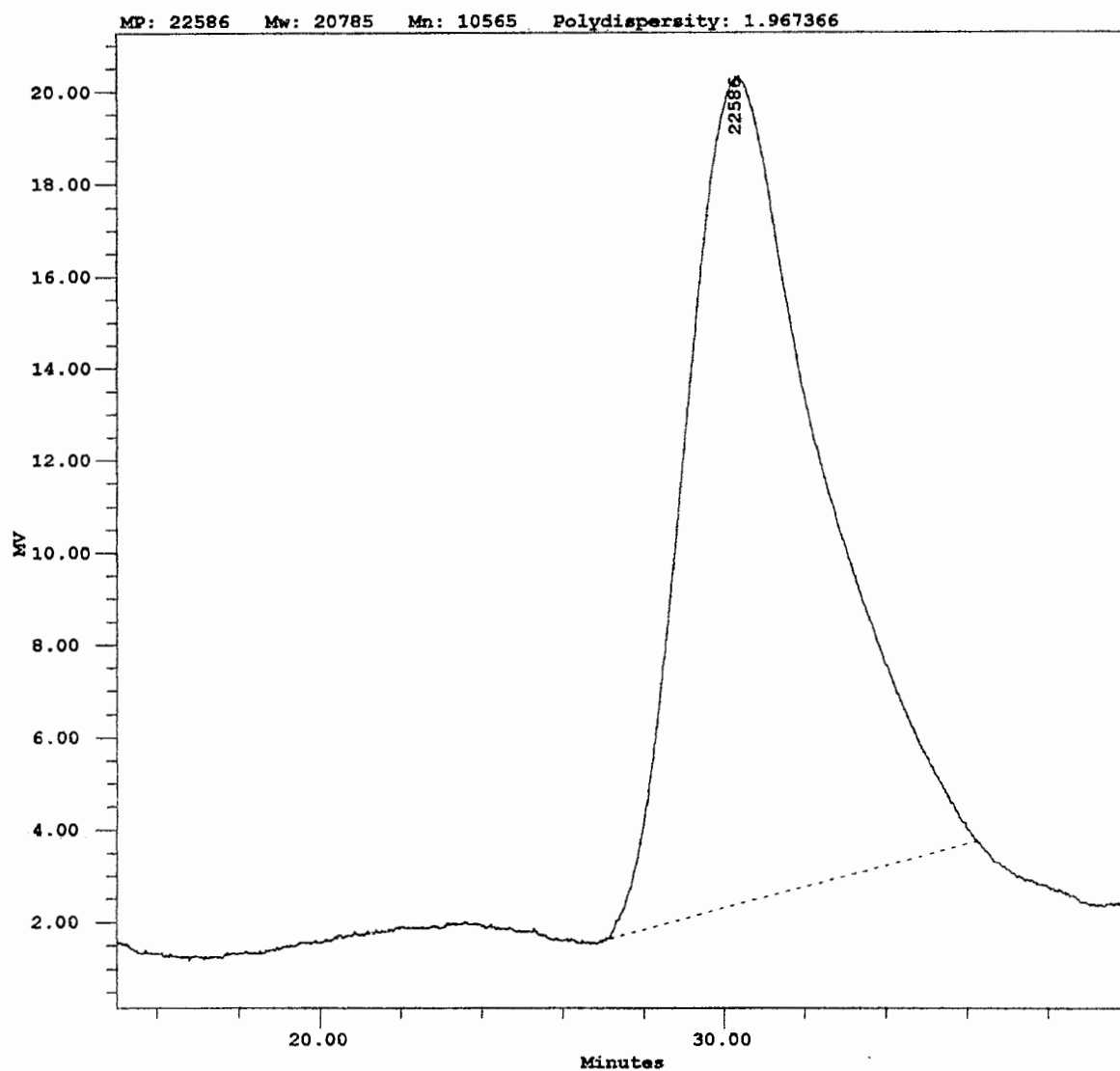
Entry 21



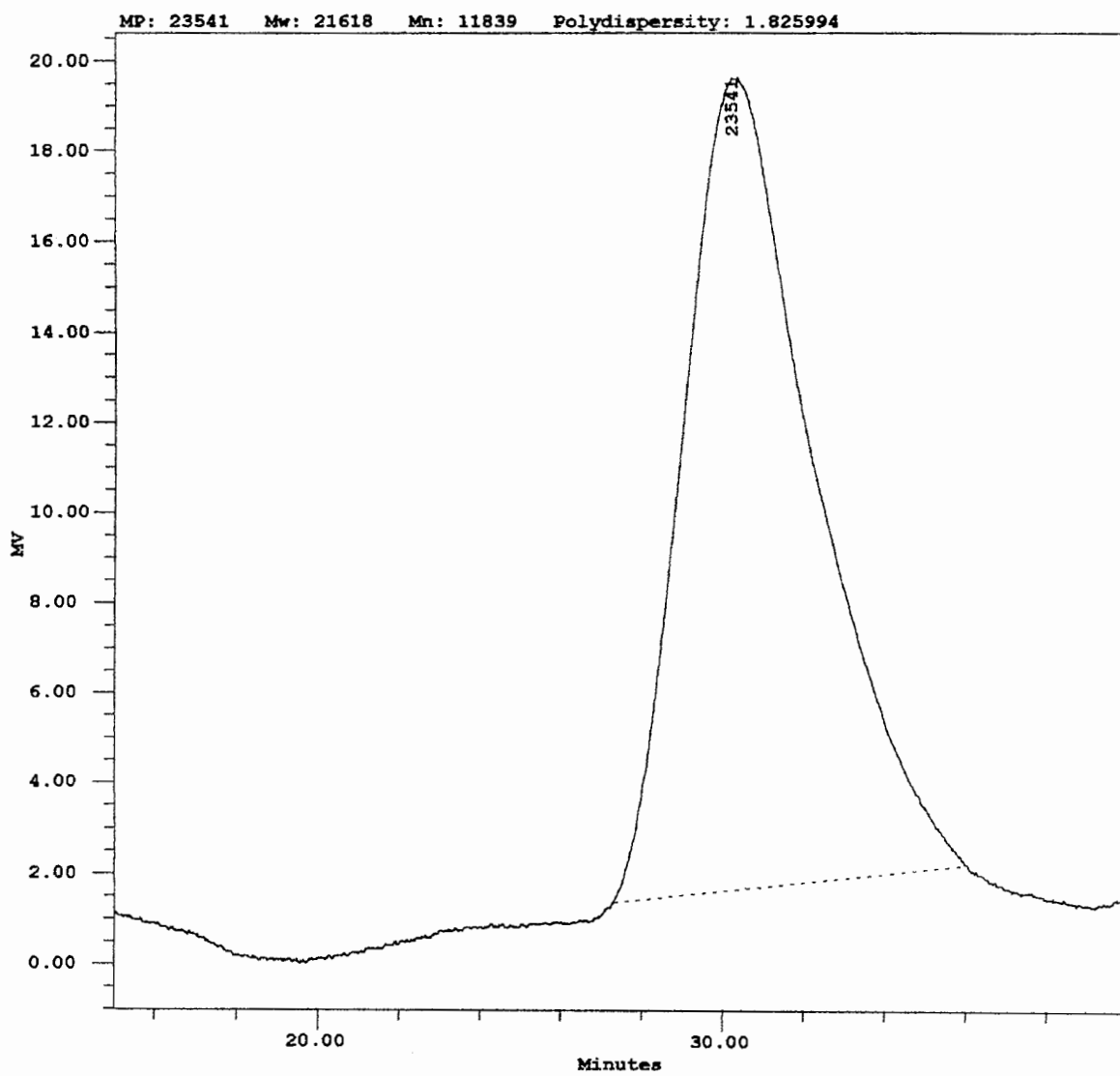
Entry 22



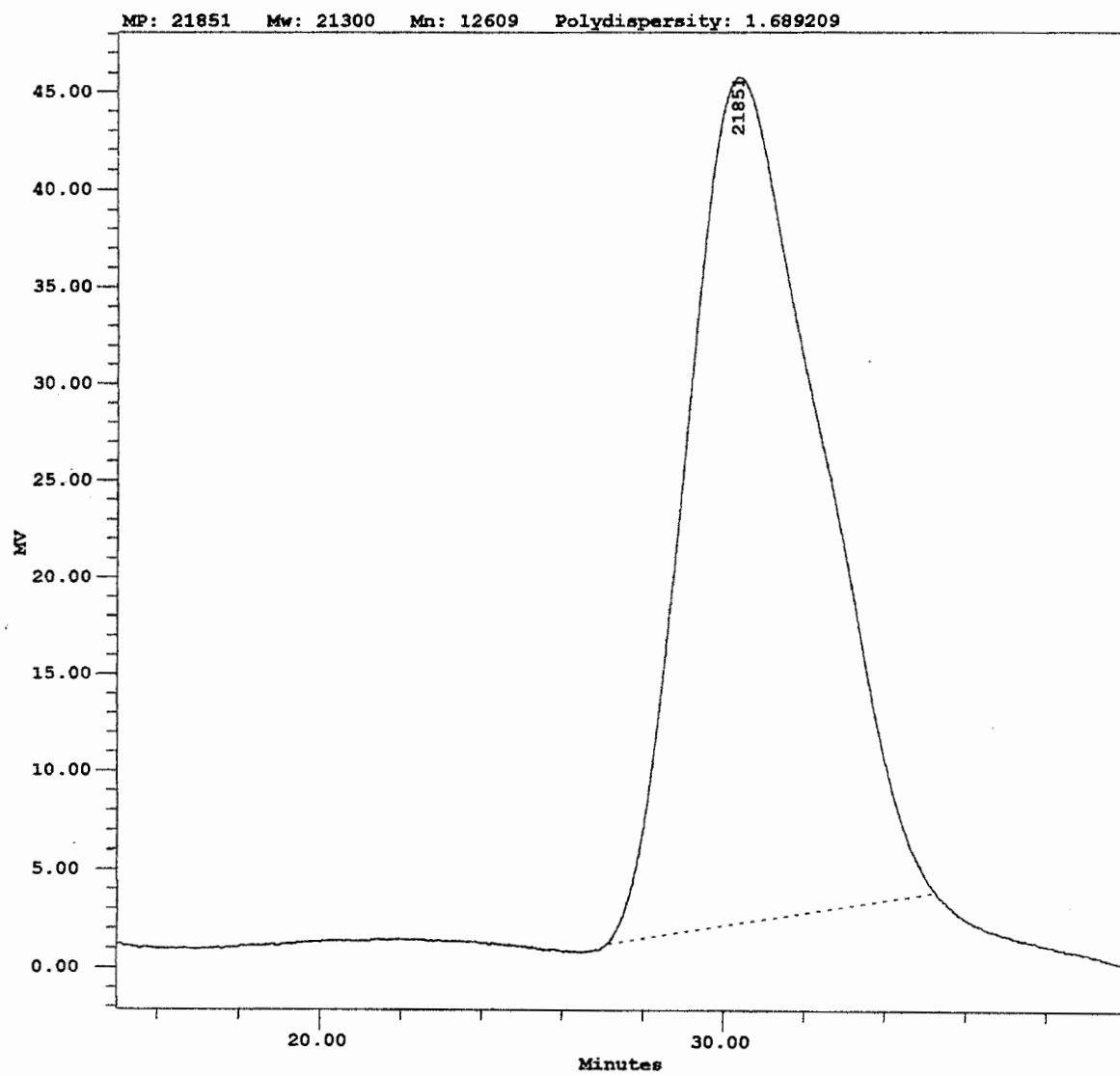
Entry 23



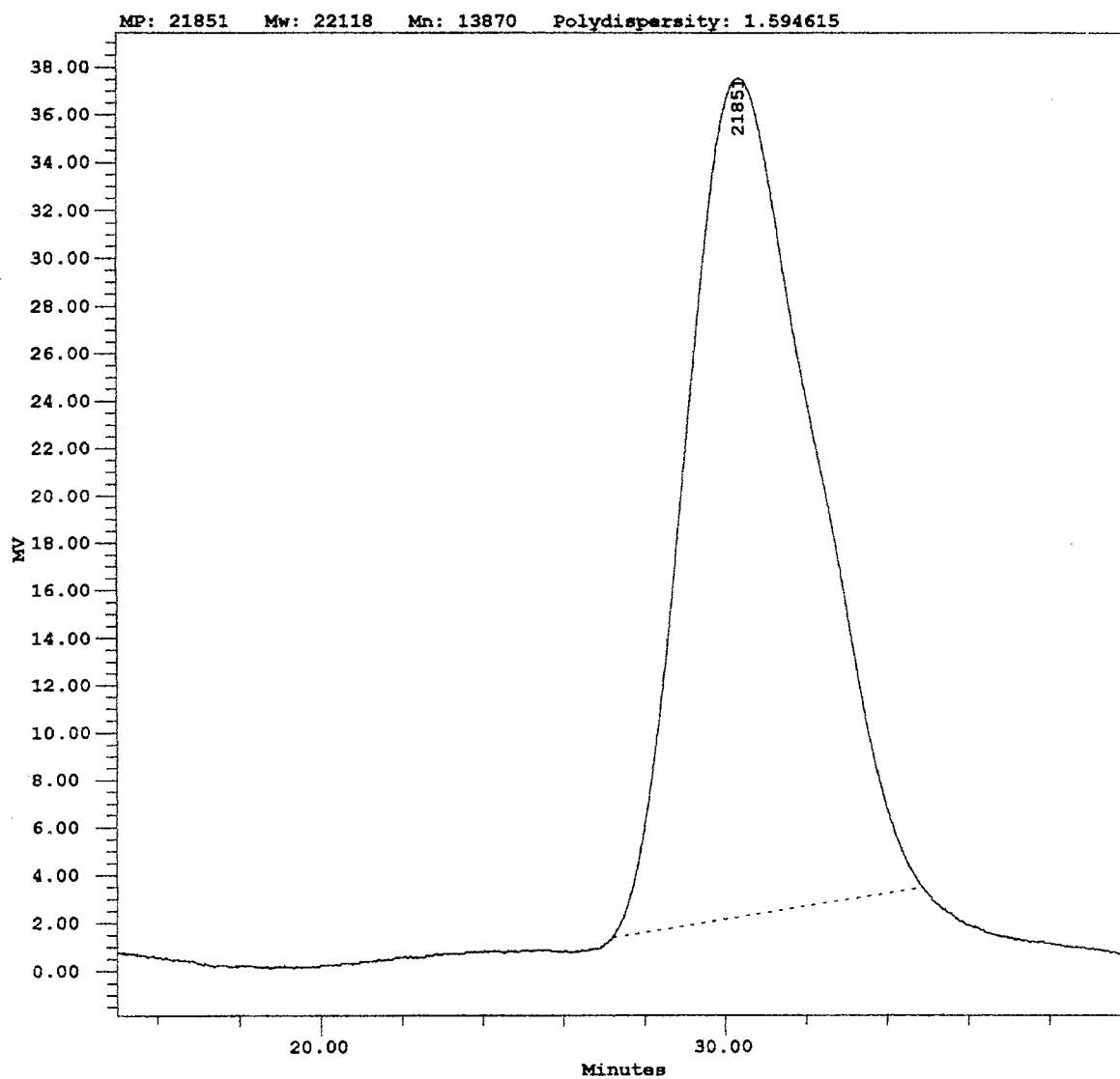
Entry 24



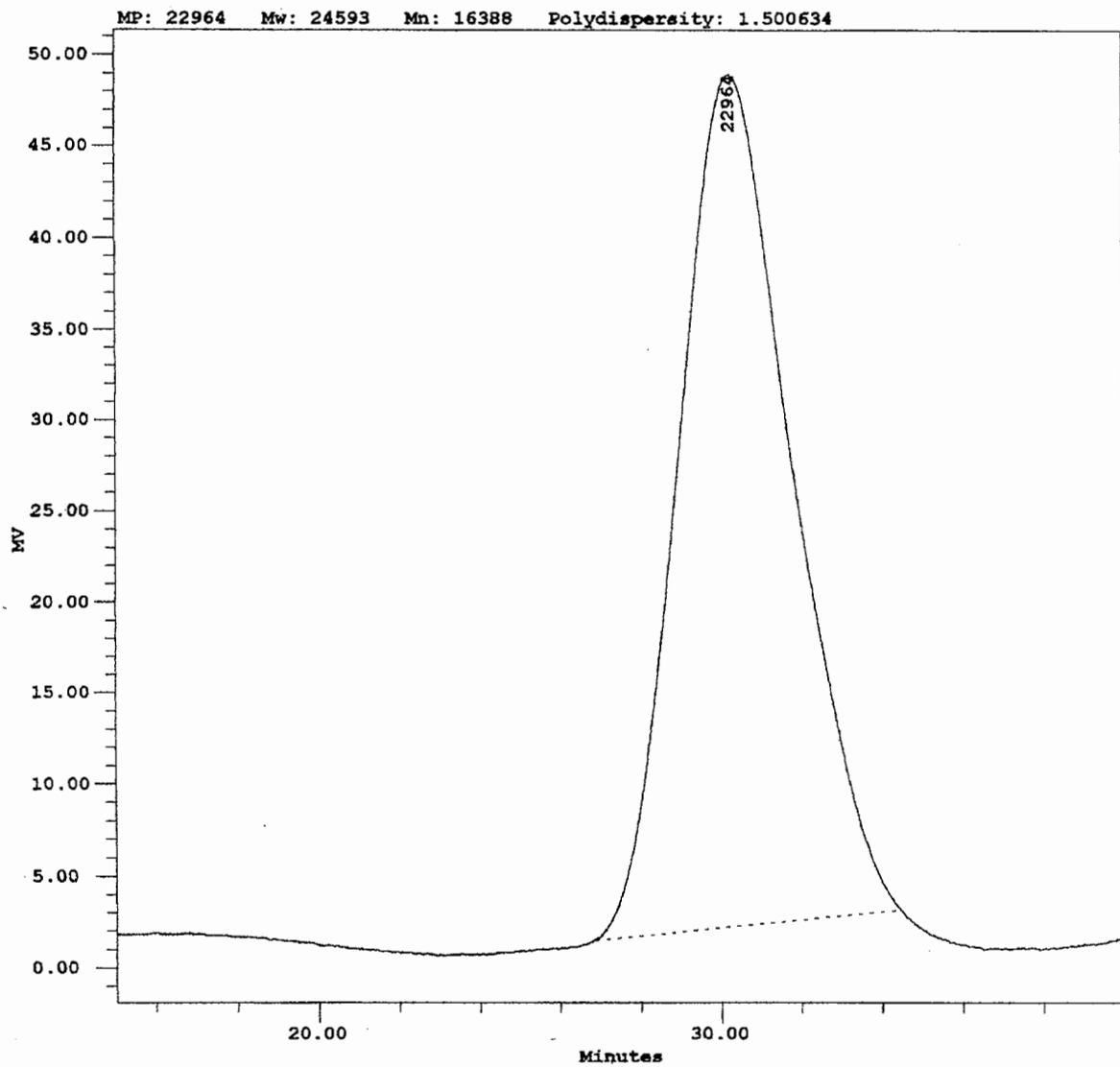
Entry 25



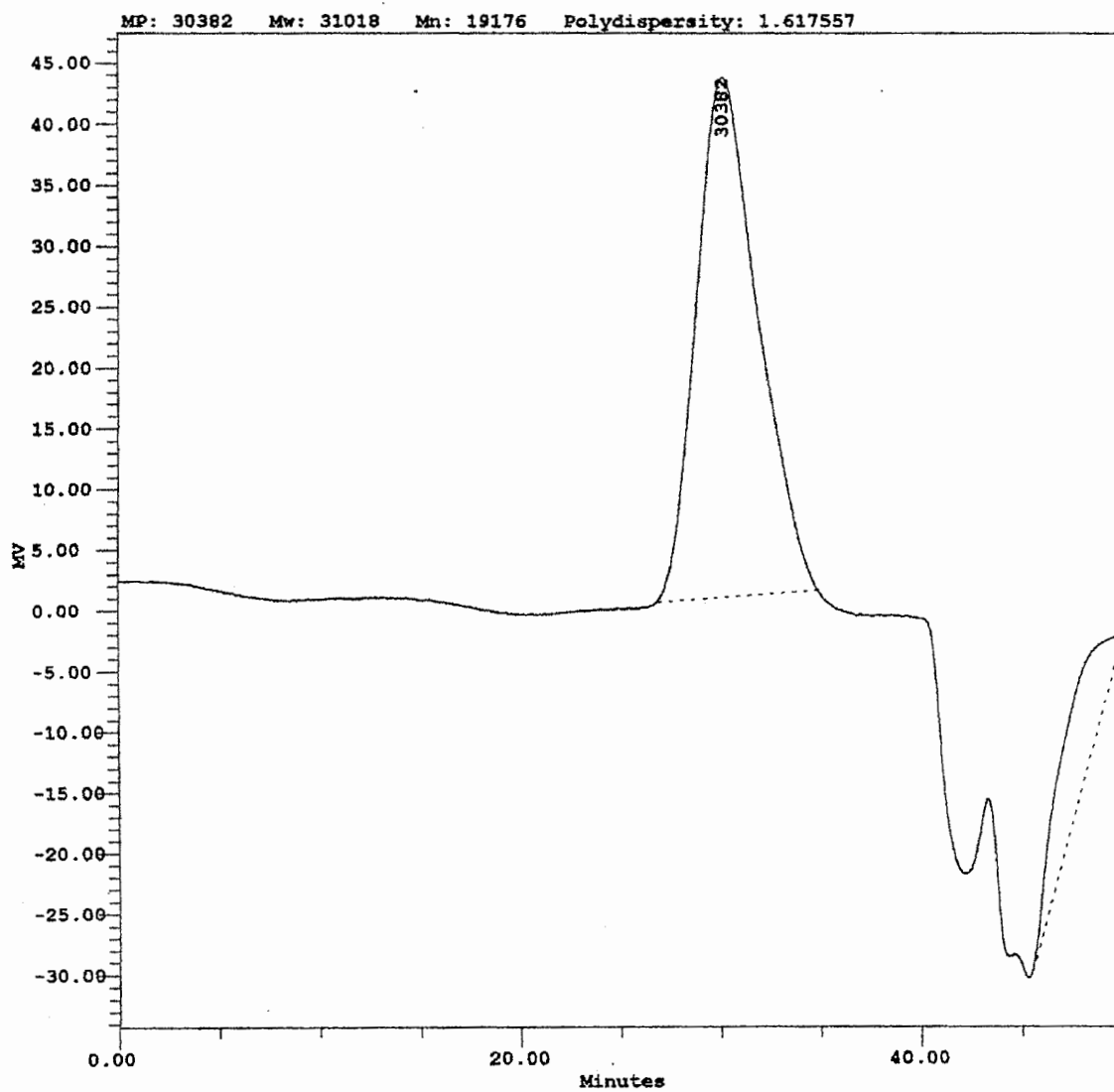
Entry 26



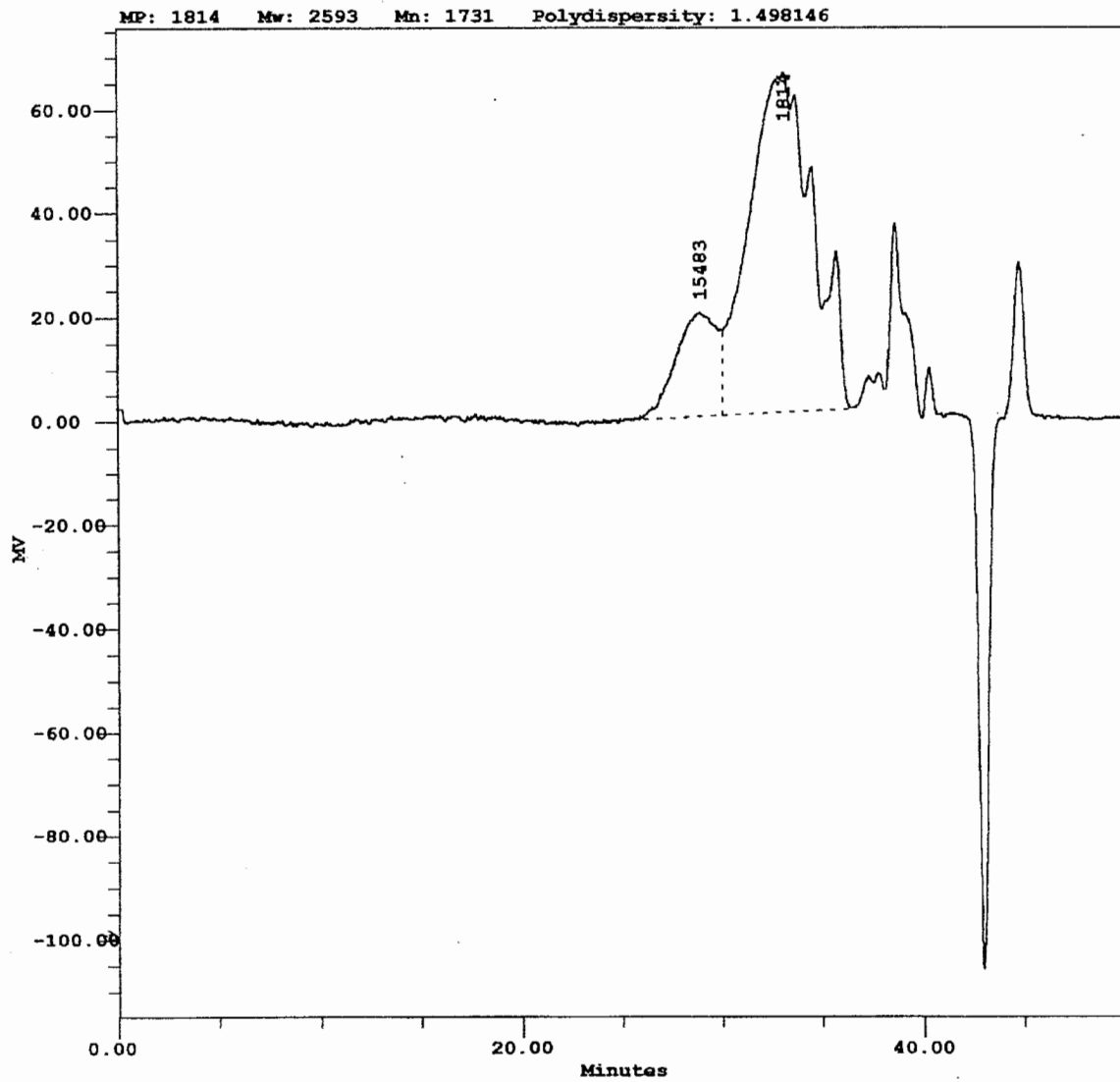
Entry 27



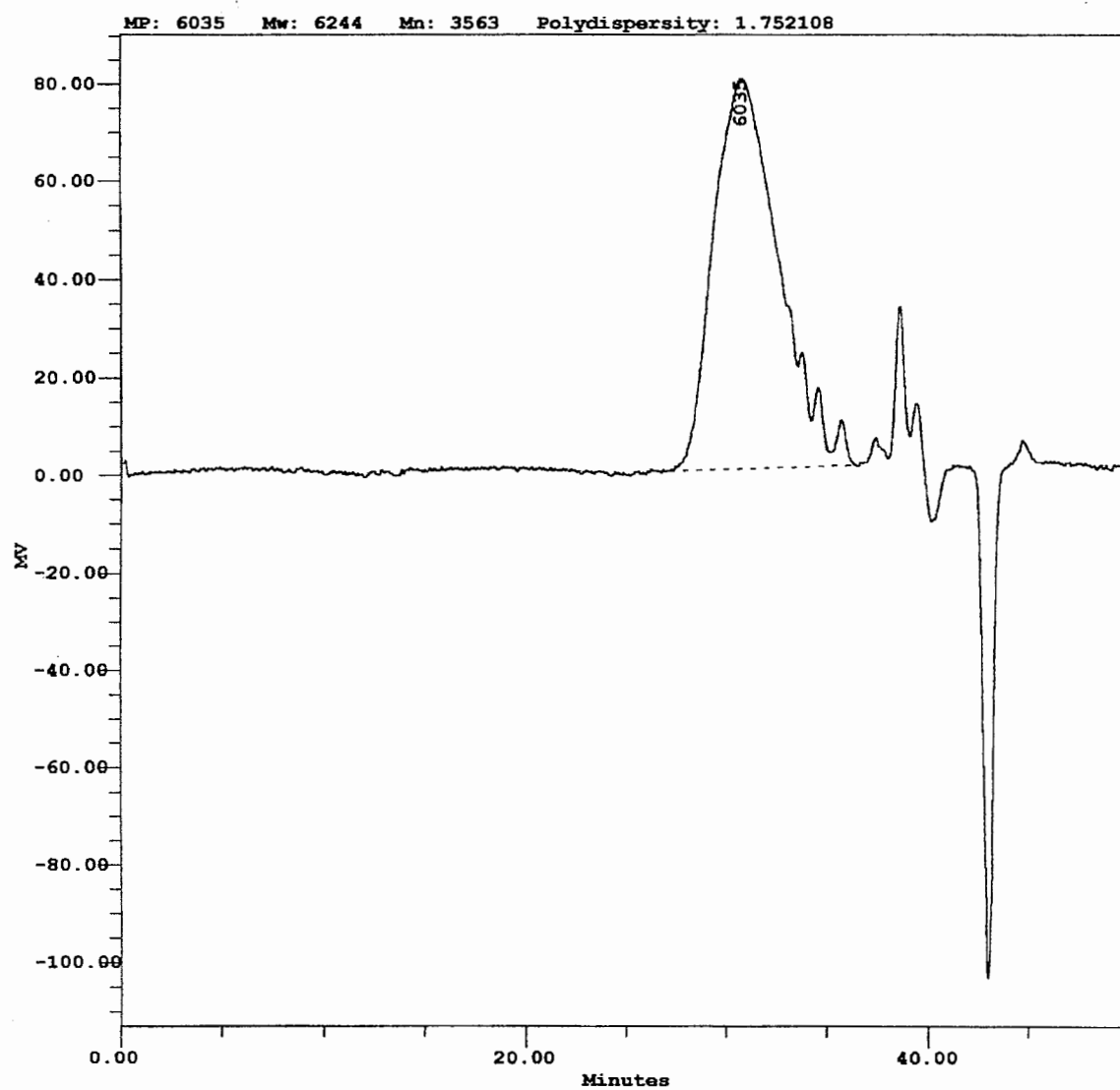
Entry 28



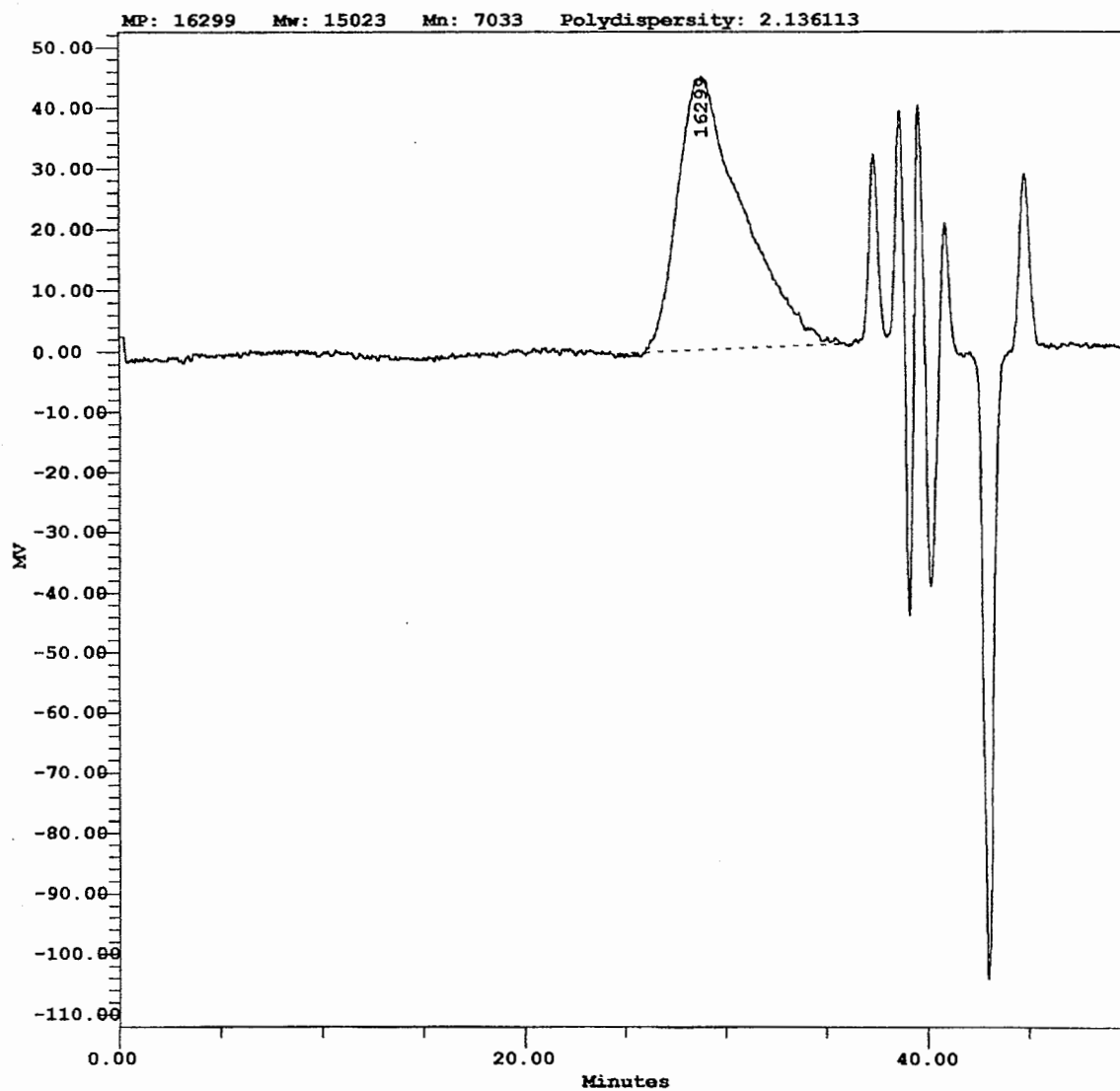
Entry 29



Entry 30



Entry 31



Entry 32

REFERENCES

- (1) Plunket, R. J. *US Patent* 2230654, **1941**.
- (2) Scheirs, J. *Modern Fluoropolymers: High Performance Polymers for Diverse Applications* London, Wiley, **1997**.
- (3) Houghan, G.; Cassidy, P.E.; Johns, K.; Davidson, T. *Fluoropolymers 2: Properties* New York, Plenum, **1999**.
- (4) Rodgers, G.E. *Introduction to Coordination, Solid State, and Descriptive Inorganic Chemistry* New York, McGraw-Hill, **1994**, 224.
- (5) Conroy, M. E.; Honn, F.J.; Robb, L.E.; Wolf, D.R. *Rubber Age* **1995**, 76, 543.
- (6) Rose, S.H. *J. Polym. Sci., Part A: Polym. Chem.* **1968**, 6, 837.
- (7) Norris, A.M.; Fiedler, L.D.; Knapp, T.L.; Virant, M.S. *Automotive Polymers and Design* **1990**, 19, 12.
- (8) Lyons, B.J. *Radiat. Phys. Chem.* **1994**, 45, 158.
- (9) Stamatoff, G.S.; Wittmann, J.W. *Chem. Abstr.* **1965**, 6318297c.
- (10) Stamatoff, G.S.; Wittmann, J.W. *French Patent* **1965**, 1394897.
- (11) Iizawa, T.; Kodou, H.; Nishikubo, T. *J. Polym. Sci., Part A: Polym. Chem.* **1991**, 29, 1875.
- (12) Tullos, G.L.; Cassidy, P.E.; St. Clair, A.K. *Macromolecules*, **1991**, 24, 6059.
- (13) Mercer, F.W.; Goodwin, A.A.; Fone, M.M.; Reddy, V.N. *Polymer*, **1997**, 38, 1987.
- (14) Hoyt, A.E.; Riecco, A.J.; Yang, H.C.; Crooks, R.M. *J. Am. Chem. Soc.* **1995**, 117, 8672.

- (15) Mohr, J.H.; Paul, D. R.; Tullow, G.L.; Cassidy, P.E. *Polymer* **1991**, 32, 2387.
- (16) Kane, K.M.; Wells, L.A.; Cassidy, P.E. *High Perform. Polym.* **1991**, 3, 191.
- (17) McGrath, J.E.; Rogers, M.E; Arnold, C.A. Kim, Y.J.; Hedrich, J.D. *Macromol. Chem., Macromol. Symp.* **1991**, 51, 103.
- (18) Kakimioto, M.A.; Iamai, Y. *J.Polym. Sci. Polym., Chem.Ed.* **1986**, 24, 3555.
- (19) Brady, R.F. *Polym. Mater Sci. Eng.* **1996**, 74, 118.
- (20) Keller T.M. . *J.Polym. Sci. Polym., Chem.Ed.* **1984**, 22, 2719.
- (21) Griffith, J.R. *Am. Chem. Soc., Polym. Mat.* **1984**, 50, 422.
- (22) Keller T.M. . *J.Polym. Sci. Polym., Chem.Ed.* **1985**, 23, 2557.
- (23) Ramharack, R. *Polym. Prepr.(Am. Chem. Soc., Div. Polym. Chem.)* **1988**, 29, (1), 146.
- (24) Misra, A.K. Tesoro, G.; Hougham, G.; Pendharkas, S.M. *Polymer*, **1992**, 33, 1078.
- (25) Griffith, J.R.; O'Rear, J.G. *US Patent* 4518508, **1986**.
- (26) Cassidy, P.E.; Ammabhair, T.M.; Reddy V.S.; Fitch, J.W. *Polym J.* **1995**, 31, 353.
- (27) Woo, E.M.; Barlow, J.W.; Paul, D.R. *J. Appl. Polym. Sci.* **1985**, 30, 4243.
- (28) Park, J.W.; Lee, M.; Lem, M.H.; Lin, J.W.; Kim, S.D.; Cheng, J.Y.; Rhee, S.B. *Macromolecules* **1994**, 27, 3459.
- (29) Ghassemi, H.; Hay, A.S. *Macromolecules* **1994**, 27, 3116.
- (30) Chung, T.S.; Kafchinski, E.R. *Polymer*, **1996**, 37, 1635.
- (31) Bruma, M.; Mercer, F.; Fitch, J.; Cassidy, P.E. *Polymer*, **1992**, 33, 3278.
- (32) Kelleghan, W. *US Patent* 4503254.
- (33) Nishihara, Y.; Ikegashira, K.; Hikabayashi, K.; Ando, J.; Mori, A.; Hiyama, T. *J. Org.*

- Chem.* **2000**, *65*, 1780.
- (34) Colon, I.; Kelsey, D.R. *J. Org. Chem.* **1986**, *51*, 2627.
- (35) Pasquale, A.J.; Vonhof, T. K.; Sheares V. V. *Polym. Prepr. (Am. Chem. Soc., Div. Polym. Chem.)* **1997**, *38*, (1), 170.
- (36) Pasquale, A.J.; Sheares, V. V. *J. Polym. Sci., Part A: Polym. Chem.* **1998**, *36*, 2611.
- (37) Pasquale, A.J.; Sheares, V. V. *Polym. Prepr. (Am. Chem. Soc., Div. Polym. Chem.)* **1998**, *39*, (1), 331.
- (38) Wang, J.; Vonhof, T. K.; Sheares, V.V. *Polym. Prepr. (Am. Chem. Soc., Div. Chem.)* **1997**, *38*, no. 1, 263.
- (39) Wang, J.; Sheares, V. V. *Macromolecules* **1998**, *31*, 6769.
- (40) Murthy, N. S.; Correale, S. T.; Minor, H., *Macromolecules* **1991**, *24*, 1185.
- (41) Lin, S.; Li, F.; Cheng, S. Z.; Harris, F. W. *Macromolecules* **1998**, *31*, 2080.
- (42) Lyon, R. E.; Waters, R. N. "A Pyrolysis-Combustion Flow Calorimeter for the Study of Polymer Heat Release Rates" *Ninth Annual BCC Conference on Flame Retardancy* Stanford, CT, June1-3, **1998**.
- (43) Lyons, R.E. *Fire-Resistant Materials: Progress Report* DOT/FAA/AR-97/100 **1998**.
- (44) Matsuura, T.; Ishizawa, M.; Hasuda, Y.; Nishi, S. *Macromolecules* **1992**, *25*, 3540.
- (45) Havelka-Rivard, P. A.; Nagai, K.; Freeman, B. D.; Sheares, V. V. *Macromolecules* **1999**, *32*, 8235.
- (46) Morisato, A.; Shen, H. C.; Sankar, S. S.; Freeman, B. D.; Pinnau, I.; Casillas, C. G.

- J. Polym. Sci., Part B: Polym. Phys.* **1996**, *34*, 2209.
- (47) Freeman, B. D.; Hill A. J., Chapter 21 Free Volume Transport Properties of Barrier and Membrane Polymers, M. R. Tant and A. J. Hill Eds., *ACS Symposium Series* **1999**, *710*, 306.
- (48) Pinnau, I.; Toy, L. G., *J. Membrane Sci.* **1996**, *116*, 199.
- (49) Paul, D. R.; Pixton, M. R., *Polymeric Gas Separation Membranes*, CRC Press, Boca Raton, Florida, **1994**, 83.
- (50) Breck, D. W., *Zeolite Molecular Sieves*, Wiley, New York, **1974**, 636.
- (51) Stern, S.; Shah, V.; Hardy, B., *J. Polym. Sci.: Polym. Phys. Ed.* **1987**, *25*, 1263.
- (52) Bondar, V. I.; Freeman, B. D.; Pinnau, I. *Polym. Prepr. (Am. Chem. Soc., Polym. Mat. Sci. and Eng)* **1997**, *77*, 311.
- (53) Takada, K.; Matsuya, H.; Masuda T.; Higashimura, T., *J. Appl. Polym. Sci.* **1985**, *30*, 1605.
- (54) Freeman, B. D.; Pinnau, I. "Polymeric Materials for Gas Separations," *Polymeric Membranes for Gas and Vapor Separations: Chemistry and Materials Science*, B. D. Freeman and I. Pinnau, I Eds., *ACS Symposium Series* **1999**, 1-27.
- (55) Shah, V. M.; Hardy, B. J.; Stern, S. A. *J. Polym. Sci.: Part B: Polym. Phys.* **1993**, *31*, 313.
- (56) Hirose, T.; Kamiya, Y.; Mizoguchi, K., *J. Appl. Polym. Sci.* **1989**, *38*, 809.
- (57) Pixton, M.R.; Paul, D. R. "Relationships Between Structure and Transport Properties for Polymers with Aromatic Backbones" *Polymeric Gas Separation Membranes*, D.R. Paul and Y.P. Yampol'skii Eds., CRC Press, Boca Raton, FL. **1994**, 83-153.

ACKNOWLEDGEMENTS

Funding was provided by the U.S. Department of Energy, Office of Basic Energy Sciences, Division of Chemical Sciences under contract W-7405-ENG-82. Support was also provided by the National Science Foundation (Research Planning Grant), Iowa State University (Start Up Funds) and the DuPont Young Faculty Award (VVS). We would like to thank Dr. Richard Lyon from Federal Aviation Administration Fire Research Program for the data on fire resistance, and Dr. Kenneth Carter from the IBM Almaden Research Center for the dielectric constant measurement. We would also like to thank Dr. Matthew Kramer and Larry Margulies from the Ames Laboratory of the Department of Energy for the WAXD experiments.